personal buildup for

Force Motors Ltd.

MTZ worldwide 4/2011, as epaper released on 07.03.2011
http://www.mtz-worldwide.com

content:

www.MTZonline.com

MTZ WORLDWIDE

04 April 2011 I Volume 72

FRICTION POWER Measurements of a Fired Diesel Engine

GAS ENGINE with Two-stage Turbocharging

QUANTIFYING and Preventing Pre-ignition

INJECTION AS KEY TECHNOLOGY

CONTENTS

COVER STORY

INJECTION AS KEY TECHNOLOGY

4, 10 I For diesel and petrol engines for passenger cars, the fuel injection system has long since been in the focus of development. However, there is still a need for further improvement – in addition to an increase in pressure, important development fields include multiple injection and metering accuracy. For decades, there has been relatively little movement in fuel injection technology for marine diesel engines. But now, the severe tightening of emissions standards is leading to a dramatic change. System pressures need to be increased, and the loads on the components are rising accordingly. At the same time, the special requirements regarding durability and cost-effectiveness remain in place.

FIGURE ABOVE AND COVER FIGURE © Audi

RESEARCH IS THE FUTURE

Dear Reader,

Many of the academic theses written at the institutes of our technical field deal with current issues relating to engine technology in a very application-oriented manner. This is by no means a bad thing for students, as it confronts them at an early stage with projects that they will encounter later on in their professional life.

Recently, I was able to take a closer look at research being carried out at the Cluster of Excellence “Tailor-Made Fuels from Biomass” at the RWTH Aachen. There, twenty institutes are jointly working on the future of our mobility. Their research approach is unique throughout the world: whereas others try to produce biofuels in such a way that they reproduce the properties of petrochemical fuels to the greatest possible extent, the researchers in Aachen focus on developing combustion processes and biofuels at the same time. Their aim is to find a fuel that provides optimum, clean combustion.

The scientists in Aachen are also pursuing new approaches towards producing fuel from biomass. The components are not first split up into individual hydrogen atoms and carbon monoxide molecules at very high temperatures and then “recombined” to produce fuel by means of Fischer-Tropsch synthesis, but a catalytic process is used to convert them directly into those molecules that can be burned in the engine. Such a process could be much more energy-efficient.

We already published a report on initial successes of this research in the December issue of MTZ. And we will, of course, intensively follow the developments. After all, even if the success of this approach, in other words its large-scale implementation, is by no means certain and will take at least another ten years, such basic research makes us future-proof!

MTZ sees itself as a technical-scientific journal that also goes beyond the articles from universities that we publish. Research in the field of drive systems and energy sources will continue to be the main focus of our reporting in the future.

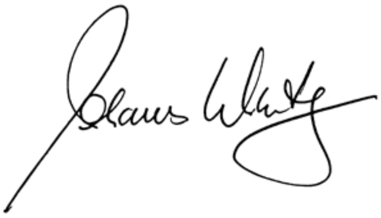

JOHANNES WINTERHAGEN, Editor-in-Chief
Jülich, 10 February 2011

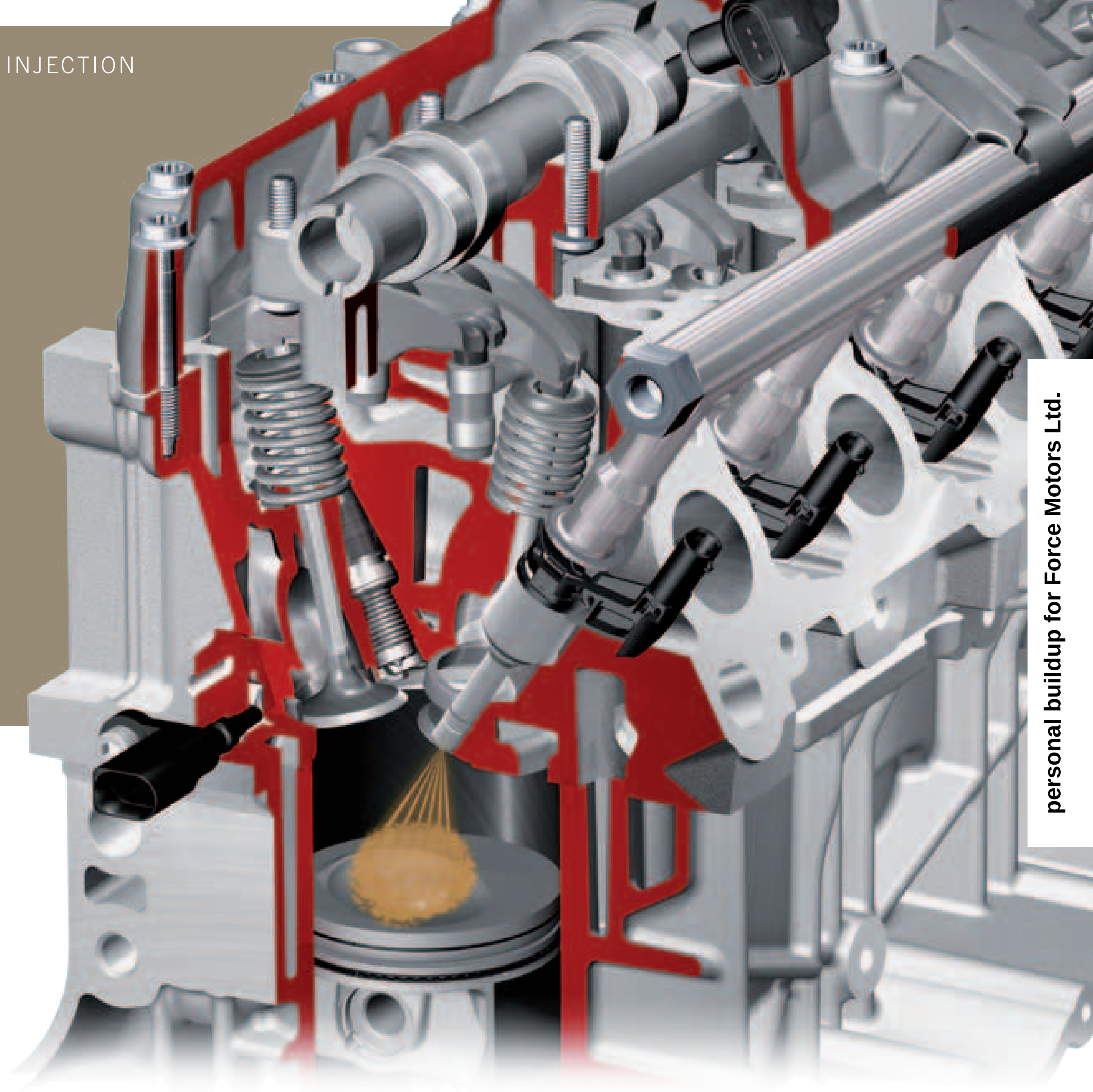

FUEL INJECTION SYSTEM
KEY COMPONENT FOR FUTURE EMISSION TARGETS

Optimum mixture formation is an essential requirement for low engine-out emissions. That applies to both diesel and spark-ignition engines. A summary by Volkswagen shows which potentials innovative direct-injection systems still offer in this field.

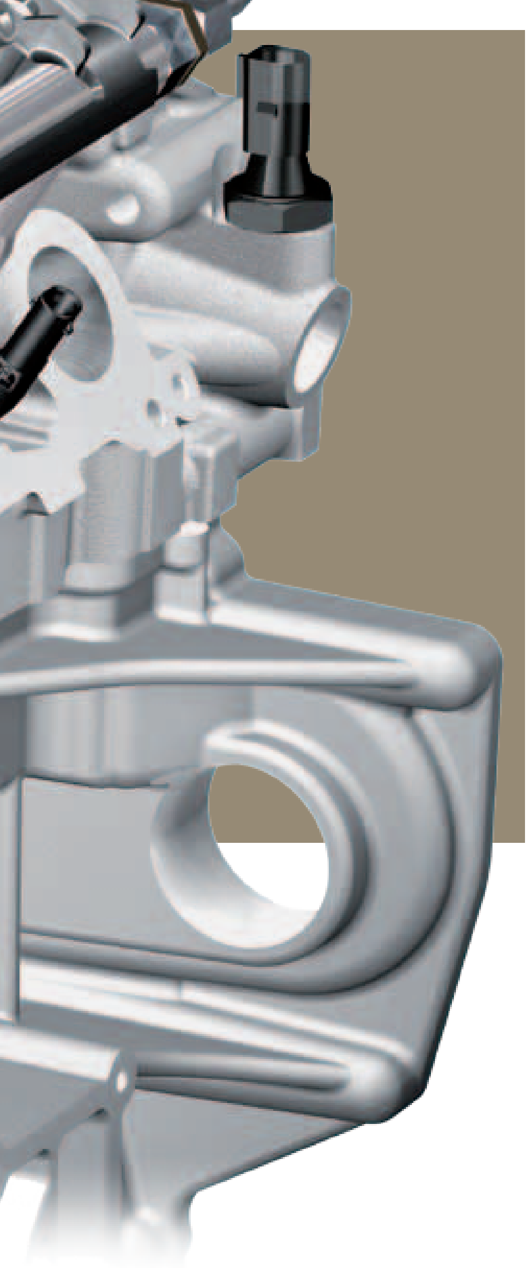

AUTHORS

DR.-ING. JÖRG THEOBALD
is Head of SI Engine Advance Engineering at Volkswagen AG in Wolfsburg (Germany).

DR.-ING. KAY SCHINTZEL
is Development Engineer for Combustion Systems, SI Engine Advance Engineering at Volkswagen AG in Wolfsburg (Germany).

ANDREAS KRAUSE
is Head of Development Diesel Injection Systems at Volkswagen AG in Wolfsburg (Germany).

ULRICH DOERGES
works at Development Diesel Injection Systems at Volkswagen AG in Wolfsburg (Germany).

INCREASING DEMANDS

The introduction of direct injection in both spark ignition (SI) and compression ignition (CI) engines has led to a continuous improvement of engine performance as well as to a significant reduction of untreated emissions. Volkswagen's first direct injection spark ignition (DISI) engine – the FSI with stratified charge and so-called swirl injectors – went into production in 1999. Since then, direct injection technology has continuously evolved. The TSI engine introduced in 2005 combined supercharging and homogeneous direct injection. The downsizing strategy pursued in this engine not only reduced emissions but also helped implement further optimization potentials with regard to CO_2. The TSI was also the first engine to use multi-hole fuel injectors in order to improve mixture formation.

The steady increase of the mean effective pressure in SI and CI engines calls for the consistent further development of key engine components, most notably fuel injectors and high-pressure fuel pumps. As regards the these two components, intensive efforts are being made to advance the technological progress for both engine types with the objective of preparing the fuel quantities required for downsizing the best possible way while, at the same time, keeping in mind the basic challenges concerning fuel consumption and emissions. The reduction in both the number of cylinders and combustion chamber volume give rise to further requirements to be met by the injection system. This, in turn, allows all advantages of downsizing with regard to weight, combustion method, and friction to be fully exploited. As Volkswagen engines are used all around the world, the issue of differing fuel qualities poses another big challenge to the injection system. The requirements concerning the quantitative accuracy of fuel injected are steadily increasing. Therefore, a deviation of $< 5\,\%$ between the cylinders of a given engine is to be aimed for at a test pressure of 20 MPa. Given multiple injection and a fuel rail pressure of 20 MPa, the required minimum fuel quantity to be injected under all circumstances is defined as < 2 mg per pulse with injection durations of < 0.5 ms.

In the field of CI engines, in which mastering smallest injection quantities has long

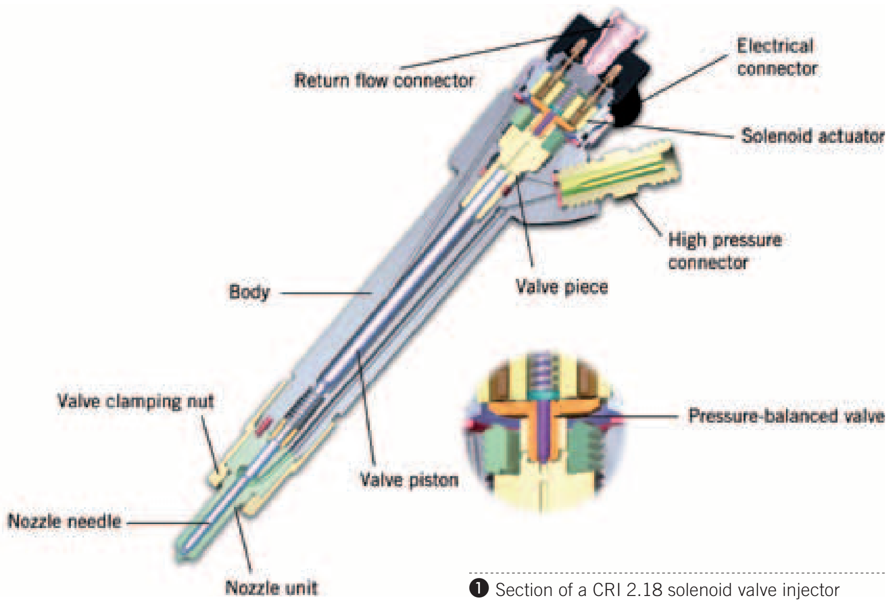

❶ Section of a CRI 2.18 solenoid valve injector

been an issue, the minimum injection quantity is currently 0.5 mg. Future requirements will be between 0.2 and 0.3 mg at pressures of 200 MPa and higher.

FUEL INJECTION IN CI ENGINES

Volkswagen's 2007 changeover to using common rail technology in diesel engines – driven primarily by the ever increasing requirements placed on exhaust treatment – marked another step towards improving flexibility and precision.

The use of piezo technology in servo-actuated common rail injectors generally allowed for both a greater number of partial injection events and shorter breaks between them. Bosch has managed to develop more cost-efficient solenoid valve injector concepts featuring the aforementioned advantages, which will be further exploited by future injection systems with increased injection pressures. When combined with pressure-compensated shift valves, the switching times of the magneto-inductive actuators are accurate enough to be used in EU5 and EU6 engine concepts. ❶ shows a CRI 2.18 injector used for injection pressures of up to 1800 bar. At Volkswagen, this injector type has almost completely replaced the CRI 3.18 piezo injector used in 2.0 l TDI engines.

Newly developed common rail injectors with directly controlled valve needle exhibit further potential for multiple injections and very stable minimum fuel quantities, even for long service lives. The needles of these injectors are no longer actuated indirectly via servo valves and pressure differences between needle seat and needle backside induced thereby. Instead, they are actuated more or less through the direct, positive locking connection with the piezo actuator.

Currently, there are two suppliers for directly actuated fuel injectors. Delphi offers the DFI 3.0 injector that was presented in 2008 and which has already been introduced in a number of series production applications. What is special about this injector is the integrated hydraulic needle motion amplifier. Its purpose is to increase the needle lift generated by the piezoelectric actuator, thereby providing adequate valve lift for injection. It also serves to ensure that the injector is sealed leak-tight when no current is applied, which is achieved by combining the motion amplifier with a closing spring. During operation, the injector is opened by discharging the piezoelectric actuator and closed by applying the control voltage between the individual injection events. Another special feature of this injector concept is that the piezoelectric actuator is accommodated within a volume of fuel located inside the injector, close to the nozzle. The aim of this setup was to significantly reduce the susceptibility to pressure waves. The challenges that had to be met in this context involved ensuring complete leak tightness of the electric components.

Continental's directly controlled injector, ❷, has already been presented on various occasions under the development name New Generation. In this injector, the piezoelectric actuator's direction of motion – which is opposite to the opening direction of the valve needle – is inverted by means of a mechanical lever system. This system features a transmission ratio ensuring that the needle is lifted sufficiently without restricting the fuel flow.

Ever decreasing injection quantities combined with the ever growing demand for precise injections have resulted in in-

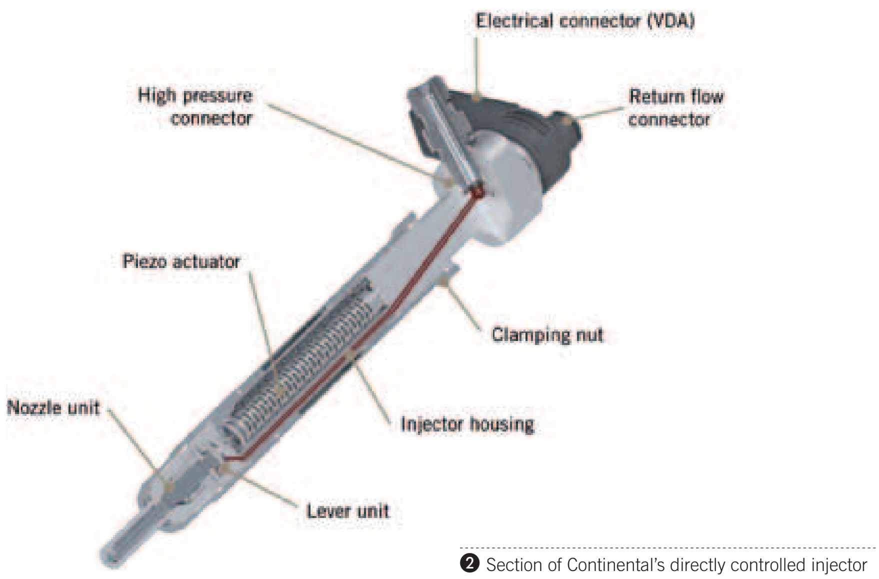

❷ Section of Continental's directly controlled injector

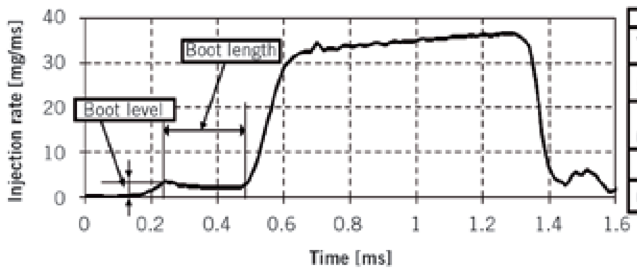

Type	NG
pRail [bar]	1650
Boot level [% of max. flow rate]	6
Boot length [ms]	0.25
mF_tot [mg/cycle]	30.5

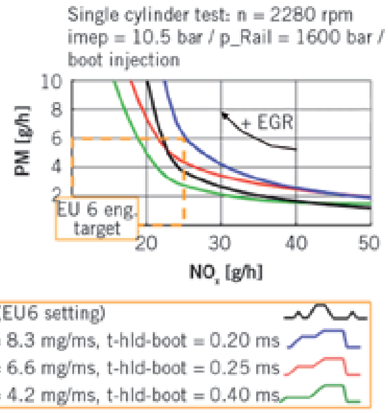

❸ Manipulating the course of the injection process during boot injection, higher part load (n = 2280 rpm / imep = 10.5 bar / p_{Rail} = 1650 bar / HR50 = 18° crk)

creased requirements placed on both the quantitative accuracy and the accuracy of injection timing. A variety of correction functions for compensating the tolerances of mechanical and electronic components used in injector systems are already established and used in series production. The future, however, will see a very interesting closed loop control system used in this particular application case. The speed of the valve needle changes abruptly when it reaches its end positions. This, in turn, produces an evaluable change in the capacitance signal which allows the injection timing to be controlled online for each individual valve lift. It thus becomes possible to compensate changes and drift on the piezoelectric actuator and on the needle seat over the entire service life.

BOOT INJECTION

Directly actuated piezo injectors allow for the course of the injection process to be manipulated, which opens up additional potentials. Although current injector systems used in large-scale production are capable of performing up to eight injections per combustion cycle, there is always a time interval of a few µs between each injection which cannot be shortened. This is due to the well-known issue of susceptibility to pressure waves in the injector which, despite the use of attenuators and compensating algorithms, still causes significant problems. ❸ shows a comparison between a standard injection process with multiple offset injection events and a boot injection process, which, e.g., improves acoustics when the engine is idling and reduces emissions in the emission-relevant range.

LEAKAGE

Fuel leakage on the injectors has turned out to be a major drawback that is characteristic of common rail injection system used to date. The leakage sources to be named are the inevitable switching leakage of the servo valves and the permanent leakage on the needle guides and the control piston which still leaves room for optimization. Keeping in mind that leakage rates ranging from 5 to 20 l/h – which correspond to the actual fuel demand of the engine – are nothing unusual, the solution of this issue bears an enormous potential for reducing CO_2 emissions. With the Delphi injector, the leakage issue has already been solved completely, and the permanent leakage rates of the Continental system are far below the values common today.

INFLUENCE ON EMISSIONS

The new possibilities allowing even smaller fuel quantities to be used during the individual injection events can be utilized to reduce emissions significantly.

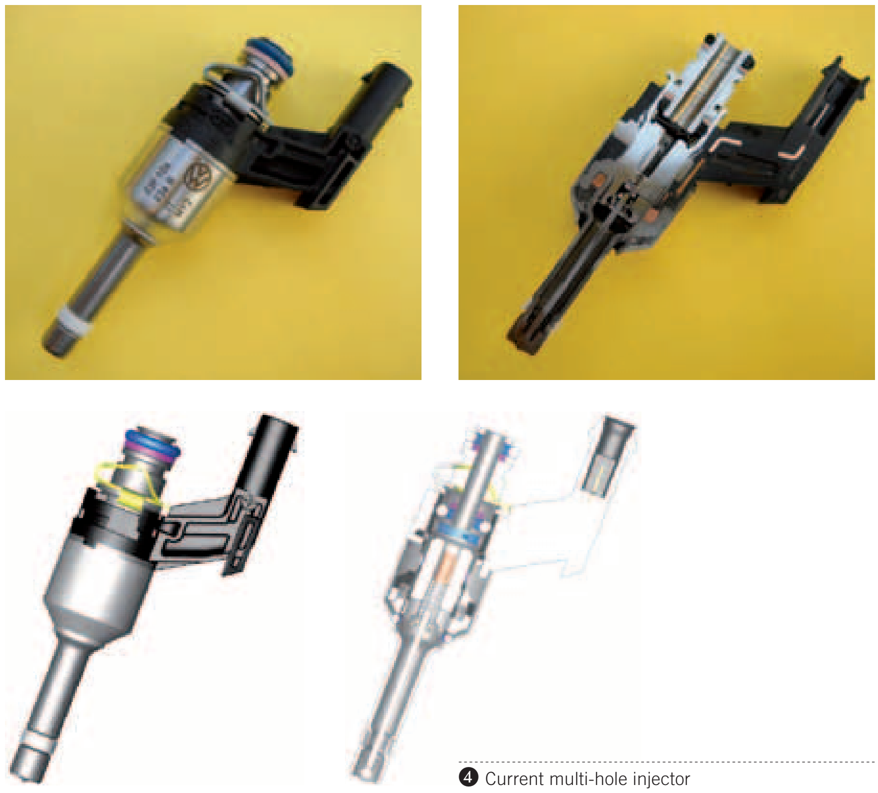

❹ Current multi-hole injector

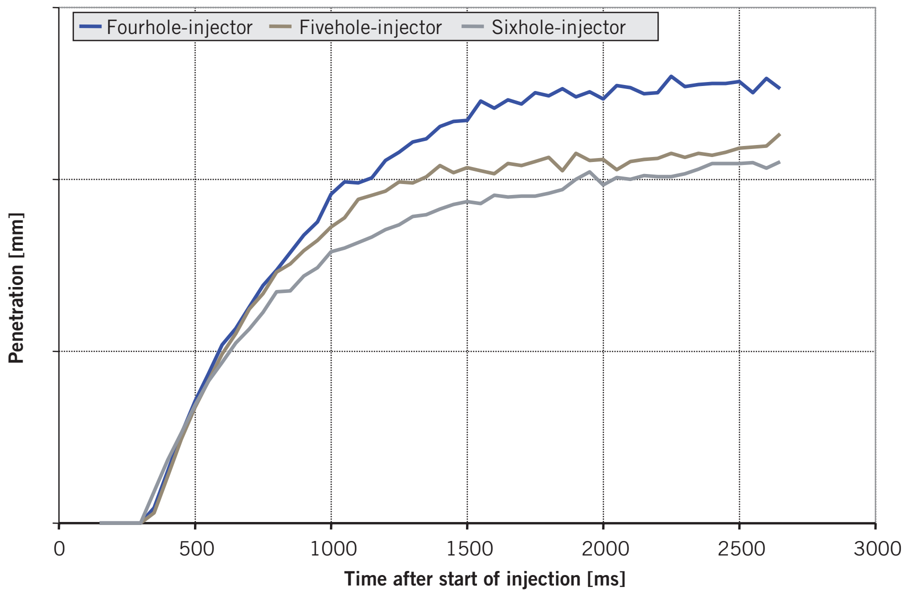

❺ Penetration curve of injectors with different numbers of holes at a rail pressure of 20 MPa (operating parameters: $p_{chamber}$ = 0.1 MPa, $T_{chamber}$ = 25 °C, T_{inj} = 25 °C, t_i = 1 ms, f_E = 5 Hz, recorded from the side)

This applies in particular to systems with high rail pressures and multiple injections. The application of exactly definable injection processes, particularly in emission test cycles with higher engine loads, increases EGR compatibility while, at the same time, reducing particle emissions by up to 30 % in some points. This, in turn, is accompanied by a reduction in pressure increase rates and thus combustion noise. The fact that this can be used to obtain higher utilizable injection pressures and to improve particle emissions is no longer a secret of diesel engine developers.

The key component of a diesel injection system is the injection nozzle which converts the fuel pressure into the foundations of efficient combustion, i.e., high jet speed and best possible atomization with smallest droplets and high penetration depth. Still, the key to obtaining high-performance nozzles is to use state-of-the-art technologies for rounding off nozzle edges in combination with matched conicity and the smallest possible hole diameter. The use of new electric discharge machining procedures allows for the efficiency of pressure conversion to be further increased. The only constraints in this context are manufacturing tolerances and the safe distance between the nozzle and surfaces with excessive smoothness, which could lead to coking of the injection holes due to the lack of microcavitation.

FUEL INJECTION IN SI ENGINES

When designing the spray geometry of state-of-the-art DISI combustion systems, various boundary conditions such as the injection hole diameter, the injector position, and the motion of the air entering the combustion chamber have to be taken into consideration. One of the main development tasks therefore consists in positioning the individual fuel jets of the multi-hole injectors, ❹, used at Volkswa-

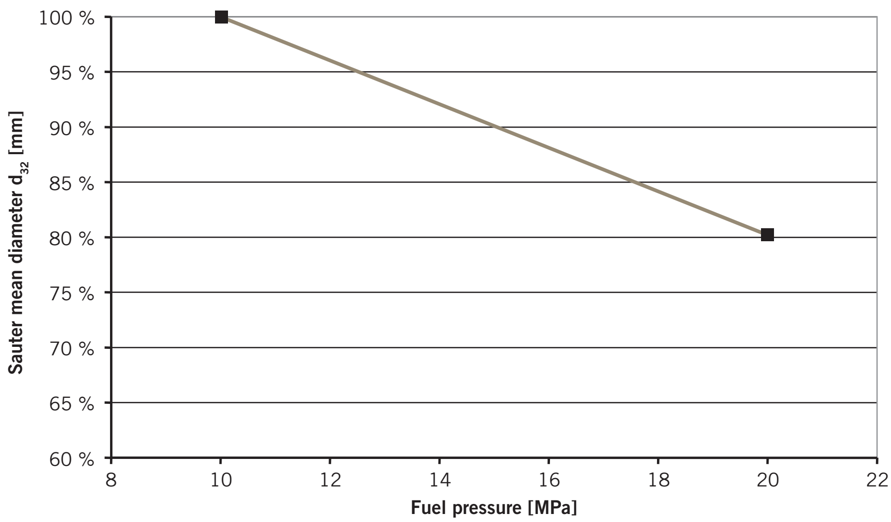

❻ Influence of the rail pressure prail on the Sauter mean diameter d_{32}

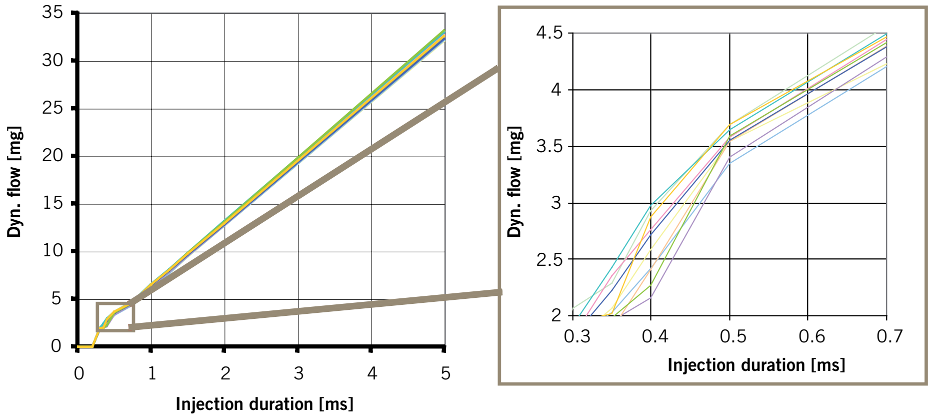

❼ Dynamic flow q_{dyn} in ten fuel injectors of the same model series

gen in such a way as to obtain the desired spray geometry.

What is aimed for when designing fuel spray geometries is to ensure that the individual fuel jets utilize the combustion chamber volume in the best possible way. Injectors with four, five, six and seven holes are tested during the design process with the objective of achieving best possible homogenization. The final decision on which spray geometry to use for which engine concept is contingent on the measurement results of the specific engine concepts. This approach is also currently being used in the development of the combustion system of the next generation TSI engines. Here, the objective is not only to achieve optimal homogenization, but also to avoid any contact between the cylinder walls and the injected fuel.

The special design of the injection holes reduces the amount of fuel wetting the combustion chamber roof and the piston as well as the amount of hydrocarbons in the vicinity of the cylinder wall (wall quenching). This also leads to a considerable reduction in the emission of pollutants, which, in the end, is also the result of a significantly reduced fuel jet penetration depth, ❺.

The development of special spray geometries furthermore reduces deposits on the piston surface and the combustion chamber roof which, again, reduces emissions. The rail pressure in the next generation of DISI engines will be increased to a maximum of $p_{Rail} = 20$ MPa, which will results in a reduction of the Sauter mean diameter d_{32}, ❻. The fine atomization of the injected fuel improves not only mixture formation, but also the emission behavior and fuel consumption.

IMPROVING THE DYNAMIC PROPERTIES OF FUEL INJECTORS

Different measures are being taken to improve the dynamics of fuel injectors. Especially the injector holes must be manufactured with a high degree of precision in order to keep variance between the individual injectors to a minimum. In operating ranges with both short and long injection durations this increases the accuracy of the injection, ❼. This, in turn, improves the overall running smoothness of the engine and reduces emissions.

Especially in systems with multiple injection, which are used in an increasing number of applications, improving the dynamic properties of injectors will result in more stable engine operation and reduced emissions.

INJECTION STRATEGIES

As mentioned above, multiple injection strategies are becoming more and more important both in catalyst heating operation and in the rest of the engine map. Current concepts use three individual injection events for engine speeds of up to n = 3000 rpm and two injection events in the engine speed range from n = 3000 rpm to n = 4000 rpm. This improves fuel economy and reduces emissions. Multiple injection offers a wide range of possibilities with an immense number of potential combinations that have to be taken into consideration during development. The first step thus consists in using automatic optimization processes based on genetic algorithms in order to parameterize all combinations and possibilities. Limited parameter spaces and parameter variations are then tested on the actual injection system in order to confirm the optimal settings. This approach reduces the time required for the application of multiple injection to a minimum.

SUMMARY

This article goes to show that – even though individual parameters may differ significantly when viewed from an absolute perspective – the development of both SI and CI engines is generally heading in the same direction as regards the rail pressure, multiple injection, and fuel metering accuracy of the respective injection systems. In addition to increasing the injection pressure, efforts are being made to develop solutions that increase the flexibility of injection as well as the fuel metering accuracy. In order to master the challenges of ever stricter emission legislation and to meet the increasing fuel consumption objectives, both engine types will feature the same design details and make use of the same materials, manufacturing methods, and required corrective functions within the software structures. The further development of injection system components will contribute significantly to achieving the primary objective of reducing untreated emissions by means of optimal mixture formation.

INJECTION TECHNOLOGY FOR MARINE DIESEL ENGINES

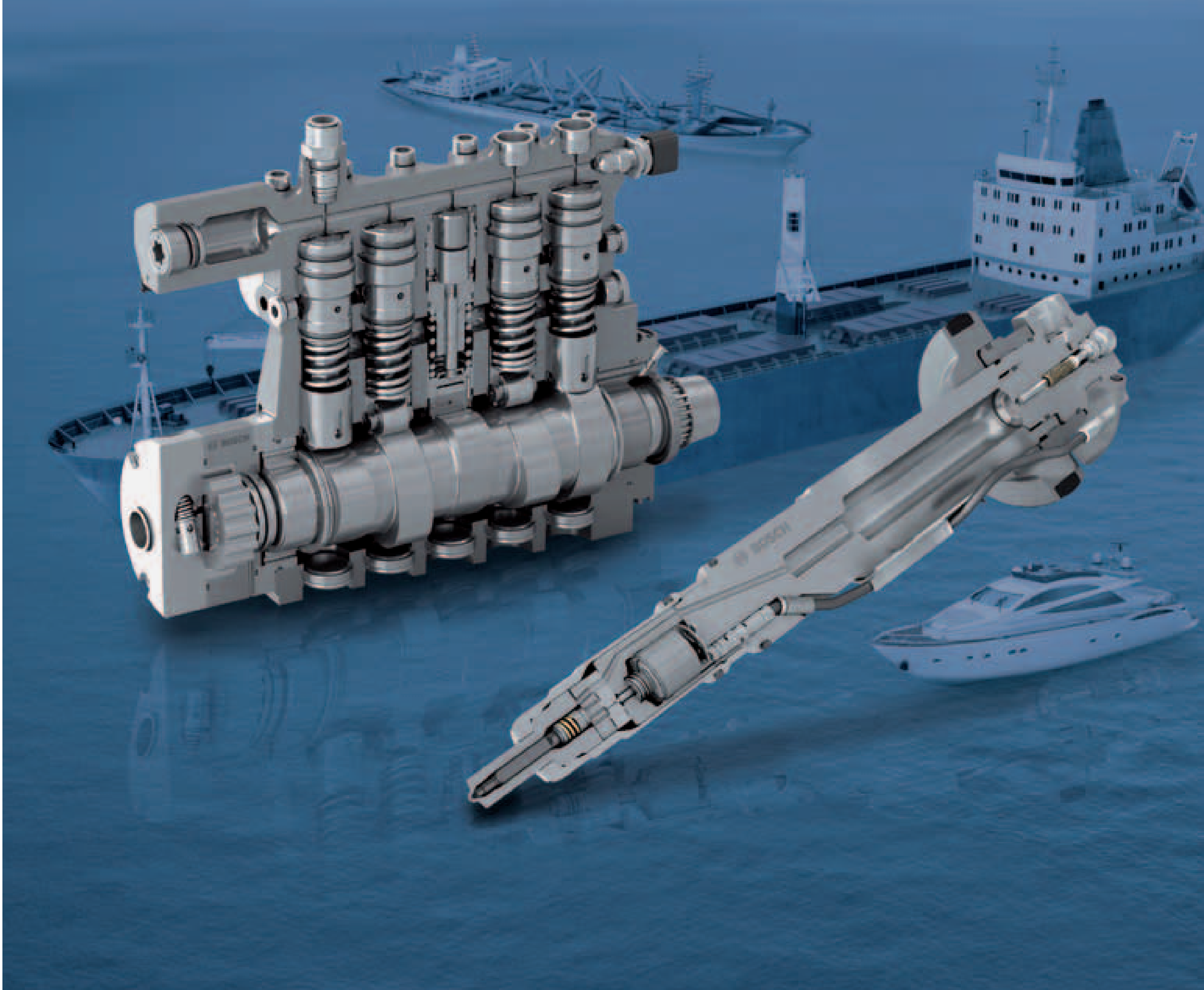

Increasingly strict emissions legislation worldwide is also resulting in further improved fuel injection systems for marine diesel engines. Bosch has developed a product range of common rail systems with an injection pressure of up to 2200 bar for medium-speed marine engines that will also be able to comply with the future Tier 4 and IMO 3 emissions standards.

AUTHORS

DR. ROLF LEONHARD
is Executive Vice President Engineering, Bosch Diesel Systems at Robert Bosch GmbH in Stuttgart (Germany).

DR.-ING. MARCUS PARCHE
is Senior Vice President Diesel Systems for Commercial Vehicles at Robert Bosch GmbH in Stuttgart (Germany).

DR. CHRISTOPH KENDLBACHER
is Head of Development Large Engines of the Commercial Vehicle Product Division at Bosch Diesel Systems at Robert Bosch AG in Hallein (Austria).

DIFFERENT REQUIREMENTS FOR DIFFERENT APPLICATIONS

For decades fuel injection systems for marine diesel engines did not change significantly. The requirements for cost, robustness, durability, packaging and function could be met with standard inline and mechanical unit pumps. The fuel injection systems are now changing dramatically due to increasing requirements for emissions and fuel consumption.

Throughout history, Inline Pumps (IP) were used to drive marine engines. They were limited in terms of variable timing and injection pressure (approximately 1200 bar). Electronically controlled Unit Pumps (UP) and Unit Injectors (UI) have one more degree of freedom, i.e. the advantage of flexible injection timing within the limits of the cam profile. These cam-driven fuel injection systems provide higher injection pressures (up to 1800 bar) based on more robust camshafts and flexible timing. Both of these modifications therefore lead to a benefit in fuel consumption and emissions.

Since emission limits became even more stringent Common Rail Systems (CRS) were introduced to the market. They have two additional degrees of freedom: injection timing and injection pressure.

Bosch is the only company in the world offering diesel injection systems and, in particular, Common Rail Systems for passenger-car, commercial-vehicle and large diesel engines. The uses to which diesel engines are put in marine applications are as varied as the demands made on the injection system. Marine engines can be segmented into the following categories, ❶:

- derivatives of commercial-vehicle engines
- high-speed engines
- medium-speed diesel and heavy-fuel-oil engines
- low-speed heavy-fuel-oil engines.

For high-speed marine engines of up to 2.5 l displacement/cylinder, Bosch offers the third generation of its Common Rail System for commercial vehicles (CRSN3), which is based on commercial-vehicle components and has been optimized for off-highway applications. For engines of over 2.5 l/cylinder, Bosch has developed the particularly robust Modular Common Rail System (MCRS) and has been active in this field in a wide variety of applications since 2004. For medium-speed diesel engines with especially long service intervals, the MCRS-T will be going into series production in 2012. Operation with heavy fuel oil makes special demands on the Common Rail System. Bosch developed together with MAN Diesel&Turbo a system especially optimized to meet these requirements, the HFO-CRS. This system is available in future also for other customers.

EMISSIONS: DRIVING FACTOR OF MARINE INJECTION TECHNOLOGY

Bosch supports its customers by developing injection and exhaust-gas treatment systems and thus permits great flexibility in the development and application of marine engines which are optimized as regards emissions and fuel consumption. An extremely long service life, many general overhauls and retrofitting with modern injection and exhaust-gas treatment systems in order to meet the most recent fuel-consumption and emission standards are state of the art. Their field of application ranges from performance-optimized

ENGINE CATEGORIES	HD-TRUCK DERIVATIVE	HIGH SPEED	MEDIUM SPEED (FOUR-STROKE-ENGINE)		LOW SPEED (TWO-STROKE-ENGINE)
Cyl.-volume (l) Cyl.-output (kW) Speed (rpm)	< 2.5 ≤ 120 ≥ 1400	2.5 – 7 ≤ 250 ≥ 1400	4 – 32 ≤ 500 ≥ 1400	33 – 290 ≤ 2100 ≥ 450	134 – 1800 ≤ 7760 ≤ 450
FIE	IP, UP, CRS	PF, IP, CRS	UP, PF, CRS	PF, CRS	PF, CRS
Application	Pleasure boats Fast ferries Coast guard Fishing boats		Ferries Tug boats River boats	Container ship Tanker Ocean liner	Main propulsion

UI = Unit injector UP = Unit pump IP = Inline pump CRS = Common rail system PF = Single plunger pump

❶ Segments of the marine engine market

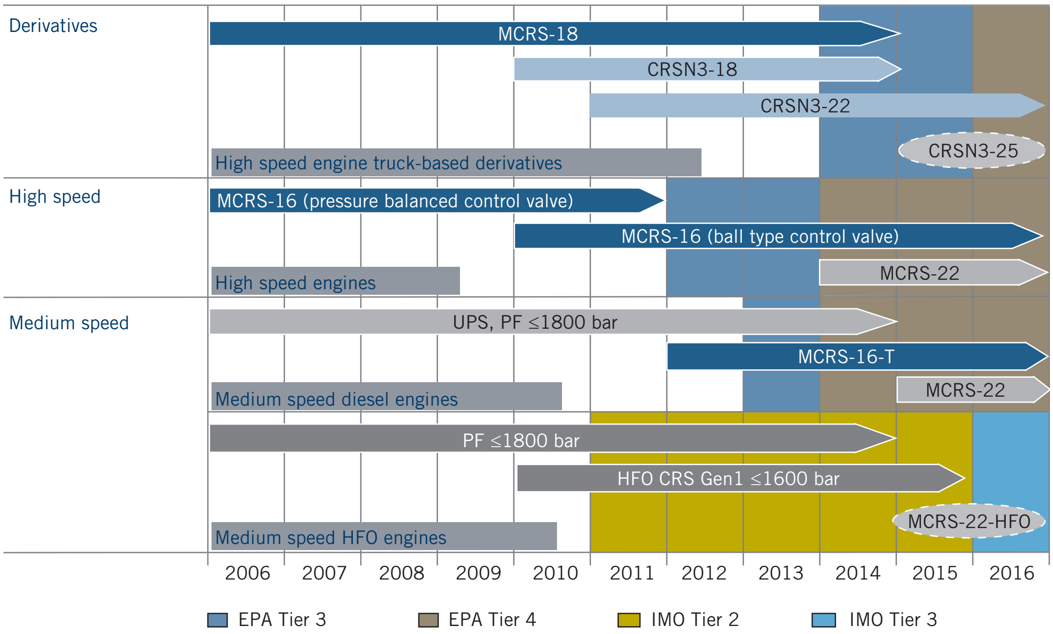

❷ Marine diesel injection technology roadmap

yachts to the robustness-optimized main drive units of tankers and container ships, ①. All applications are subject to the relevant legal exhaust-gas regulations (e.g. EPA, IMO) which will be significantly tightened up in the years between 2012 and 2016, ❷.

To fulfill future emission limitations, measures inside and/or outside the engine will be required. Here, too, Bosch is primary relying on Common Rail technology. This meets the demands for the necessary flexibility of injection rates and multiple injections, permitting further increases in pressure while at the same time minimizing hydraulic losses. Individual customer-specific stipulations determine the type of Common Rail System applied to specific engine types and sizes.

Today approximately one tenth of the world's entire nitrogen-oxide emissions are attributable to shipping. Shipping is seen as a large-scale emitter of sulfur dioxide and soot particulate. The International Maritime Organization (IMO) has thus decided to reduce the exhaust-gas threshold levels in stages. From 2011 on, emissions of nitrogen oxide must be reduced by 20 %, from 2016 by 80 %. A start toward reducing the high emissions of particulate and nitrogen oxide can be made via the fuel used or via the ship's engine itself (inside-engine measures and injection technology) as well as via attention to the exhaust-gas system.

To reduce the emission of particulate, the sulfur content of the fuel is to be drastically cut down. Here there are a variety of threshold limits: "Global Caps" apply on the high seas. Zones with emission regulations (Emission Control Areas, ECAs) have considerably stricter limits. The Global Cap for sulfur in heavy fuel oil is at present 4.5 %. On 1st January 2012 it will be reduced to 3.5 % and, probably from 2020 on, to 0.5 %. The top limit for sulfur in fuels used in Emission Control Areas was reduced from 1.5 % to 1.0 % in March 2010. From 2015 it will be further reduced to 0.1 %. On the drive side, the emission limits valid from 2011 can be achieved via optimized combustion processes. For the next stage, special techniques are needed to reduce NO_x emissions. The EPA also defines limits for particulate emissions. At 0.04 g/kWh for Tier 4 applications, these present a particular challenge, calling not only for optimization of the combustion processes but also for a further increase in fuel injection pressure to 2200 bar.

TECHNOLOGIES TO FULFILL IMO AND EPA EMISSION LIMITS

The CRSN 3, ❸, with injector, high-pressure pump, rail with ancillary components (pressure sensor, pressure limiter, pressure-control valve) and control unit offers excellent preconditions for optimizing the combustion method, with the capability of up to seven injections per cycle. It has been in production since 2008 and supports engines with an output of < 120 kW/cylinder 2200 bar have been available since 2010. The system pressure required is generated without pressure amplification by the high-pressure pump and stored in the rail. The excellent hydraulic efficiency is determined by the pump and the injector.

Injector performance (CRIN3):
: injection pressure range 250 to 2200 bar (2500 bar planned)
: nozzle flow 400 to 1300 cm^3/30 s at 100 bar with calibration oil DIN ISO4113
: injection quantity 1.5 to 450 mm^3/stroke
: possibility of seven consecutive injections
: efficiency increase (vs. 1800 bar injector)
: reduced backflow quantity (~ 50 %)
: no leakage.

Design:
: plug and play to former generations (same outer geometry)
: no internal leakage (increased efficiency)
: reduced steering volume
: flexible interface to the engine.

For engines < 120 kW/cylinder, a high-pressure pump (CPN5-22/2, 2200 bar, inline plunger pump with two cylinder elements) is used. This is a fuel-lubricated pump of modular construction.

Pump performance (CPN5-22/2):

: pressure level of 2200 bar released, 2500 bar in development
: inlet pressure 0.35 to 1 bar abs
: back pressure 1.8 bar abs
: inlet temperature -25 °C to 80 °C
: integrated gear pump and fuel metering unit
: maximum output 250 l/h (2500 bar).

Design:

: fuel lubricated
: two cylinders inline
: weight-reduced design (-30 % vs. previous generation).

The Modular Common Rail System (MCRS) has been developed for high-speed engines > 120 kW/cylinder and has been adapted to meet the needs of marine engines. The MCRS is unique in its design and differs significantly from a standard Common Rail System. The MCRS does not have a rail to distribute fuel to the various injectors and therefore can be adapted “modularly” to different engine types, e.g. six, eight and ten cylinder in-line engines, or eight, ten, twelve and 16 cylinder V-type engines. The volume of the rail has been integrated into the High Pressure Pump (HPP) and the injector. Both of them dampen the pressure spikes from pumping and injection events. The MCRS consists of high pressure pump, pressure limiting valve, injectors, ECU and several sensors.

A cross-section through the MCRS injector reveals details, showing pressure

❸ CRSN3 system layout and injection program map

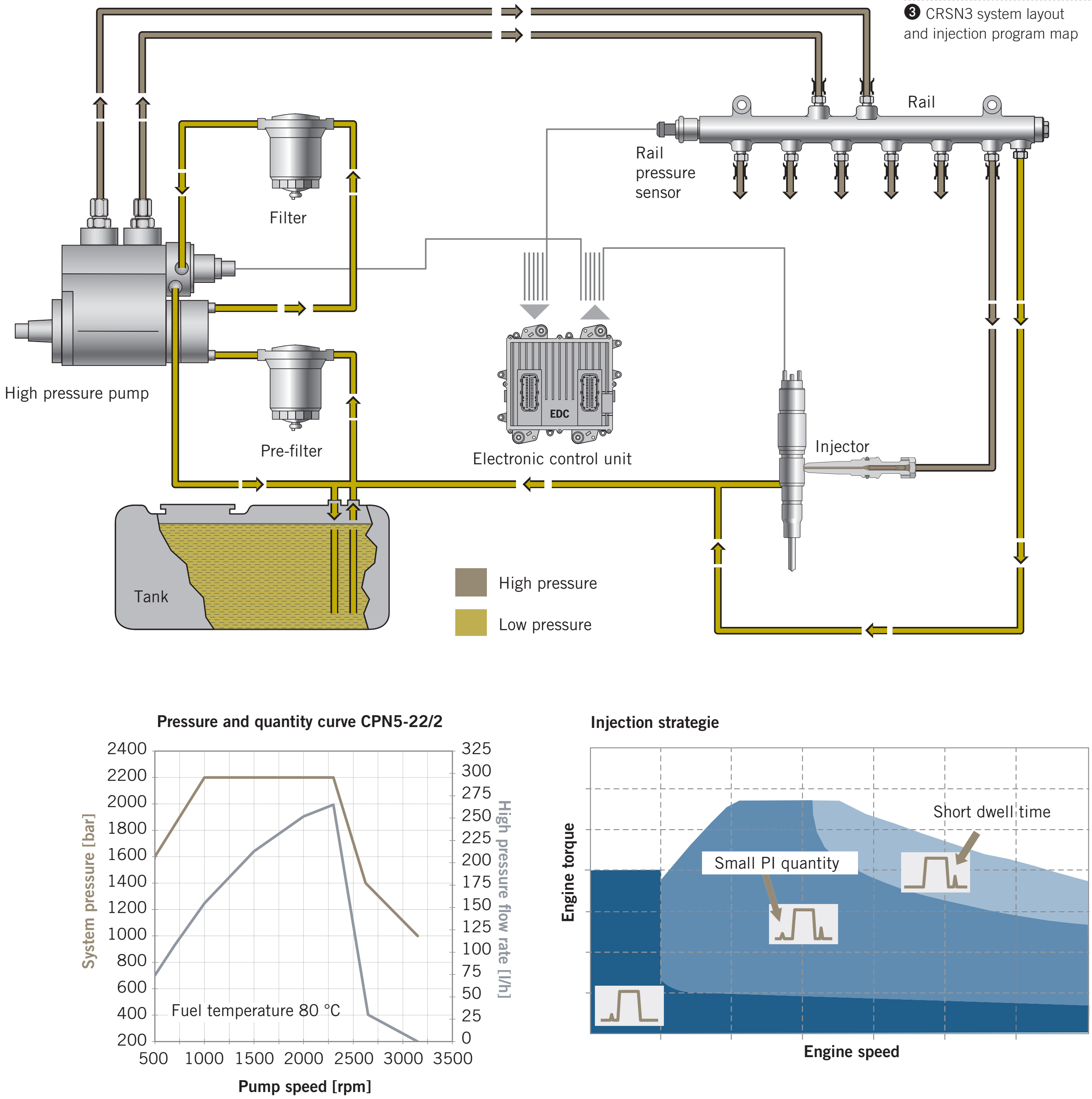

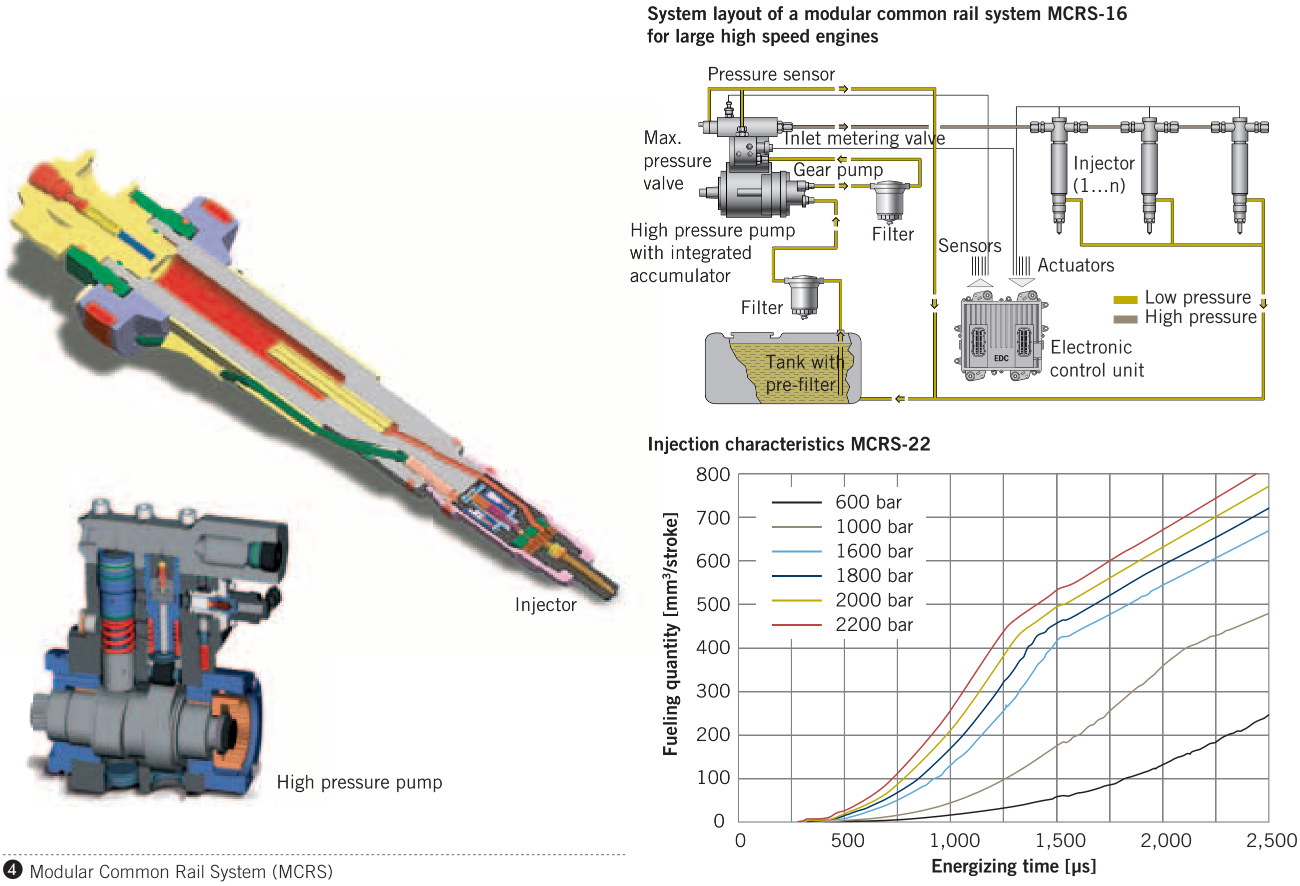

❹ Modular Common Rail System (MCRS)

damper, internal volume, the robust ball type solenoid valve and the cavitations' and wear optimized nozzle, ❹. A injection characteristic is optimized for minimum amounts and the stable characteristics across the entire program map are mandatory necessary for Tier 4 applications. The family of pumps from L2 to L5 covers fuel delivery to engines of between 0.5 and 2.25 MW and, with dual-pump drive, up to 4.5 MW.

CHALLENGE: FUEL QUALITIES

A particular challenge for Common Rail Systems in marine applications are the regional variations in fuel quality. High particulate loading and deposits from fuels led to the development of the especially robust injector control valve, which is based on a particulate-resistant ball-seat valve. The rotation of the ball ensures that initial damage caused by particulate does not lead to the formation of erosive channels. As the valve does not contain any conduits subject to high pressures, the danger of deposits building up in narrow passages is also minimized.

For medium-speed engines the MCRS-16-T was developed, which is extending the advantages of the MCRS-16 to performance classes up to 500 kW/cylinder and permitting the use of plug-in pumps (CP9.2). The existing installation space and cam drive of PF or UP drives can also be ideally utilized for the MCRS.

Above and beyond this, Bosch offers a Common Rail System for heavy-fuel-oil engines < 270 mm bore, which fulfills the IMO Tier 2 emission regulations with considerably reduced particulate emissions, ❺. There are two variants for different engine-power classes. Control of the Bosch heavy-oil injector does not require a servo system. This results in reduced losses, rapid response behavior and a reduction in the complexity of the injection system. The nozzle is pressure-controlled and thus only subjected to pressure during injection. This prevents undesired long-duration injections. Exchanging nozzles on the spot is possible without restrictions. The Common Rail high-pressure pump compresses the heavy oil to an injection pressure of maximal 1600 bar. The unit involved is a cam-driven high-pressure pump with built-on metering unit to control the system-pressure. The pumps have been optimized to prevent gumming and the special sealing design of the scavenging valve guarantees wear-free operation.

The heavy-oil Common Rail System for marine engines and auxiliary machines with over 270 mm bore, ❻, was developed with MAN Diesel&Turbo and differs from the above system by separating the control valve from the injector. This permits the use of a conventional nozzle-and-holder assembly (DHK). Conversion from conventional to Common Rail technology is thus simple to implement. Servicing the nozzle-and-holder assembly can be carried out separately from the control valve on board.

A single feed pipe is available to supply two engine cylinders each. Injection is controlled by a robust control unit with 2/2 and 3/2 valve on each accumulator end cover, switching the high pressure

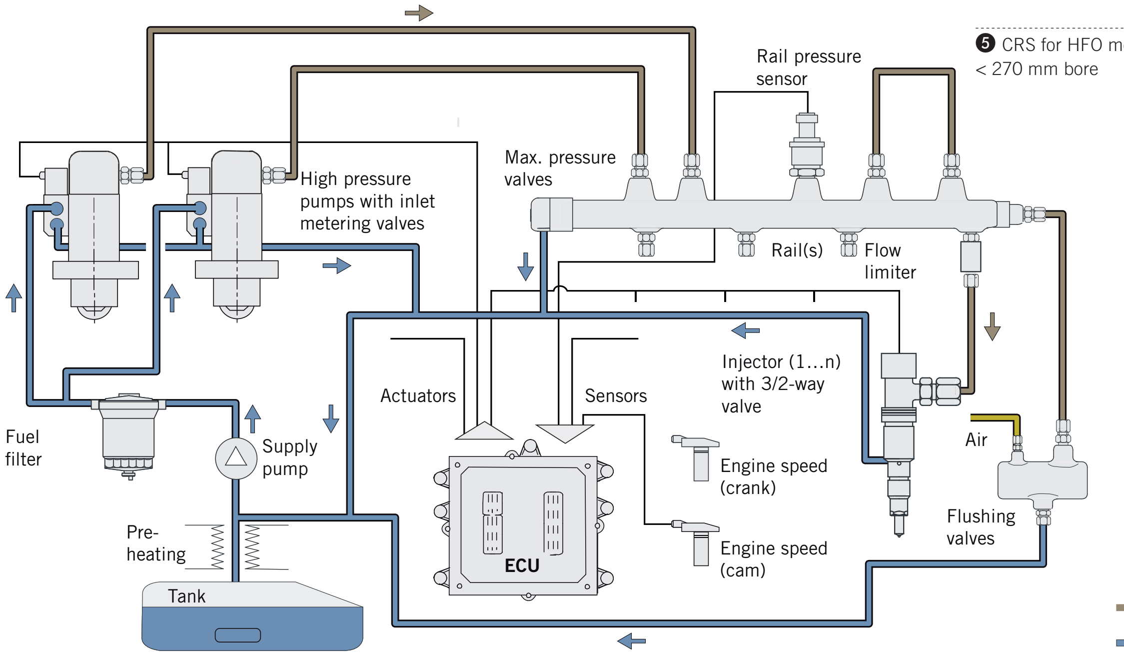

❺ CRS for HFO medium speed engines < 270 mm bore

between accumulator pipe and mechanical DHK. The flow-limiter valve in the accumulator pipe prevents the injection of unintentionally large amounts. A pressure limiter in the system ensures that no excessive system pressure is created in the case of a fault in either the metering unit or the pressure sensor. Bosch developed components are the 3/2 way valve, flow limiter, circulation valve, maximum pressure valve and the inlet metering valve for the high pressure pumps. The System responsibility has MAN Diesel&Turbo and they developed the high pressure pump, accumulator and mechanical nozzle-holder assembly. ECU and fuel lines are also in responsibility of MAN Diesel&Turbo.

Both injection systems considerably reduce black-smoke emissions and improve part-load fuel consumption.

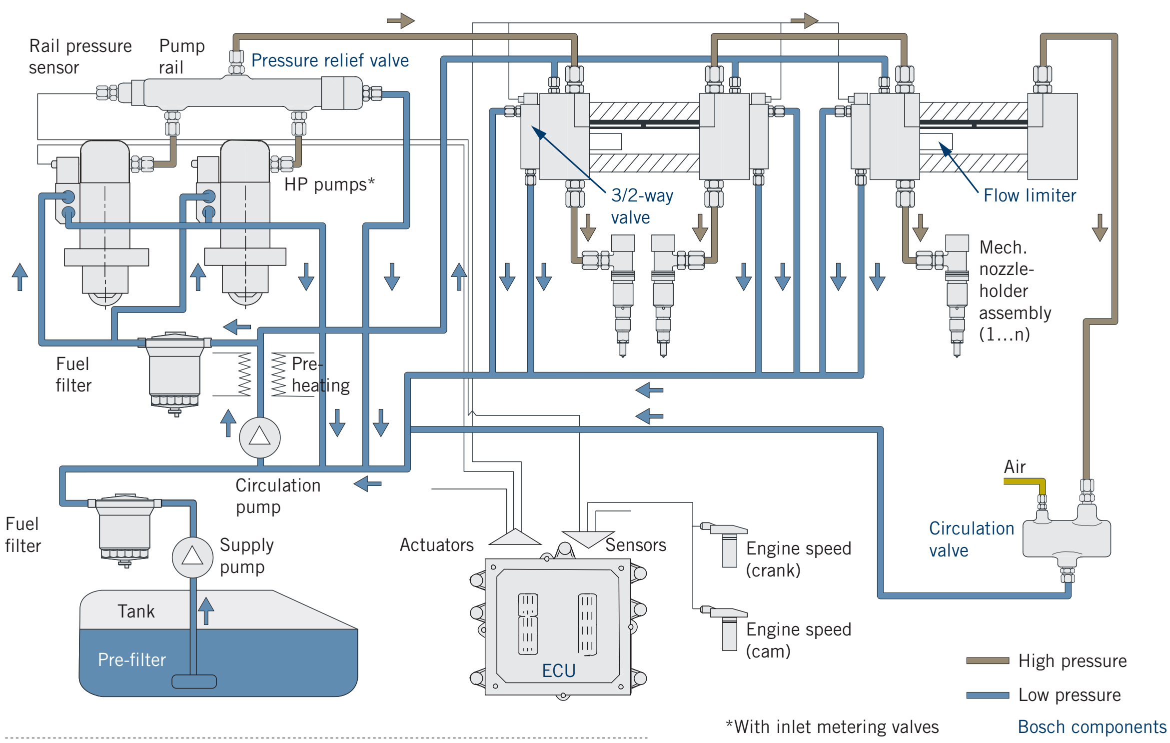

❻ CRS for HFO medium speed engines > 270 mm bore

OUTLOOK

The introduction of new emission limits faces modern injection systems with new challenges. Increasing the system pressures puts higher loads on the injection components as regards stability, wear and temperature. At the same time, the robustness and economy must be retained. To further develop the existing diesel Common Rail platforms for marine engines, Bosch is working on increasing pressures to 2200 bar. This system for distillated fuels will be available from 2012 and will be introduced in stages for all high-speed and medium-speed engines. Conscious use will be made of the experience gained and technologies already used for increasing injection pressures in the automobile sector.

In order to be able to achieve the emission targets via measures inside the engines or exhaust-gas treatment as well as good fuel-consumption values for the engines the full flexibility of the CR injection system and injection pressures up to 2200 bar for the future emission stages Tier 4 and IMO 3 will be needed.

Bosch is already working together with MAN Diesel&Turbo on the second system generation of the heavy-oil Common Rail Systems with injection pressures of up to 2200 bar and the possibility of multiple injections permitting further combustion optimization. A feasibility study on this is being carried out. This system generation will help to meet the emission targets of IMO 3 (from 2016).

REFERENCES

[1] Kendlbacher, C.; Müller, P.; Bernhaupt, M.; Rehbichler, G.: Large engine injection systems for future emission legislations. 26. CIMAC World Congress on Combustion Engine Technology for Ship propulsion, Power generation, Rail traction

[2] Kendlbacher, C.: Large Engine Injection Systems for Future Emission Legislation. Injection Systems for IC Engines. 13-14 May 2009 IMechE, One Birdcage Walk, London

[3] Parche, M.; Sassen, K. P.; Krüger, M.: Zukünftige Emissionsvorschriften für On- und Off-Highway-Nutzfahrzeug-Applikationen-Herausforderungen für Motormanagement und Einspritzsystem. MTZ Konferenz Heavy Duty-, On- und Off-Highway-Motoren, November 2009 in Friedrichshafen

[4] Heider, G.; Kremser, T.; Gritzko, T.: More than 100.000 running hours field experience in HFO operation with CR injection systems on MAN medium speed diesel engines. CIMAC 2010 Paper 36

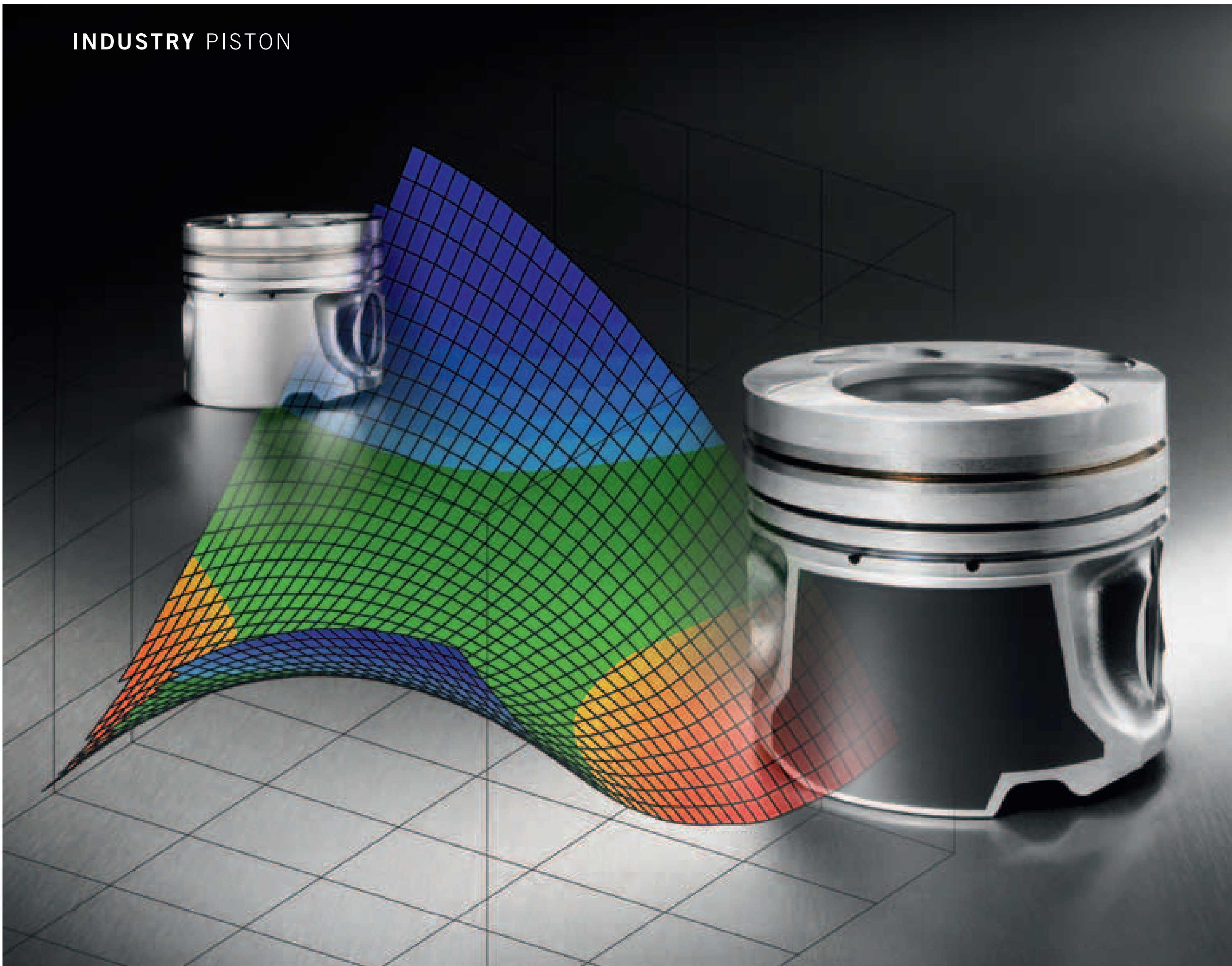

FRICTION POWER MEASUREMENTS OF A FIRED DIESEL ENGINE – INFLUENCE OF PISTON SKIRT COATINGS

Reducing engine-internal friction is one of the most important development goals in engine design. With extensive tests on fired diesel engines, Mahle engine testing has determined the potential of individual design parameters for the piston group. In order to be able to classify the potential of piston skirt coatings as the parameter studies were conducted, three different coating materials were also tested with respect to friction and wear.

AUTHORS

DIPL.-ING. THOMAS DEUSS
is Ph.D. Student in the Engine Test Laboratory at Mahle International GmbH in Stuttgart (Germany).

DIPL.-ING. HOLGER EHNIS
is Development Engineer in the Engine Test Laboratory at Mahle International GmbH in Stuttgart (Germany).

DR. REINHARD ROSE
is Head of Materials Science Surface Engine Systems and Components Europe at Mahle GmbH in Stuttgart (Germany).

DR.-ING. REINER KÜNZEL
is Director of the Engine Test Laboratory at Mahle International GmbH in Stuttgart (Germany).

FRICTION MEASUREMENT

Various measurement methods can be used to determine friction losses. ❶ shows a series of methods for determining the friction of individual frictional pairs as well as of complete engines. These range from external engine testing of individual engine components, via methods using motored engines, to several methods based on different measurement principles using fired engines. The most suitable measurement method is selected based on the parameters to be investigated.

Tribometer testing allows coatings to be evaluated by determining their coefficients of friction. Both the dry coefficient of friction and a coefficient of friction for a defined lubricant amount can be determined. The complex frictional and lubrication conditions in the tribological system of the piston group, however, cannot be reproduced exactly. Conclusions about the potential friction savings in a real engine are therefore only of limited use.

Measurements of a motored engine, due to their nature, do not provide any information about the actual effects of load on engine friction. If the engine is externally charged while being motored, the effects of gas pressure can indeed be simulated, but not under the true temperature conditions. Therefore the associated thermal expansion of the components does not occur, due to the lack of combustion. This means that a significant change in operating clearances under increasing load, and the associated change in lubrication conditions, cannot be assumed to occur. Results from baseline studies [1, 2], however, show that it is precisely these phenomena, in addition to the engine speed, that have a significant influence upon the friction losses of a combustion engine. Engine friction tests, particularly of components of the piston group, should therefore be performed on a fired engine whenever possible.

Measurements based on the floating liner method can be performed in either motored or fired operation. The operating range of the engine, however, is limited for this method. At the moment measurements taken in respect to the crank angle, can only be made up to speeds of 3500 rpm and peak cylinder pressures up to 120 bar. The cylinder distortion that occurs in a complete engine can also not be simulated using a floating liner engine. For this reason, the friction conditions that are created do not correspond exactly to the reality of a complete engine.

Friction losses of a complete engine can be determined using the indication method. The indicated mean effective pressure is determined using pressure sensors, which together with the high precision torque measurement allow a difference to be determined and this is the friction mean effective pressure.

Fuel consumption measurements provide information about the overall efficiency of an engine. In order to be able to trace back to changes in mechanical efficiency (mechanical friction), all other efficiencies that are used to calculate the overall efficiency must remain constant. The combustion and gas exchange must therefore be monitored by high-pressure and low-pressure indication. Exhaust gas measurements are performed sporadically as additional verification. If the derived fuel consumption improvement is correlated to the mechanical friction losses of the engine, then a comparative evaluation of changes in friction losses of components can be performed using fuel consumption or CO_2

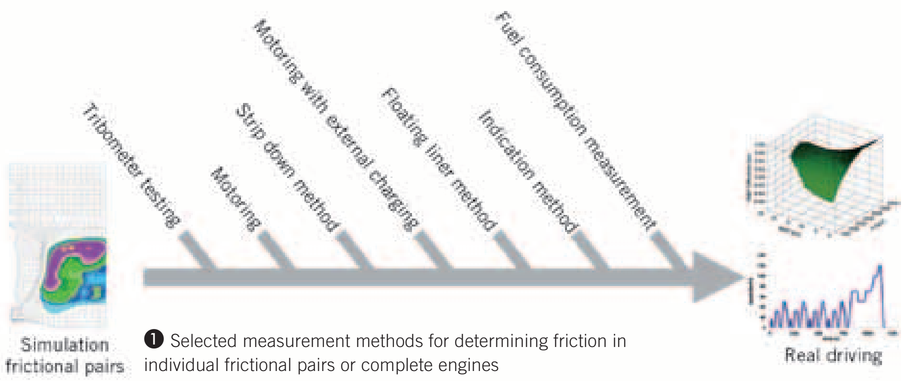

❶ Selected measurement methods for determining friction in individual frictional pairs or complete engines measurements. However, this requires a great deal of measurement effort, even exceeding that of the indication method.

The engine results presented below were obtained using the indication method with a 2.0 l diesel engine. The engine-external results are based on tribometer testing.

PISTON SKIRT COATINGS

Coating of the piston skirt is primarily intended to prevent local welding between the piston and the cylinder, the piston seizing. A risk of seizing exists under extreme operating conditions, such as

: lack of local clearance, caused by mechanical and/or thermal deformation of the cylinder
: lack of clearance due to thermal overload of the piston
: insufficient oil supply, such as during a cold start
: insufficient lubrication capability of the engine oil, caused by fuel contamination in the oil, extremely high operating temperature, or excessive aging of the oil, during a cold start and during late injection for exhaust gas treatment
: ”green” engine, when the piston, rings, and cylinder have not yet been run in.

In a series of tests, using a piston profile that has a risk of seizing and by reducing the installation clearance of the piston, such an extreme situation is created deliberately. The friction mean effective pressure for coated and uncoated pistons is compared for fired operation in each case, until the uncoated piston seizes.

The friction mean effective pressure for three different loads is plotted against the installation clearance in ❷. It is evident that the minimum friction results at an installation clearance of about 120 µm. With increasing installation clearance, the friction mean effective pressure increases again, due to more significant secondary piston motions, with greater tip angles. The friction mean effective pressure also increases again as the installation clearance is reduced. This increase in friction mean effective pressure can be traced to lower hydrodynamic proportions and greater mixed friction proportions for the piston skirt.

Starting from the full-load operating point 2, the advantages of a piston skirt coating can be demonstrated strikingly. With the coating, under identical operating conditions, the friction mean effective pressure of the engine (measured without auxiliaries) can be reduced by up to 8 %; see operating point 3. If the focus is not on reducing friction losses, but on the requirement to have smaller installation clearances, then the present example also demonstrates this potential. For the same friction mean effective pressure, a skirt coating allows significantly lower installation clearance while providing the same assurance with respect to seizure resistance; operating point 4. ② shows clearly that the effect of the skirt coating on frictional power increases greatly with low clearances.

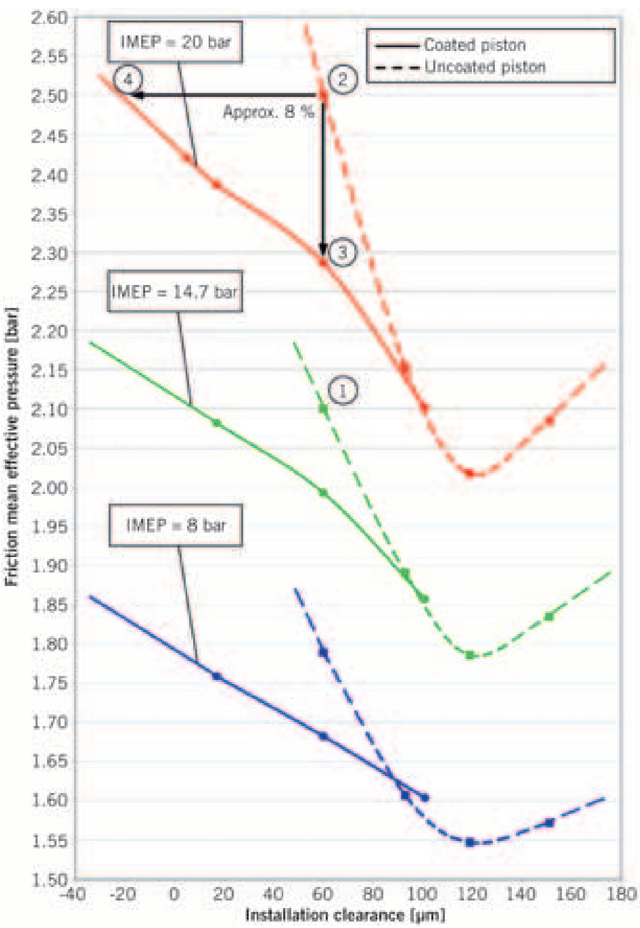

❷ Effects of installation clearance and skirt coating on friction mean effective pressure; engine temperature 90 °C, speed 4000 rpm

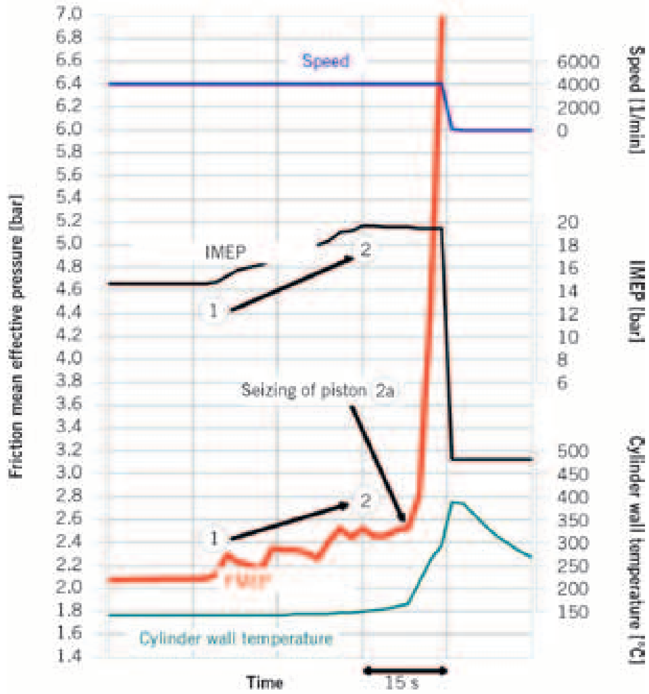

❸ Friction power loss measurements as piston seizure occurs

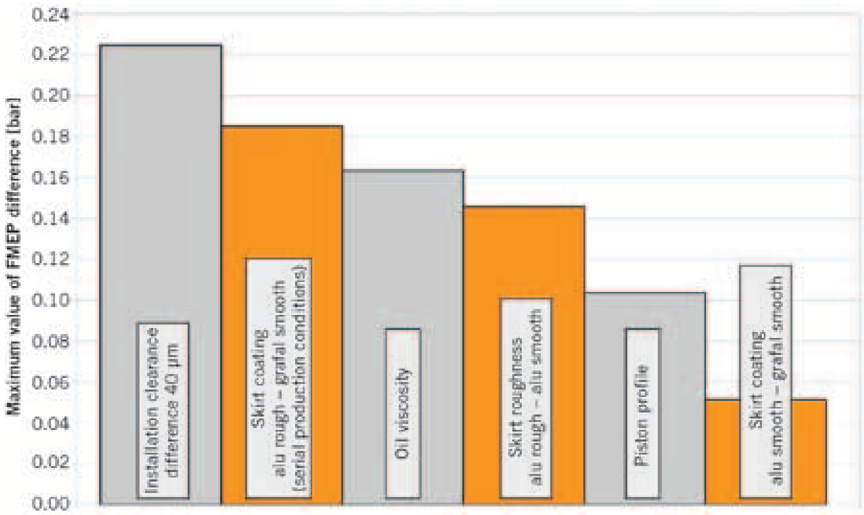

❹ Maximum values from friction mean effective pressure difference maps, at an engine temperature of 90 °C – the values are taken in the run-in state

In ② and ❸, 1 indicates a partial load operating point, running without a skirt coating. If, starting from this operating point, the load is increased further at a constant speed (operating point 2), this leads to increased thermal and mechanical loads on the piston, and thus to a reduction in operational clearance. With the uncoated piston, this leads to piston seizing after running for only a short time. This is indicated by an extremely large increase in friction mean effective pressure and in the cylinder wall temperature.

SKIRT ROUGHNESS

The extent to which a reduction in friction power loss can be attributed to the surface roughness of the skirt, and the extent to which it can be attributed to the coating material, is shown in ❹.

The previously demonstrated difference in friction power loss with and without coating is based on the different serial production conditions "rough aluminium" and "smooth Grafal," which have very clear differences in surface roughness in run-in condition. If the parameter of skirt roughness is investigated in isolation, then it can be seen that even aluminium with a smooth surface leads to lower friction losses. A direct comparison of coated and uncoated piston skirts, with comparably smooth surfaces, indicates only a slight potential for improvement. The appreciable advantage of a coating can therefore be attributed to the change in surface roughness. This result leads to the conclusion that the friction on the piston skirt can be chiefly improved by increasing the hydrodynamic proportion, and less so by the coating material and its coefficient of friction.

NEW PISTON COATING

The side loads on the piston skirt increase as engines are subjected to higher loads (downsizing), therefore future skirt coatings must provide improved wear resistance in the tribological system of the piston/cylinder bore, over the entire lifespan of the engine, without increasing friction losses in the engine.

In order to be able to meet these requirements, several skirt coating materials were tested for suitability. External engine tribometer testing as well as engine friction and wear measurements were used. The specifications of the tested coatings are summarized in ❺.

The results obtained are shown in ❻. The two top bar charts show results from external engine tribometer tests, and the

COATING TYPE	BASE RESIN	SOLID LUBRICANT	PROPORTION IN THE COATING	WEAR-RESISTANT ADDITIVES
Grafal 255	Polyamide-imide	Graphite	Approx. 35 %	No
Evo Glide	Polyamide-imide	Graphite	Approx. 35 %	Yes
Molykote D-6024	Polyamide-imide	MoS_2	Approx. 45 %	No
		Graphite	Approx. 5 %	

❺ Coating specifications: all coatings consist of solid lubricant particles dispersed in resin, and are printed onto the piston skirt and cured

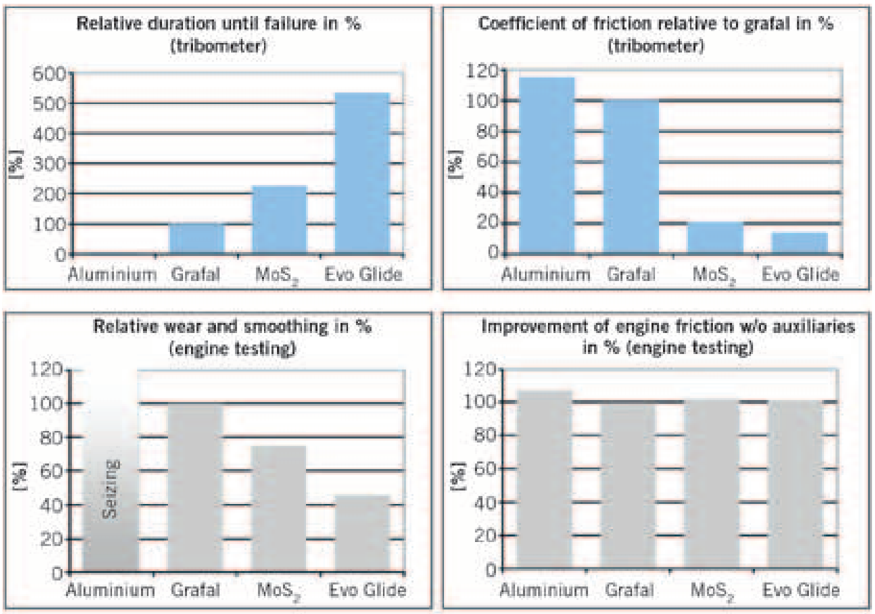

❻ Results for friction and wear from tribometer testing, compared to results from engine tests (averaged over the operating map)

❼ Derived friction mean effective pressure difference map for fired engine operation, using Grafal and Evo Glide as a skirt coating

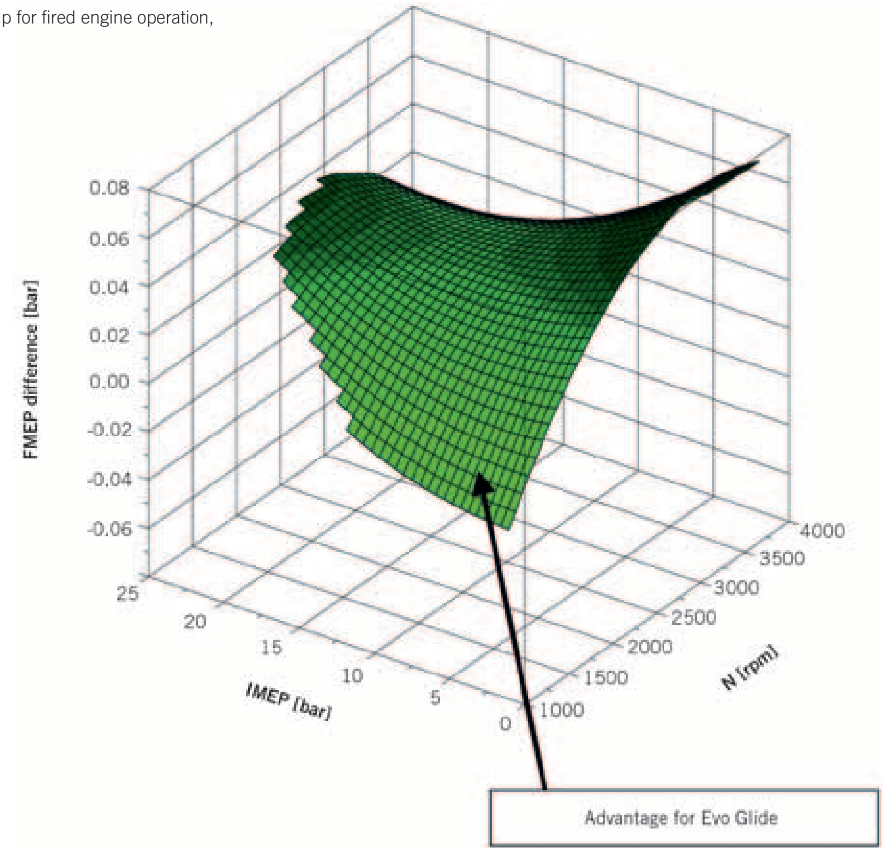

two bottom charts show those from engine testing.

Three different skirt coatings were tested in the tribometer tests, using a grey cast iron test body as a frictional partner. The elapsed time until failure of the coating in the unlubricated condition was used as the measurement variable. In addition, the coefficient of friction of the friction pairs is determined for the lubricated state after a certain run-in period. Here it is evident that only a moderate improvement in the coefficient of friction, relative to an uncoated aluminium skirt, can be obtained with a typical graphite skirt coating. The coating containing MoS_2 and the new Evo Glide coating, in contrast, achieve a coefficient of friction that is many times lower.

Because these material characteristic values obtained from external engine test benches only insufficiently represent the real conditions in the engine, the coatings were further tested in a fired engine run for wear resistance and friction power performance. The wear and smoothing of the various coatings after a defined period of time are shown at the bottom left of ⑥. They were determined using roughness measurements over the entire skirt length, at several different defined locations on the piston skirt, and therefore represent an integral value for the skirt. In case of wear, the result from the tribometer tests can be reproduced very well, and the same ranking order is evident. ⑥, at the bottom right, shows additionally the friction power loss savings potential of the various skirt coatings, as determined in the engine. Therefore the friction mean effective pressures for each variant are integrated over the entire engine operating map and shown in comparison. The large change in the friction coefficient of the MoS_2 coating and the Evo Glide coating from the tribometer tests cannot be reproduced in the engine. This leads to the presumption that the piston skirt appears to run under largely hydrodynamic lubrication conditions in normal engine operation.

FRICTION MEAN EFFECTIVE PRESSURE DIFFERENCE MAPPING

⑥ shows that all of the piston coatings tested – averaged over the operating map – are at the same level of friction. A closer examination of the friction mean effective pressure difference map, however, shows that the different coatings can be associated with slight advantages that depend upon the operating point. The MoS_2 coating, for example, shows slight advantages at higher speeds and loads. The Evo Glide coating, on the other hand, shows advantages more in the range of the operating points relevant to the fuel consumption cycle, ❼.

CONCLUSION

With new coating materials on the piston skirt, improvements in wear behaviour can be achieved, particularly in highly loaded engines. For the case of suitable combinations of the new coating materials with design measures, such as clearance, piston profile, and piston skirt roughness, additional friction power loss potentials can be opened up that would have been considered insignificant just a few years ago.

REFERENCES

[1] Deuß, T.; Ehnis, H.; Freier, R.; Künzel, R.: Reibleistungsmessungen am befeuerten Dieselmotor – Potenziale der Kolbengruppe. In: MTZ 71 (2010) No. 5, p. 326-330
[2] Mahle GmbH (Hrsg.): Produktkunde Kolbensysteme: Kolben und motorische Erprobung. Vieweg+Teubner, 1. Auflage 2010

THANKS

The authors would like to thank Dipl.-Ing. Rudolf Freier for his effort on this article.

VARIABLE FLOW SPUR GEAR OIL PUMP FOR UTILITY VEHICLE ENGINES

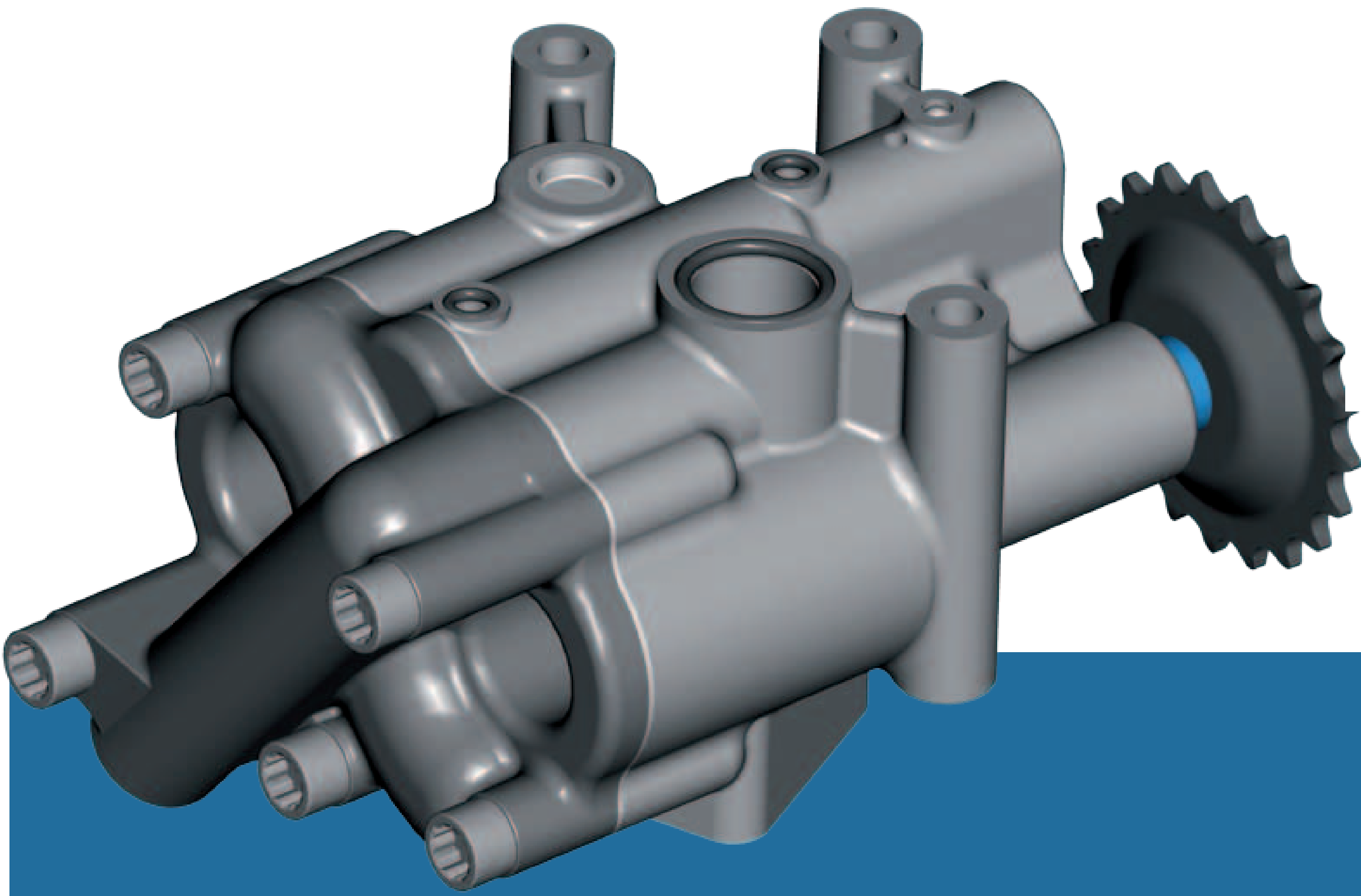

By the use of variable flow oil pumps for the lubricating of internal combustion engines advantages in fuel consumption and CO_2 emission of up to 3 % can be achieved. While variable flow oil pumps increasingly can be find in passenger car engines, in future this trend might spread also to utility vehicle engines. Therefore IFM Motorentechnik has developed a new variable flow oil pump to meet the specific demands of utility vehicle engines.

AUTHOR

DIPL.-ING. DIETER VOIGT
is Owner of IFM Motorentechnik
in Braunschweig (Germany).

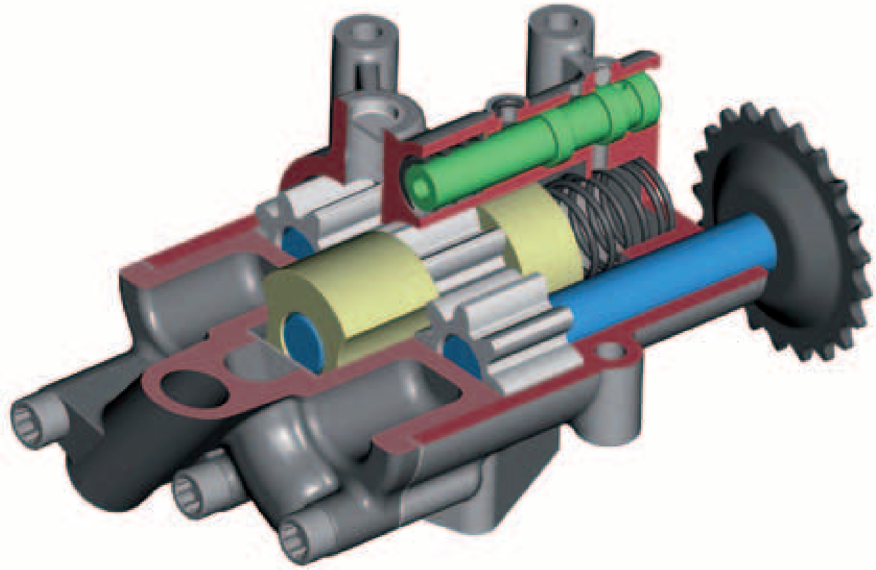

❶ Two step variable flow oil pump

OBJECTIVE

Based on long-standing developing experiences in variable flow oil pumps [1] for passenger car engines the objective was to develop a variable flow oil pump for utility vehicle engines. Utility vehicle engines are almost exclusively diesel engines and differ from passenger car engines essentially by bigger displacements and higher cylinder figures. They have a maximum engine speed of 3000/min and are mostly operated in continues working. Variable flow oil pumps for utility vehicle engines must correspond to these demands and must work in particular about a long durability.

The well known constructions of variable flow oil pumps of passenger car engines, like spur gear pumps [2, 3], "Pendelschieber" pumps [4, 5] and vane cell pumps [6, 7], are basically also usable for utility vehicle engines. After comparing their specifically usability for utility vehicle engines finally the conception of a variable flow spur gear pump with two delivery units was pursued, which promises advantages concerning complexity, production costs and wear resistance.

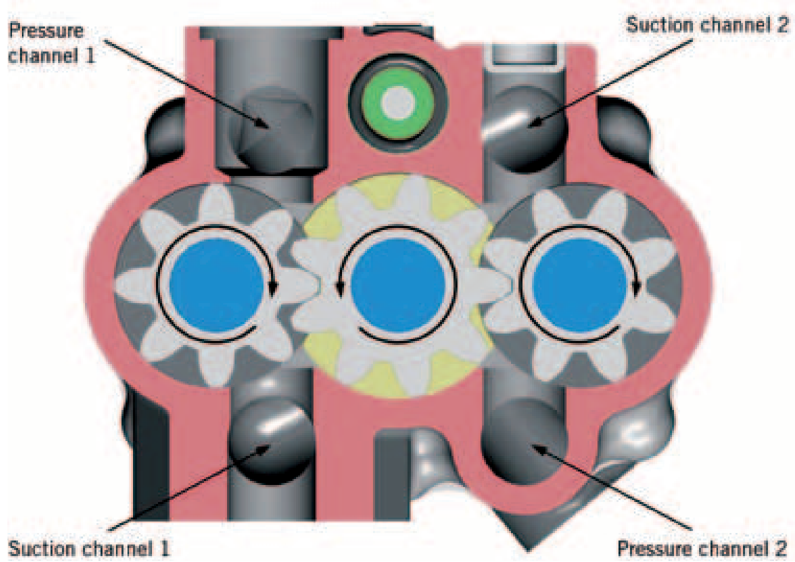

❷ Sectional view onto the gearwheels

PUMP DESCRIPTION

The conception of the variable flow spur gear pump has two parallel working delivery units with a total of only three gearwheels. With a size interpretation for small utility vehicle engines a compact pump building was designed, which is shown in ❶. The middle one of three side by side located gearwheels is part of a sliding unit, which is movable in the pump housing by oil pressure against a spring and a regulating pressure in the spring chamber. By the variable axial adjustment of the middle gearwheel relative to both other gearwheels the oil flow quantity can be varied. A control piston, positioned above the sliding unit, controls the regulating pressure in the spring chamber. Deviations to the requested engine oil pressure level are corrected automatically by the control piston by a suitable adaptation of the oil flow quantity.

The cover of the pump housing connects by two channels, ①, the suction and the pressure sides of the two pump units. For these connections via the cover the pump housing has two suction channels and two pressure channels, as shown in the sectional view in ❷. As a result of the different rotation directions of the three gearwheels the pressure sides of both delivery units are in diagonally opposite positions, and the suction sides too. The oil pressure creates radial forces from both pressure sides onto the sliding unit, but they are compensating themselves. This leads to a minimal friction between the movable sliding unit and the pump housing. By this advantage on the one hand a high precision for oil pressure regulation is achieved and on the other hand the wear between the sliding unit and the pump housing is minimized for a long pump durability. A rise in pump life time is caused too by using different gearwheel cog numbers with eight cogs for both external gearwheels and nine cogs for the middle gearwheel for alternating cog interventions.

Caused by small sizes of the pump gearwheels a relative high pump speed is realizable without any cavitation problems. Therefore the engine driven pump can be operated by a chosen pump transmission ratio of 1.8 in speedy translation. The relative high pump speed combined with two pump delivering units lead to a high pump flow quantity.

Both connected pump delivering units suck in the oil below suction channel 1, while above pressure channel 1 the oil flows to the engine. Alternatively both pump delivering units could supply their oil flow via two pressure channels to different oil systems, for example for separated crankshaft and valvetrain lubrication. A survey of the main technical data of the variable flow oil pump:

: pump construction: spur gear / 2 delivering units
: module: 3.5
: number of gearwheels: 3
: cog numbers: 8 / 9 / 8
: gearwheel length: 25 mm
: pump flow quantity: 26.6 cm³ / rev
: pump transmission ratio: 1.8.

Oil pressure regulation by varying the oil flow quantity can be done by different regulation systems. For the utility vehicle oil pump a two-step pressure regulation by a control piston was chosen like used in passenger car engines [2, 7]. This achieves appreciable fuel consumption advantages with only low expenditure. Furthermore by the control piston about the whole engine lifetime a constant oil pressure level is guaranteed, independent of increasing oil flow quantity caused by more and more engine wear. Therefore the oil pressure level can be adjusted relatively low with increased advantages in fuel consumption. For the two-step pressure regulation the control piston is pressure acted on two surfaces, on the first surface permanent and on the second surface switchable by a magnetic valve. This electrically easiest changeable engine oil pressure allows for example a general pressure level at 3.5 bar and a reduced pressure level at 2 bar for maximum fuel reduction at low engine speed. Utility vehicle engines predominantly operated in the upper engine speed range do not need the two-step regulated oil pressure level. That causes cost and complexity advantages by cancelled electric components without appreciable fuel consumption disadvantages.

TEST OPERATION

A prototype of the oil pump, ①, was produced and tested on a pump test bench. For the simulation of a realistic engine oil flow rate at cold and warm conditions in the test temperature range between 20 °C and 100 °C, the test bench oil cycle used an especially developed flow resistor. The measured pressure behind a filter module in the test bench cycle was used as the "engine oil pressure" for acting the pump regulation. The pump was operated directly driven by an electric motor up to a maximum pump speed of 5000/min. For result evaluation the engine speed later was calculated by the factor 1.8 of the simulated transmission ratio.

At first the variable flow oil pump was tested for generally checking up the pump functions. Then the two-step pressure regulation system, switched by a magnetic valve, was optimized. The nearly frictionless adjustment of the movable sliding unit led to a very sensitive pressure regulation with high ability for reproduction.

For evaluation the improvement potential, finally the variable flow oil pump was also operated as a simulated constant flow oil pump with full oil flow by a blocked sliding unit and manual adjusted bypass pressure regulation.

PRESSURE REGULATION AND OIL FLOW

The two-step switchable engine oil pressure levels are shown in ❸ above the engine speed. Orientated to a linearly rising pressure demand the electrically switched E1/E2 pressure change-over between the

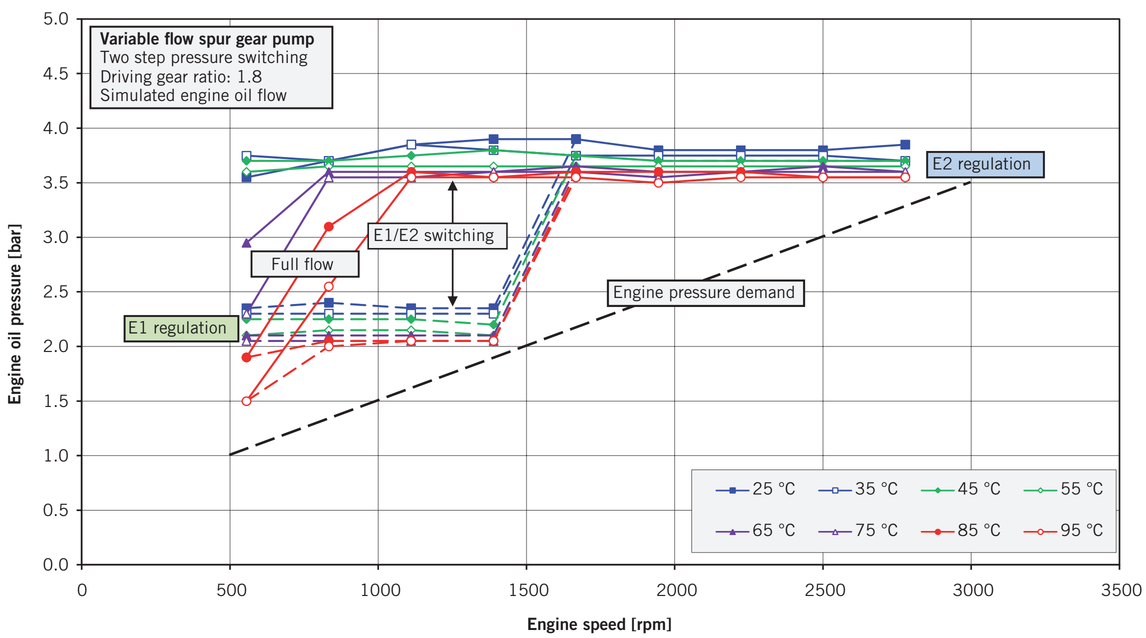

❸ Engine oil pressure

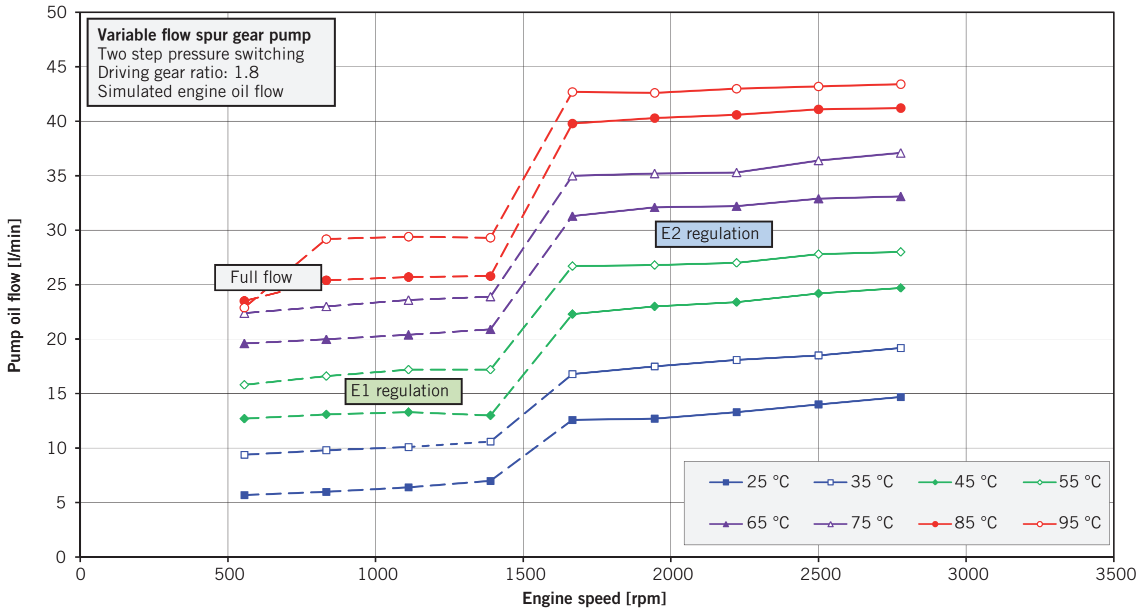

❹ Pump oil flow

elected pressure levels of 2 and 3.5 bar was chosen at 1500/min. Because the pressure regulating control piston works as a pressure sensor, the engine oil pressure is only minimal influenced by the oil temperature. Near engine idling and above 90 °C the variable flow oil pump works at full oil flow, so the not more increasable engine oil pressure drops under the E1 pressure level, but remains above the engine pressure demand. If necessary later with real engine oil supply the maximum pump oil flow must be increased to guarantee enough oil pressure at hot idling. At more pressure demand, for example to activate piston cooling, the engine oil pressure can be raised in the lower engine speed range also to the E2 pressure level.

In ❹ the pump oil flow, dependent on the simulated engine oil flow resistance, is shown for the two-step pressure regulation. While at the E2 pressure level and 95 °C the oil flow amounts 44 l/min, the oil flow decreases at the E1 pressure level and higher oil viscosity at 25 °C up to nearly 5 l/min. Near idling and above 90 °C due to the chosen pump size the oil flow decreases and causes a reduced engine oil pressure, like shown in ③.

PUMP DRIVING POWER

Substantially for the aimed fuel consumption advantage of variable flow oil pumps is their reduced pump driving power by the engine compared to conventional constant flow pumps with bypass regulation. This advantage in pump driving power of the tested prototype is shown in ❺. For

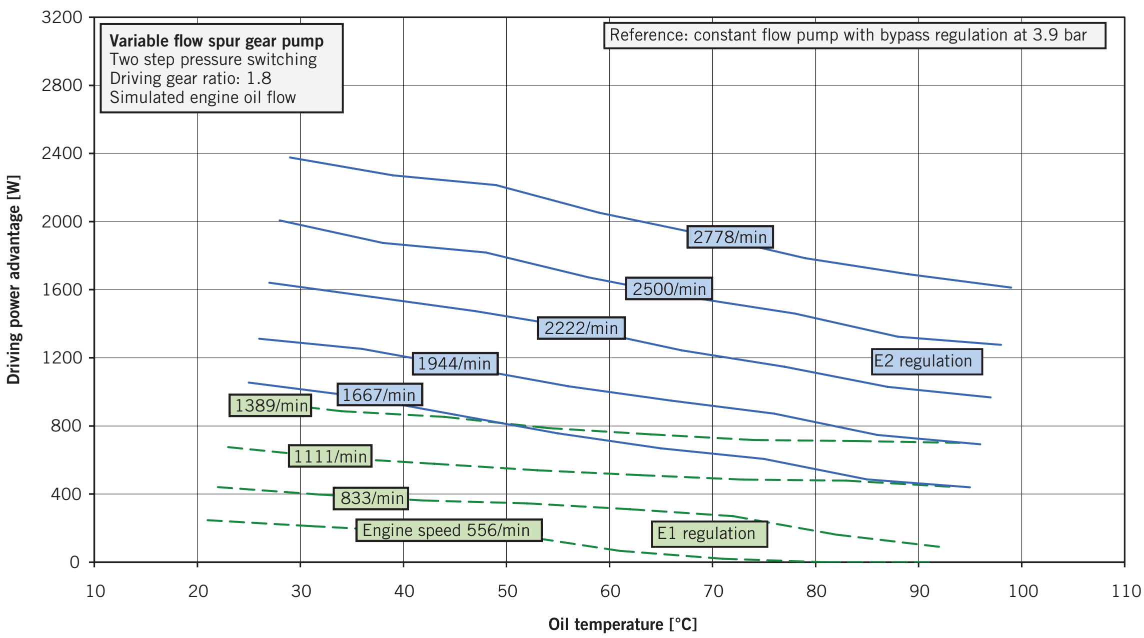

❺ Advantages in pump driving power

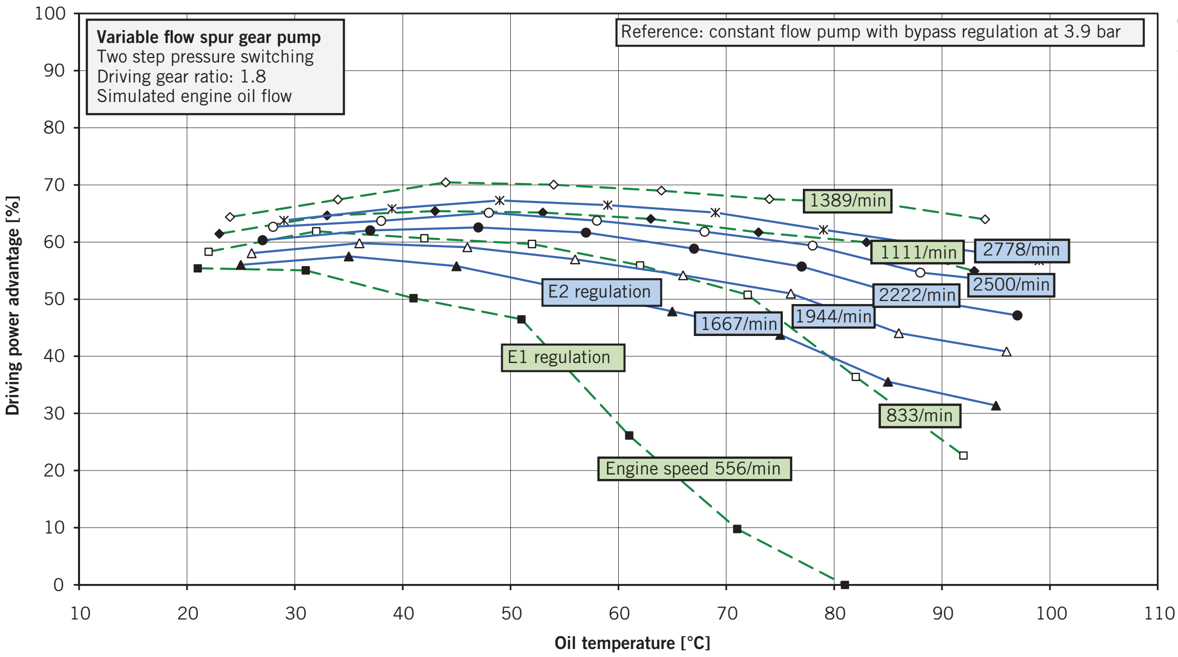

❻ Proportional advantages in pump driving power

this comparison the simulated constant flow pump was manual bypass regulated at a pressure of 3.9 bar. Depending on engine speed and oil temperature the advantages in pump driving power are up to 2.4 kW. The pressure reduction to the E1 pressure level in the lower engine speed range causes raised advantages in pump driving power, what is expressed by the partial overlapping of the E1/E2 characteristic curves.

Evident in the proportional representation of the advantages in pump power input in ❻ is, that the two-step pressure regulation of the variable flow oil pump leads to advantages between 50 and 70 % compared with a conventional constant flow pump. Nevertheless at low engine speed and higher temperatures these advantages decrease, and latest at hot idling with full oil flow the advantage of the variable flow oil pump drops to zero. These proportional advantages in pump driving power of the tested variable flow oil pump are also be expected for bigger utility vehicle engine/pump interpretations.

SUMMARY

The prototype tested variable flow spur gear oil pump with two delivery units is a compact pump construction, which recommends itself by easy to manufacture pump parts and high wear resistance for application in utility vehicle engines. While for engines operating mostly in the upper engine speed range a constant level pressure regulation is already advantageous in fuel consumption, the more improvement potential of a two-step pressure regulation can be used for engines often operating in the lower engine speed range. Compared with conventional constant flow oil pumps with bypass regulation pump driving power advantages of up to 70 % are achievable by using variable flow oil pumps. This advantages lead to a higher engine power as well as reductions in fuel consumption and CO_2 emissions. The increasingly application of variable flow oil pumps in passenger car engines can be expected also for utility vehicle engines in future.

REFERENCES

[1] Voigt, D.; Kraftstoffverbrauchsvorteile durch Regelölpumpen. In: MTZ 64 (2003), No. 12, p. 1050
[2] Böhme, J.; Fröhlich, G.; Dornhöfer, R.; Grigo, M.: Der neue 1,8-l-TSFI-Motor im Audi A4. In: ATZ/MTZ extra 9/2007, p. 72
[3] Neußer, J.: Die neuen 4,8-l-V8-Ottomotoren von Porsche mit Benzindirekteinspritzung und variabler Ventilsteuerung. In: MTZ 68 (2007), No. 12, p. 1018
[4] Klüting, M.; Landerl, C.: Neuer Sechszylinder-Ottomotor von BMW. In: MTZ 65 (2004), No. 11, p. 868
[5] Jensen, H.; Janssen, M.; Beez, G.; Cooper, B.: Kraftstoffeinsparpotenzial der geregelten Pendelschieberpumpe. In: MTZ 71 (2010), No. 2, p. 104
[6] Bauder, R.; Bach, M.; Köhne, M.; Streng, C.; Hoffmann, H.; Rossi, D.: Der neue 3,0-l-V6-TDI-Motor im Audi Q5. In: ATZ extra 6/2008, p. 36
[7] Doll, G.; Waltner, A.; Lückert, P.;Kemmler, R.: Der neue 4,6-l-V8-Ottomotor von Mercedes-Benz. In: MTZ 71 (2010), No. 10, p. 670

J624 – WORLD'S FIRST GAS ENGINE WITH TWO-STAGE TURBOCHARGING

Stationary gas engines are an important part of decentralized energy supply. This is because of their low emissions, a high level of availability, the large fuel flexibility – and their high efficiency. GE's new J624 for instance, the world's first two-stage turbocharged gas engine, achieves an electrical efficiency of 46.5 %.

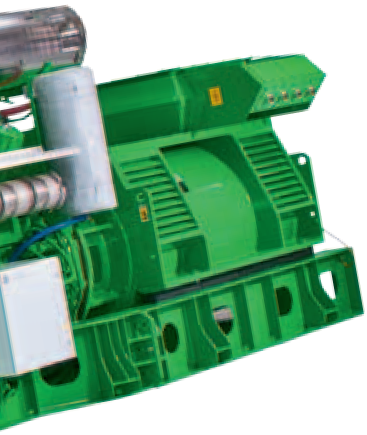

AUTHORS

DIPL.-ING. JOHANN KLAUSNER
is Senior Engineer Charging and Charge Exchange at the Jenbacher Gas Engine Division of General Electric Corporation in Jenbach (Austria).

DIPL.-ING. JÜRGEN LANG
is responsible for Charge Exchange within the Thermodynamics Department at the Jenbacher Gas Engine Division of General Electric Corporation in Jenbach (Austria).

DR.-ING. CHRISTIAN TRAPP
is Head of Thermodynamics at the Jenbacher Gas Engine Division of General Electric Corporation in Jenbach (Austria).

GAS ENGINES MEET STRINGENT EMISSION STANDARDS BY ENGINE MODIFICATIONS

For years gas engines have been gaining importance within the global energy mix. One reason for that is the comparatively good, long term availability of natural gas, combined with the option to burn special gases, such as biogas, landfill gas, coal mine gas or steel gases, while maintaining a high level of efficiency. In addition to that GE's Jenbacher gas engines meet the most stringent emission standards, for example the German Technische Anleitung Luft (TA Luft). This makes large gas engines a comparable cleaner technology for supplying electricity and heat around the globe as part of a decentralized structure.

The ambient conditions, ranging from the temperate latitudes to arctic areas and to a hot and humid tropical atmosphere, pose very high requirements to engine robustness: Annual operating time can be as long as 8000 hours with an availability of over 95 % for a very long lifetime mostly under full load conditions. Jenbacher gas engines fulfill these requirements along with the most severe emission standards despite varying gas quality and gas composition. In accordance with TA Luft 2002 the engine emission level is warranted to be ≤ 500 mg of nitrogen oxides (NO_x) per Nm³ and an even more severe ≤ 250 mg/Nm³ (at 5 % O_2 in the exhaust gas) for densely populated areas. Currently a suggestion is being discussed within the EU to lower this limit to a maximum of 200 mg/Nm³ NO_x. In contrast to the diesel engine, future gas engines will continue to be able and meet these challenging standards without exhaust gas after treatment.

For more than 50 years GE's Jenbacher gas engine division has been developing solutions for the never-ending list of new technological challenges to stationary gas engines and is thus driving technology forward. The latest product is the two-stage turbocharged 24-cylinder lean burn engine J624, ❶. It produces 4.4 MW of electric power and reaches an electrical efficiency of 46.5 % by combining a set of blocks featuring new technology.

TECHNOLOGICAL TRENDS

The GE's type 6 gas engine provides a perfect historical trend of how highly effi-

	P_{el}	η_{el}	η_{tot}	LENGTH	WIDTH	HEIGHT	WEIGHT GENSET
50 Hz	4400 kW	46.5 %	89.0 %	12 m	2.5 m	2.9 m	44 t
60 Hz	4360 kW	46.0 %	88.5 %	14 m	2.5 m	2.9 m	47 t

❶ Technical data of the two-stage turbocharged 24-cylinder lean burn engine J624 Methan number > 80, 500 mg/Nm³ NO_x

cient gas engines developed: By increasing the brake mean effective pressure (BMEP) in combination with a continuous improvement of combustion and optimization of the charging as well as the charge exchange process, the electrical efficiency (η_{EL}) of the generator set could be increased from an original 38 % in 1994 (at 12 bar BMEP) to 45.6 % in 2009 (at 22 bar BMEP) while always meeting TA Luft.

The new J624 with two-stage turbocharging, portrayed in this paper, has an η_{EL} of 46.5 % and produces 4.4 MW (at 24 bar BMEP). It follows the same general path of development. However, new technology blocks are combined to push the limits of current serial engines. The road to far advanced Miller valve timing and the optimized lean-burn combustion process, enabling highest efficiency levels and lowest NO_x emissions, was paved by two-stage turbocharging, ❷.

Combined with the optimized Moris high energy ignition system along with refined control strategies and algorithms, these technology blocks facilitate a sufficiently wide operating band between the knock and misfire limits. In particular they make operation possible at high altitudes and under tropical hot conditions without compromising efficiency.

ENGINE AND CHARGING

The new J624 is based on a modular build consisting of the three units base engine, turbocharger auxiliary module, and the generator. Like all previous GE's Jenbacher gensets, the new engine runs at 1500 rpm to generate a grid frequency of 50 Hz.

The J624 version of the type 6, which had gone into customer operation in 2009, provided the basis for development work. Up to that point it was the GE's Jenbacher gas engine with the highest electrical output of 4 MW. Type 6 engines work with exterior mixture preparation, which is done in a gas mixer located before the compressor, and with Miller valve timing plus a lean-burn combustion process with a gas-enriched pre-chamber.

To further increase the power and efficiency while improving the potential for bringing down nitrogen oxide emissions technology blocks had to be developed which would facilitate a substantial increase of the air-fuel ratio λ and a reduced knock tendency despite higher compression and higher specific power.

Far advanced Miller valve timing reduces the knock tendency, however, it also increases the required charge pressure beyond the level needed for the increased λ.

Using single stage charging the required compression ratio of considerably > 6 would have been just about achievable with special turbocharger technology. But even so the turbocharger efficiency would have dropped dramatically to a value of under < 60 % which would have offered no buffer for future improvements. Therefore the decision was made to develop a two-stage turbocharging which offers a potential peak pressure level of up to 10 bar at a charging efficiency of > 73 %.

The newly developed charger module consists of a low-pressure compressor with subsequent intercooling, a high-pressure compressor with mixture cooling and the corresponding high- and low-pressure turbocharger turbines on the exhaust side, ❸. Power control of the engine is done via a compressor by-pass. All three possible by-pass options – by-passing both compressors, high-pressure compressor by-pass, and low-pressure compressor by-pass – were analyzed during the early development phase together with the optimum design of turbine and compressor wheels.

The optimum realization of the two-stage turbocharging not only provides the required pressure level in the intake pipe to facilitate far advanced Miller valve timing but it also provides the necessary pressure differential of 1000 mbar between inlet and outlet side. To avoid scavenging losses caused by mixture charging (HC emissions and loss of efficiency) the valve timing was further optimized, particularly during the overlap phase, to find a trade-off between flushing (residual gas level) and HC-slip.

Closing the inlet valves very early leads to a charge expansion and re-compression in the cylinder which considerably brings down the compression end temperature and the temperature in the end zones and thus the knock tendency. The valve timing of the new J624 is defined to avoid knock during the entire engine lifetime despite a maximum permissible mixture temperature after the intercooler of above 70 °C and despite 24 bar BMEP, and varying gas fuel quality.

This high temperature level in the intake system avoids mixture condensation even under tropical conditions and thus allows to achieve full efficiency and power at ambient temperatures of over 40 °C, given a suitable design of the turbo chargers.

In addition the heat from the mixture cooler can be dumped by much smaller horizontal air coolers under the above

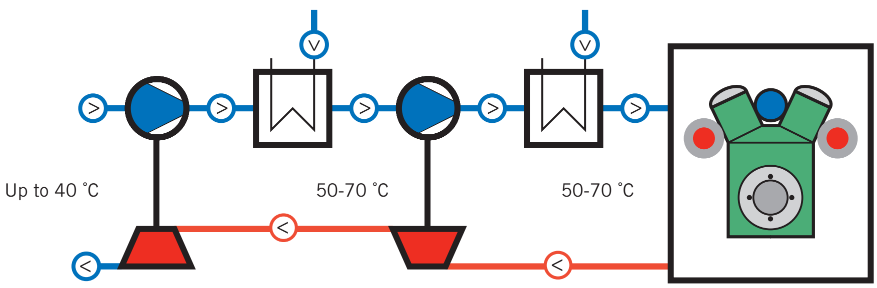

❷ Principle design of the two-stage turbocharging and intercooling mentioned tropical conditions and without the need for a cooling tower. In a combined heat and power installation this heat can be fed into the heat circuit and can help to increase the overall plant efficiency to more than 90 %.

The new J624 combustion process is based on burning a lean mix in combination with a gas-enriched pre-chamber. The very lean mixture ($\lambda > 2$) in the main combustion chamber is ignited by the flame jets emerging from the pre-chamber, which ensures a complete combustion. Within the pre-chamber the lean mixture, which is enriched by additional gas, is ignited by a special spark plug that ensures ignition even at 60 bar firing pressure. This combustion process and in particular the tuning of flame orifice channel shape, charge movement, piston and pre-chamber design had to be newly developed to warrant an optimum combustion timing and a complete combustion even under very lean conditions, ❹. The new J624 development was completed by more sophisticated and improved control strategies and algorithms which mostly serve to control power, knock and emissions, but which are still based on the Leanox concept's patented approach.

DEVELOPMENT METHODOLOGY

It takes a lot to keep up or even exceed the high level of quality during a new development while pushing previous limits at the same time: On top of 50 years of experience a powerful and reliable development methodology is also needed, ❺. It integrates the various tools and methodologies, such as databases, simulation processes and tests, in a simultaneous engineering process.

❸ The turbochargers in the auxiliaries module; the arrow indicates the exhaust flow

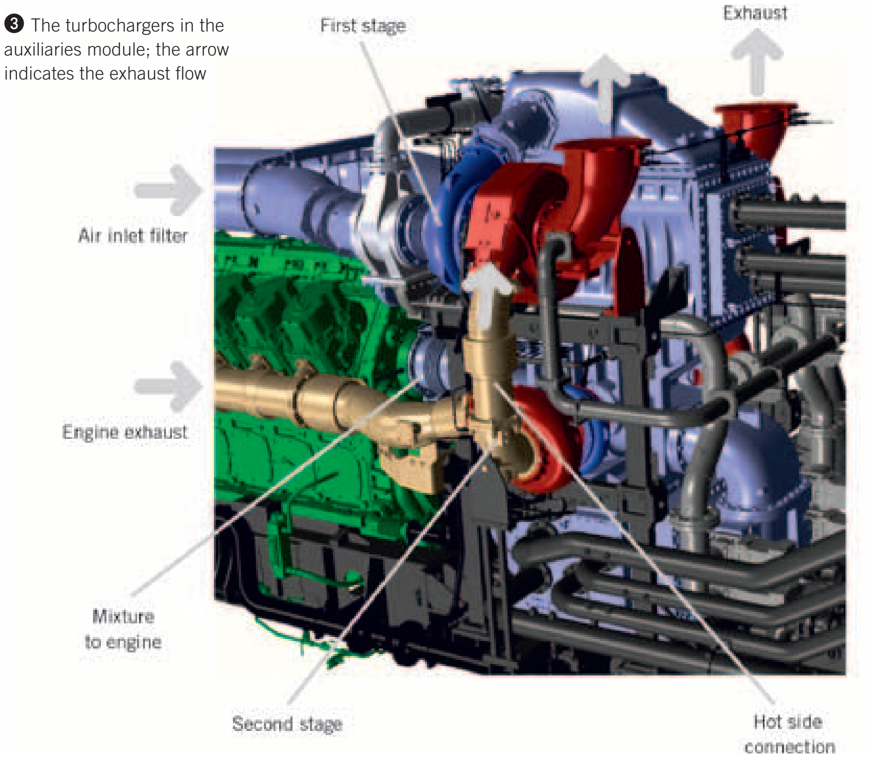

The beginning of any development is formed by analyzing requirements in detail, which in turn is based on a profound understanding of customer requirements and legal standards around the world. These are driven down from the product level to functions, systems, and sub-systems, right to the individual component. During this the engine base design is defined, a process that draws on databases, experience with similar types, competition analyses, working-process calculation as well as 1D flow simulation. As early as in the first concept stage the most important target parameters of the engine, such as power, efficiency, emissions, but also cost, have to be modeled with sufficient precision to be able and evaluate the influence of operating conditions, gas quality, plus engine and systems concepts.

During the next step the concepts are described in more details via more powerful simulation, such as 3D in-cylinder flow and combustion, FEA analyses, single cylinder engine testing and component testing. Along with the progress more and more test results either confirm or replace the simulation data. Within the detail design phase the final engine construction is defined and the individual component design is simulated with a focus on service-life considerations. Full engine test-

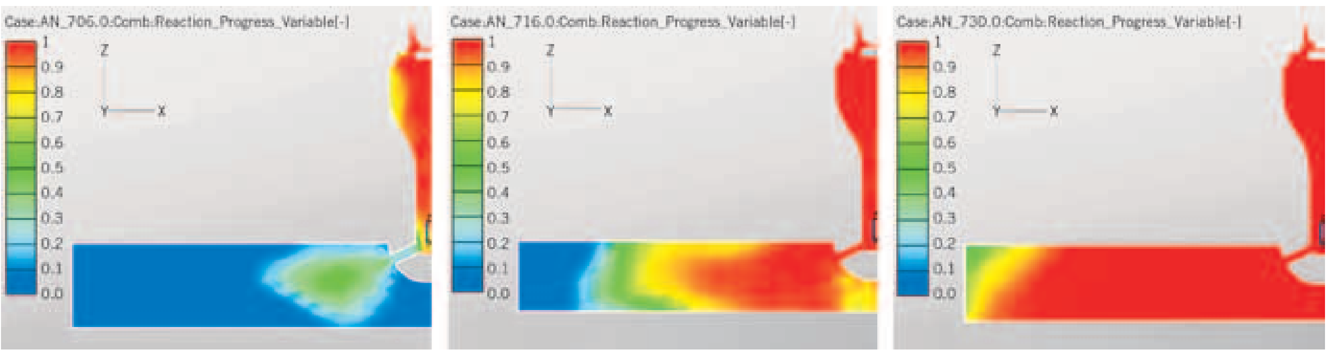

❹ Flame progress of the combustion and level of burn-out

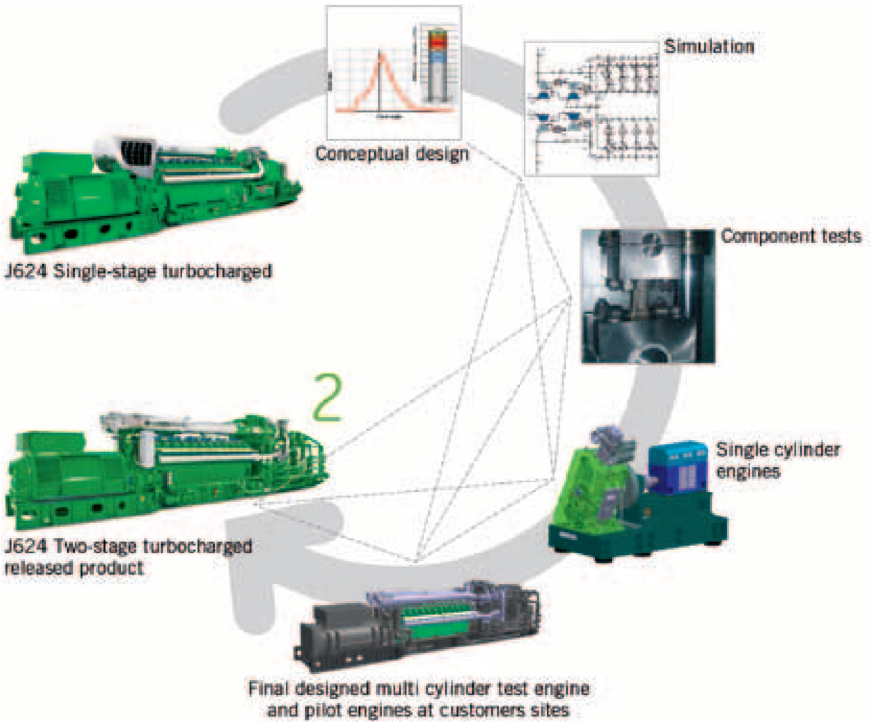

❺ Schematic view of the development methodology

ing, which serves to optimize systems and components, forms the transition from the development phase to validation. It is now, that the engines have to demonstrate their readiness for production on the test beds. Finally, pilot customers together with the development teams carry out the ultimately decisive field testing. Only after this phase a new product such as the new J624 gets approval for serial production.

SUMMARY AND OUTLOOK

After many years of continuous improvements, there is still potential for stationary gas engines. An intelligent combination of innovative technology blocks with two-stage turbocharging at their very core makes it possible to push previous limits even further: Higher brake mean effective pressures, higher levels of efficiency and wider operating areas. However, only by simultaneously optimizing, charge exchange, valve timing, combustion process and control strategy, these potentials can be utilized. The new J624 underpins this with an electrical efficiency of 46.5 % at 4.4 MW power while meeting TA Luft emission requirements in an impressive way. This makes it the starting point of a new generation of GE engines.

Within the near future this will facilitate efficiency levels close to the 50 % threshold with NO_x emissions > 200 mg/ Nm³ (5 % O_2-level) while maintaining the robustness and reliability which GE's Jenbacher gas engines have been demonstrating for decades.

REFERENCES

[1] Wimmer, A.; Redtenbacher, C.; Trapp, C.; Klausner, J.; Schaumberger, H.: Aktuelle Herausforderungen bei der Entwicklung von Brennverfahren für Großgasmotoren. 1. Rostocker Großmotorenkonferenz 2010

[2] Trapp, C.; Klausner, J.; Schaumberger, H.; Haidn, M.; Lang, J.: Der Gasmotor der Zukunft – innovative Brennverfahren und Hochdruckaufladung für höchste Wirkungsgrade. CIMAC World Congress 2010, Bergen

[3] Trapp, C.; Klausner, J.; Haidn, M.; Lang, J.: Zweistufige Hochdruck-Turboaufladung für Gasmotoren mit hohem Wirkungsrad. Aufladetechnische Konferenz 2010, Dresden

MEASURING METHOD FOR EXHAUST GAS TURBOCHARGER WITH PULSATING HOT GAS FLOW

The exhaust gas turbocharger is an effective device for reducing fuel consumption by shifting the operating point to operating points of better efficiency. To provide the largest possible enthalpy to the turbocharger turbine, exhaust systems are extremely compact. Thus, the turbocharger and the internal combustion engine have to be optimally matched. Continental and the University of Applied Sciences Ravensburg-Weingarten present a new method which measures turbocharger characteristics under engine-relevant operating conditions.

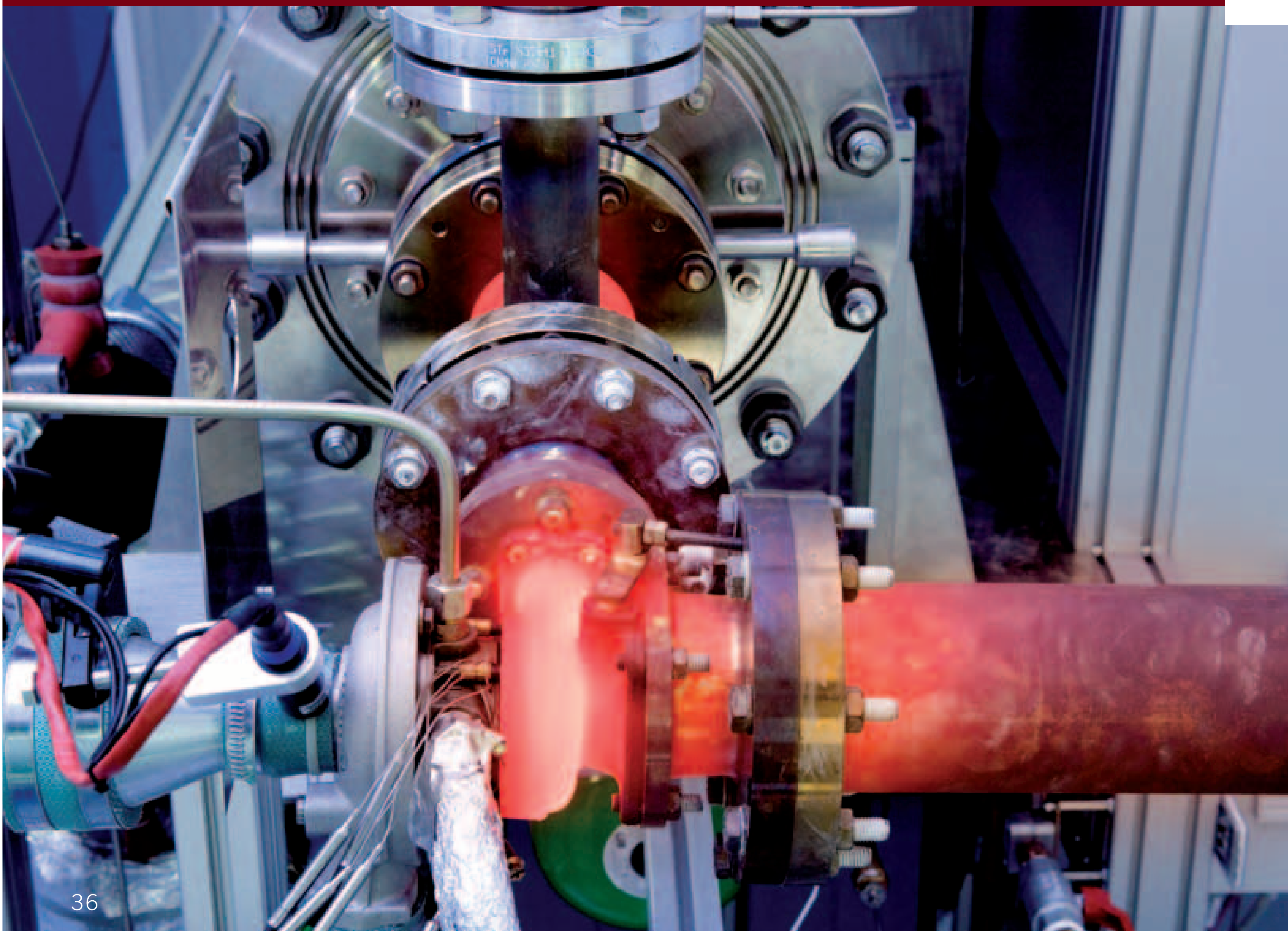

AUTHORS

DR. STEFAN REUTER
is responsible for the Validation Turbocharger at Continental in Regensburg (Germany).

DR. ANDRE KAUFMANN
teaches Thermodynamics and Fluid Mechanics at the University of Applied Sciences Ravensburg-Weingarten (Germany).

ACHIM KOCH
is Head of Development Turbocharger at Continental in Regensburg (Germany).

MOTIVATION

Modern turbo engine development focuses not only on fuel economy, but also on drivability and response characteristics at the lower end of the engine speed range. Apart from test rig trials, simulation of the internal combustion process can deliver decisive information on turbocharger suitability for a specific engine. This requires precise knowledge of the turbocharger gas flow characteristics. Decisive in particular are the mass flow behavior and efficiency as well as the rotating inertia.

Turbocharger characteristics are usually measured and recorded according to the "Turbocharger Gas Stand Test Code SAE J1826". Compressor and turbine power are balanced so that the speed remains constant. Due to the high exhaust gas temperature heating the turbine volute and causing convective heat flux, adiabatic turbine conditions are not given. The efficiency cannot therefore be determined by downstream temperature measurement, but only by establishing a power balance with the compressor. From the compressor power and the mass flow as well as expansion ratio of the turbine, the efficiency can be derived. The power balance implicitly includes mechanical power, so that the turbine efficiency as measured on the hot-gas test facility also takes account of mechanical losses. Due to power balance with the compressor, measurement of the turbine characteristics is limited to a small range. This range is too restricted for turbocharger selection and engine process simulation, because the engine causes pressure pulses on the exhaust side, and the turbine operating condition lies outside the statically measured characteristics [1]. It is therefore common practice for the engine process simulation to extrapolate the characteristics measured under steady-stage conditions. This is, however, extremely unsatisfactory due to the errors caused by extrapolation. Various methods were developed in the past for extending the turbine characteristics measuring range [2].

One of these methods is to increase the mass flow through the compressor, to which purpose the compressor is operated in closed loop mode at higher density. This increases the compressor power demand so that a higher expansion ratio is required on the turbine side and the measuring range can be extended accordingly. A drawback of this method is the difference in axial thrust compared with pulsating on-engine operation. This may cause a change in mechanical efficiency and therefore in the measured turbine efficiency. The overall efficiency of the turbocharger within the limiting conditions of the engine is decisive for optimal turbocharger selection. The turbocharger measurements should therefore be taken under on-engine conditions. Measurement of mass flow, pressure ratio and temperature directly on the internal combustion engine, however, is difficult and time-consuming. Furthermore, the turbine intake temperature cannot be freely adjusted. With the method described here, the turbocharger is operated on the test stand using pulsating hot gas flow, so that while not identical, the conditions are much nearer to on-engine operation than with the previously mentioned methods, ❶. On the hot-gas test facility, the turbine inflow temperature, pressure amplitude and mean pressure ratio can moreover be adjusted with special pulse generators. Unsteady mass flow and temperature measurements are also possible. This method can therefore be used to complement turbocharger characteristic measurements made on the steady-state hot gas test stand.

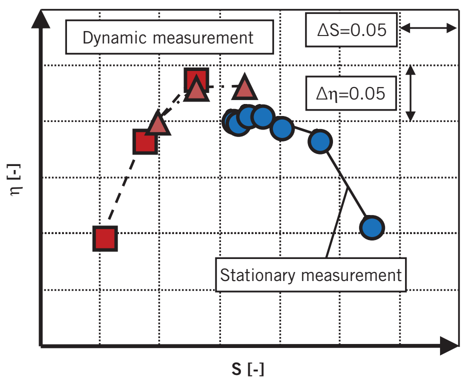

❶ Extended turbine maps using pulsating hot gas flow

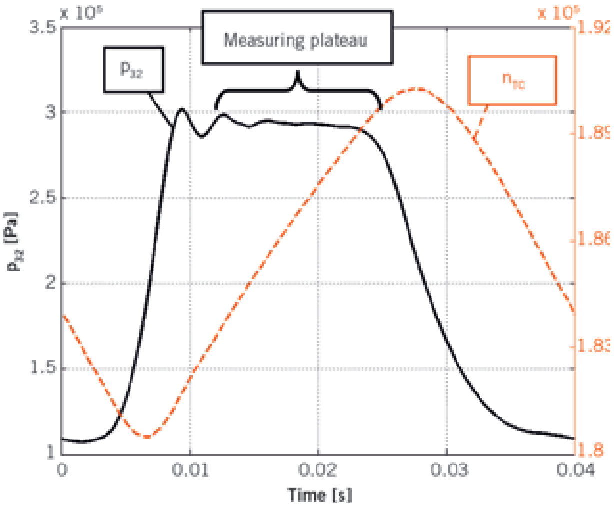

❷ High temporal resolution of static intake pressure at the turbine intake and turbocharger speed

CONCEPT AND SYSTEM

This method for extending turbocharger maps determined by steady-state measurement is based on creating turbine expansion ratios and unsteady mass flows similar to those in on-engine conditions.

In addition to the steady-state power balance between turbocharger compressor and turbine, the acceleration power is also taken into account. By impacting the turbine with pulsating hot gas, the turbocharger can be operated in a similar mode to the internal combustion engine. During an exhaust pressure pulse, the available exhaust gas enthalpy and thus power $P_{T,\,is}$ at the turbine intake rises rapidly. Since the turbine rotor takes time to come up to speed due to its inertia, the turbocharger briefly runs under high-pressure conditions. Afterwards the turbine inflow pressure decreases and the turbocharger speed falls. This procedure repeats periodically and an average speed is established. ❷ shows the time profiles of static pressure p_{32} at the turbine intake and delayed response of turbocharger speed n_{ATL}. By time-resolved analysis of all the relevant parameters, the turbine flow characteristics can be determined. For time-resolved analysis of the turbocharger characteristics it is important to take account of the filling and emptying effects caused on all flow-conducting components by impacting the turbine with pulsating hot gas.

Pressure, temperature and mass flow measurements are taken directly at the inlet to the turbine intake. Due to the finite speed of convection and sound, the impact of mass flow and pressure on the turbine rotor is delayed. Even taking account of the resultant phase shift, the instantaneous flow efficiency cannot be determined. To this purpose it is necessary to have stable conditions upstream and downstream of the turbine rotor for a short time. For dynamic analysis of the turbine, the turbocharger is impacted with a defined pulsating flow. ② shows one period of this defined flow characteristic with quasi-stable measurement plateau.

The pressure profile can be subdivided into three zones. After a rising phase, with sufficiently steep flank gradients, the pressure stabilizes at a high level (quasi-stable plateau) before falling again to an expansion ratio of almost unity. ❸ shows on the left the time-resolved and measured efficiency, Eq. 1, over the blade speed ratio, Eq. 2.

EQ. 1

$$\eta_T\,(t) = \frac{P_T'(t)}{P_{T,\,is}\,(t\text{-}\varphi)}$$

EQ. 2

$$S = \frac{u_{T\text{-}ein}}{C_S} = \frac{n_{ATL}\cdot\pi\cdot D_{T\text{-}ein}}{\sqrt{2\cdot c_{p,\,T}(t)\cdot T_{03}(t)\cdot\left(1-\left(\frac{p_4(t)}{p_{03}(t)}\right)^{\frac{\kappa_T(t)-1}{\kappa_T(t)}}\right)}}$$

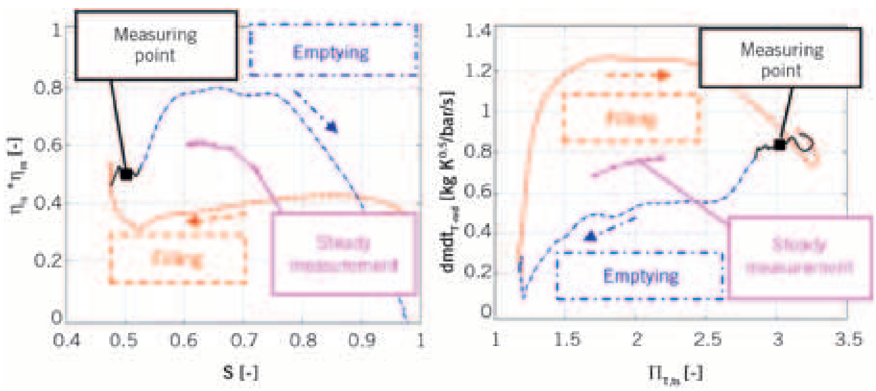

❸ Instantaneous calculation of turbine flow characteristics

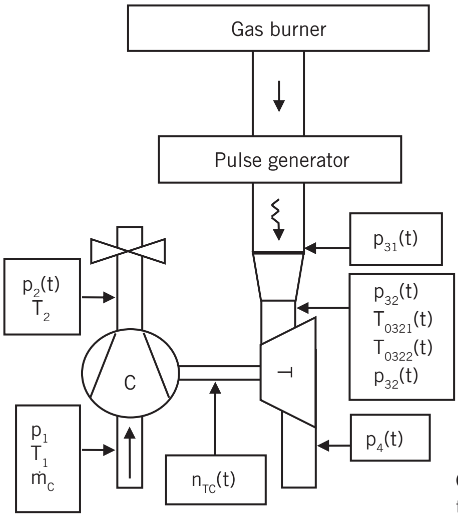

❹ Schematic layout of turbocharger instrumentation

During the pressure pulse rising phase, the flow passages from the measuring plane to the turbine are filled. The turbine flow at the measuring point, (③, right), is therefore larger, and the turbine efficiency seems correspondingly lower since it is calculated from the mass flow. The calculated efficiency follows the curve at the bottom. Due to the almost constant expansion ratio and turbine flow, the efficiency then remains on a quasi-stable plateau. During this phase the flow passages are completely full, the pressure and temperature readings remain nearly constant, and the efficiency can be measured under almost steady-state conditions. For a short time the turbine efficiency remains constant as a function of blade speed ratio, and the readings taken on this measurement plateau are dependable. When the turbine intake pressure falls off, the flow passages empty. The pressure at the measuring point is therefore lower and the blade speed ratio reduces. Since the flow at the measuring point is comparatively too small, the calculated turbine efficiency is too high.

To extend the measuring range, the pressure amplitude, frequency and pulse width are varied.

The turbine speed variations due to the pressure pulsations also change the compressor operating point. This change of operating point is taken into account by interpolation from steady-state measurement of the compressor characteristics based on instantaneous speed and boost pressure measurements.

TEST FACILITY ARRANGEMENT

To examine the characteristics of exhaust gas turbochargers in engine-relevant operating conditions, the test facility must be extended to generate a pulsating flow of hot gas. A pulse generator and a pulse damper are therefore installed between the hot-gas combustion chamber and the exhaust gas turbocharger. Due to the sensitivity of hot-gas combustion chambers to expansion ratio fluctuations, the pressure waves reflected off the pulse generator are damped before reaching the combustion chamber. Apart from damping the reflected pressure waves, the pulse damper also has a significant effect on the pressure profile at the turbine intake. The design and arrangement of the pulse generator, pulse damper and connecting piping determine the hot gas pressure and flow characteristics. For dependable test results, the pressure and flow characteristics generated should be comparable with those during engine operation. In particular the temperature, and hence the Mach number at the turbine intake, influence the mass flow and the efficiency. To ensure consistently comparable flow conditions between engine and test facility, engine-like turbine intake temperatures are therefore necessary. To investigate the dynamic characteristics of turbochargers, measuring techniques with high sampling rates are used. ❹ shows the schematic instrumentation layout.

Since adiabatic turbine conditions are not given, due to the high exhaust gas temperature, a balance is drawn between compressor power and acceleration performance as per Eq. 3.

EQ. 3
$$P_T'(t) = P_V(t) + P_{beschl}(t)$$

In general, the turbine efficiency is derived from the ratio of actual to isentropic turbine power as per Eq. 1. With pulsating inflow to the turbine, the former is derived as per Eq. 4 from the sum of compressor power and acceleration performance.

EQ. 4
$$P_{T,\,is} = \dot{m}_T(t) \cdot c_{p,\,T}(t) \cdot T_{03}(t) \cdot \left(1-\left(\frac{p_4(t)}{p_{03}(t)}\right)^{\kappa_T-1/\kappa_T}\right)$$

The change in compressor power, Eq. 5, is determined by measuring the instantaneous compressor outflow pressure $p_2(t)$ and speed $n_{ATL}(t)$.

EQ. 5
$$P_V = \frac{1}{\eta_{V\text{-}korr}} \cdot \dot{m}_V \cdot c_{p,\,V} \cdot T_{01} \cdot \left(\left(\frac{p_{02}}{p_{01}}\right)^{\frac{\kappa_V-1}{\kappa_V}} -1\right)$$

Using these two measuring signals, compressor power variations are interpolated in the steady-state compressor characteristics.

The acceleration power P_{acc} is derived from the moment of inertia of the turbine rotor, the speed, and the change in speed, Eq. 6.

EQ. 6
$$P_{beschl} = \frac{2 \cdot \Pi}{60} \cdot I_{ATL} \cdot n_{ALTL}(t) \cdot \frac{\partial n_{ATL}(t)}{\partial t}$$

The instantaneous isentropic turbine power $P_{T,is}$ is proportional to the turbine mass flow, the turbine inflow temperature, and a function of the turbine expansion ratio, Eq. 1. The turbine expansion ratio is determined using water-cooled piezoresistive absolute pressure transducers.

The time-resolved gas temperature is measured by thermocouples. Due to their transmission time characteristics, thermocouples cannot measure the gas temperature with high temporal resolution. To measure the instantaneous gas temperature, two thermocouples with different time constants are therefore installed in the

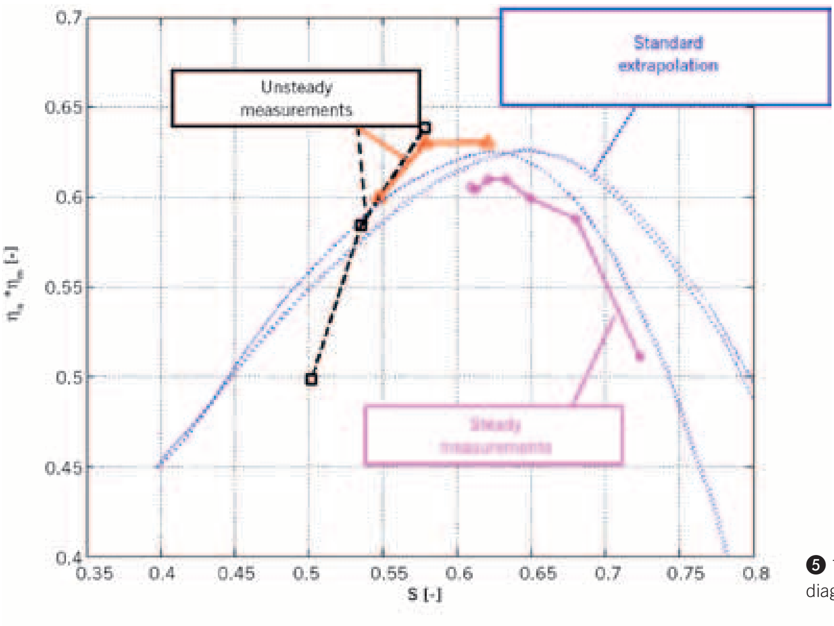

❺ Turbine operation within the extended efficiency diagram

hot gas flow immediately adjacent to each other. The time constant τ, Eq. 7, of a sensor depends on its specific characteristics and heat transfer coefficients.

EQ. 7	$T_G - T_W = \tau \cdot \frac{\partial T_W}{\partial t}$

Neglecting thermal conduction and radiation, the ratio of the time constants of two thermocouples can be taken as the ratio of their sensor diameters and of the local Reynolds and Nusselt number [3].

The time-resolved turbine flow is measured with an ISA–1932 nozzle immediately downstream of the turbine intake.

All parameters are simultaneously recorded with high resolution and have to be corrected with respect to each other for transport time characteristics. Thermodynamic measurements for determining the isentropic turbine power are taken a few millimeters upstream of the turbine spiral-casing intake. The phase shift due to convection and sonic speed is discussed in numerous publications [4]. Neglecting wave effects, the phase shift φ can be taken as the ratio of the distance L (from the measuring plane to 180° downstream of the spiral casing tongue) and the local flow velocity c_{32}, Eq. 8.

EQ. 8	$\varphi = \frac{L}{C_{32}}$

The instantaneous turbine efficiency is derived from the phase-corrected isentropic turbine power, Eq. 1.

RESULTS

By varying the expansion ratio and pulse form in pulsating flow, this new measuring method enables turbocharger turbine analysis under engine-like conditions and over a significantly wider measuring range. The form of pulsating flow influences the turbine behavior under quasi-steady operating conditions. Furthermore, the turbine operating range can be varied by adjusting the intake temperature. Due to changing heat flows, the turbine inflow temperature should lie within engine-relevant limits while taking measurements. For dependable interpolations of turbine characteristics, a sufficient number of measurements must be taken along the respective speed curves. ❺ compares steady-state measurement with the extension of a typical efficiency-speed curve. Also shown is the efficiency curve for turbocharger operation on a downsizing engine, numerically extrapolated from steady-state measurements. Combining the two concepts results in high-resolution extension of the dynamic characteristics.

The pulsating measurement of turbine characteristics is therefore an effective way of optimally adapting turbochargers to improve the performance and efficiency of internal combustion engines.

REFERENCES

[1] Scharf, J.; Schorn, N.; Smiljanovski, V.; Funken, B.; Pischinger, S.: Messung des Turbinenwirkungsgrades bei niedrigen Turboladerdrehzahlen, Tagungsband 13. Aufladetechnische Konferenz, Dresden, 2008, p. 99-128
[2] Pucher, H.; Nickel, J.: Vermessung erweiterter Kennfeldbereiche von Fahrzeugmotoren-Turboladern; Tagungsband 8. Aufladetechnische Konferenz, Dresden, 2002, p. 321-339
[3] Reuter, S.; Koch, A; Kaufmann, A.: Extension of Performance Maps of Radial Turbocharger Turbines using Pulsating Hot Gas Flow, Tagungsband 9th Int. Conference on Turbochargers and Turbocharging, London, 2010, p. 263-280
[4] Martinez-Botas, R. F. et al.: Performance and Exit Flow Characteristics of Mixed-Flow-Turbines. In: International Journal of Rotating Machinery 3 (1997), No. 4, p. 277-293

ENTHALPY-BASED APPROACH TO QUANTIFYING AND PREVENTING PRE-IGNITION

In spark-ignition engines, continuous downsizing increases the risk of pre-ignition phenomena. IAV has developed a concept in which the specific enthalpy at top dead centre can be used as an indicator for pre-ignition tendencies.

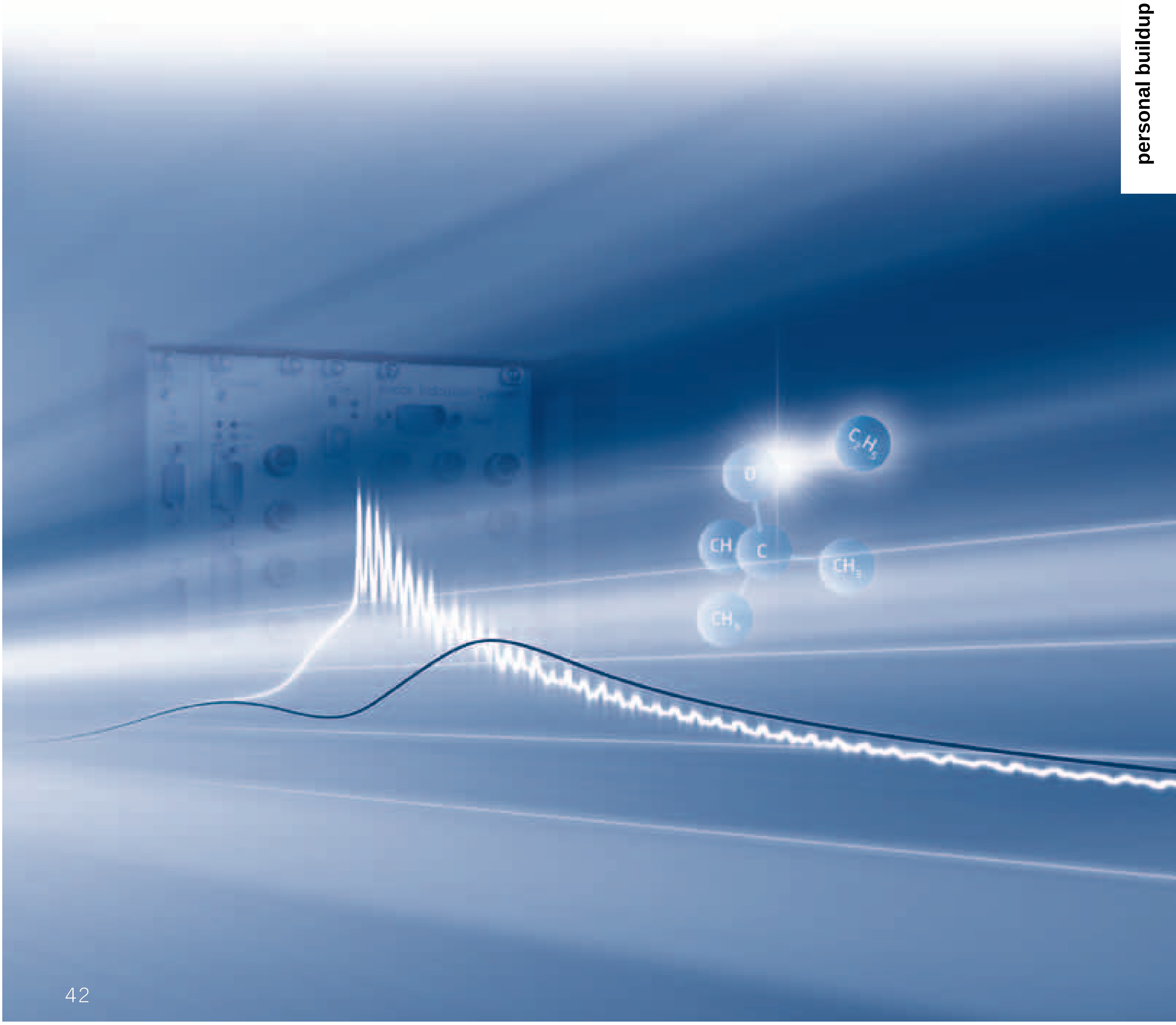

AUTHORS

DIPL.-ING. MICHAEL GÜNTHER
is Head of the Department Thermodynamics Gasoline Engines at IAV GmbH in Chemnitz (Germany).

DR. RALF TRÖGER
is Development Engineer in the Department Thermodynamics Gasoline Engines at IAV GmbH in Chemnitz (Germany).

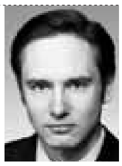

DIPL.-ING. MATTHIAS KRATZSCH
is Senior Vice President Development Gasoline Engines at IAV GmbH in Berlin (Germany).

PROF. DR.-ING. STEFFEN ZWAHR
is Professor of Internal Combustion Engines/Working Processes at the West Saxon University of Applied Sciences Zwickau (Germany).

PRE-IGNITION COUNTERACTS FUEL CONSUMPTION REDUCTION

Against the backdrop of tighter exhaust-emission legislation and the demand for better fuel economy, downsizing concepts with high-pressure turbocharging and unthrottled load control are and will continue to play a particularly important part. They are capable of providing significant potential for reducing fuel consumption of spark-ignition engines. Yet higher boost rates exacerbate the problems encountered in the context of knock and pre-ignition. Engines with high mean pressures at low engine speeds are particularly prone to pre-ignition. In some cases, combustion occurs well before the regular ignition point, with the subsequent, very early release of heat capable of producing extremely high pressure amplitudes. To avoid damaging the engine, the charging rate must be limited. This, in turn, prevents the consumption-cutting potential of downsizing strategies from being exploited to the full.

DEFINITION OF PRE-IGNITION

Pre-ignition can be distinguished very easily from knock since it is the result of combustion that is not initiated by the spark plug. As clearly evident from ❶, heat release causes pressure to rise before the ignition point. Combustion can be initiated by ignition sources, such as glowing soot particles or lubricant droplets [2], and also in local mixture zones with a high concentration of radicals (exothermic reactors).

The premature initiation of combustion causes high peak pressures and, as a result of high combustion rates, extreme pressure gradients. This is also accompanied by high-frequency, strong pressure peaks that can be compared with extreme knock. Sequences that involve alternating combustion cycles are particularly harmful. Heat release of at least 1 % at the ignition point has proven to be a good criterion for providing a clear definition of pre-ignition [2].

ENTHALPY-BASED APPROACH TO PRE-IGNITION

Exceeding a critical energy level is one possible mechanism for triggering premature combustion. This is governed by various influencing variables that cannot be manipulated individually on the engine test bench. For example, adjusting ignition timing while keeping mean pressure constant also changes the fresh and residual-gas mass as well as residual-gas temperature. A model-based approach provides the capability of considering all individual parameters separately. Enthalpy is an appropriate variable for describing the energy contained in the cylinder charge, Eq. 1. During the gas exchange, energy flows in and out in the form of enthalpy with outgoing and incoming masses. The first law of thermodynamics, Eq. 2, describes the energy balance. This makes it possible to quantify enthalpy inflow and outflow caused by fresh cylinder charge, residual gas or fuel vaporization or the exchange of heat and work done. Evaluating the state at TDC provides a suitable basis for map points with typical ignition timings after TDC.

EQ. 1

$$H = U + p \cdot V = c_v \cdot m \cdot T + p \cdot V$$

EQ. 2

$$dQ_{burn} - dQ_{wall} = dU + pdV - H_{fuel} + dH_{blow} - dH_{in} + dH_{out}$$

As absolute enthalpy is governed by charge mass, and thus also by engine size, specific variables are formed in relation to compression volume (energy density, Eq. 3). This global variable can be used for separating changes in the states of energy and analyzing them independently of the measurement program. The enthalpy-based approach permits evaluation of the influences individual parameters have on overall enthalpy in the charge. This provides a basis for quantifying the effectiveness of measures that prevent pre-ignition.

EQ. 3

$$h^*_{TDC} = \frac{H_{TDC}}{V_C} = \rho_{OT} \cdot h_{TDC}$$

At the same time, however, it is only possible to evaluate engine concepts or development stages by comparing the mean enthalpy prevailing in the cylinder with a critical enthalpy occurring at the pre-ignition threshold. This means the function parameters leading to the critical level of enthalpy at the pre-ignition threshold can be determined for different engines. Generating a model capable of being calibrated accordingly permits objective assessment of pre-ignition propensity.

In just the same way as the actual charge energy level, the maximum permissible enthalpy itself is governed by local states in the cylinder. It is assumed that in line with local fluctuations in the state of cylinder charge, individual zones diverge from the mean mixture state and sporadically reach a critical state sooner. This means using mean variables demands a sufficient interval between limit enthalpy and actual overall charge enthalpy.

TOOLS FOR ANALYZING PRE-IGNITION

Given the many individual contributors, consideration must be given to all of the processes involved in enthalpy changes. An IAV simulation tool is used for computing the entire engine process. Gas exchange simulation delivers the masses and enthalpies of fresh charge and residual gas. The effects of fuel vaporization on charge temperature and cylinder charge are computed using a vaporization model. Technical work and heat balances are also determined. The high-pressure process and enthalpy changes resulting from fuel vaporization, wall heat exchange, blow-by losses and work delivered from compression are computed starting from "inlet closes". Adding the individual components produces the overall level of energy at TDC.

LEVEL OF ENTHALPY IN THE CYLINDER CHARGE

Parameters influencing charge enthalpy were examined in comprehensive measurements. In this context, the key variables were determined as being charge temperature/charge mass, fuel mass/injection (vaporization) timing and residual-gas mass/residual-gas temperature. ❷ presents examples of the effects charge temperature and mass have on enthalpy and pre-ignition tendency. It shows the increase in pre-ignition events classified on the basis of p_{max} in comparison to the value of specific enthalpy at TDC. It is clear to see that both variables correlate exceedingly well. Variations in injection timing and residual-gas content also showed close relationships, albeit with less of an effect.

LIMIT ENTHALPY LEVEL

Limit enthalpy is defined as being the level of charge at which pre-ignition events just start to take place in the engine without producing any harmful effect. Parameters influencing the level of limit enthalpy are for example air-fuel ratio, fuel properties or lubrication oil content of the charge.

Extensive testing on different engine concepts was also necessary for determining the limit enthalpy level. By way of example, the following looks at the effects of lambda and lubrication oil components in the combustion air – mentioned above in [3]. ❸ shows the relationship between pre-ignition frequency and lambda. The

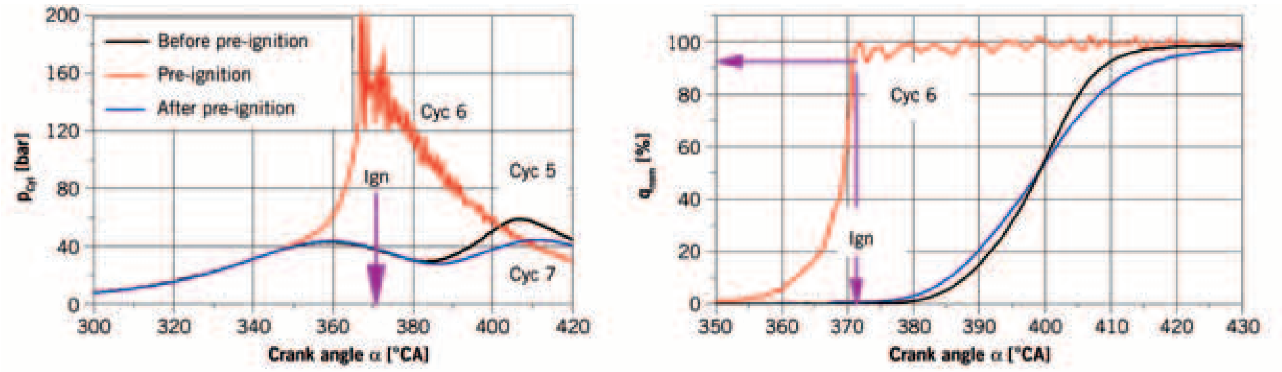

No. Cyc	Comb.cycle	q_norm@ign (%)
1	Normal	0.1
2	Pre-ignition	0.5
3	Normal	0.0
4	Pre-ignition	5.4
5	Normal	0.0
6	Pre-ignition	93.7
7	Normal	0.0
8	Pre-ignition	93.4
9	Normal	0.2
10	Pre-ignition	20.1
11	Normal	0.0
12	Normal	0.1
13	Pre-ignition	38.2
14	Normal	0.1
15	Pre-ignition	15.9

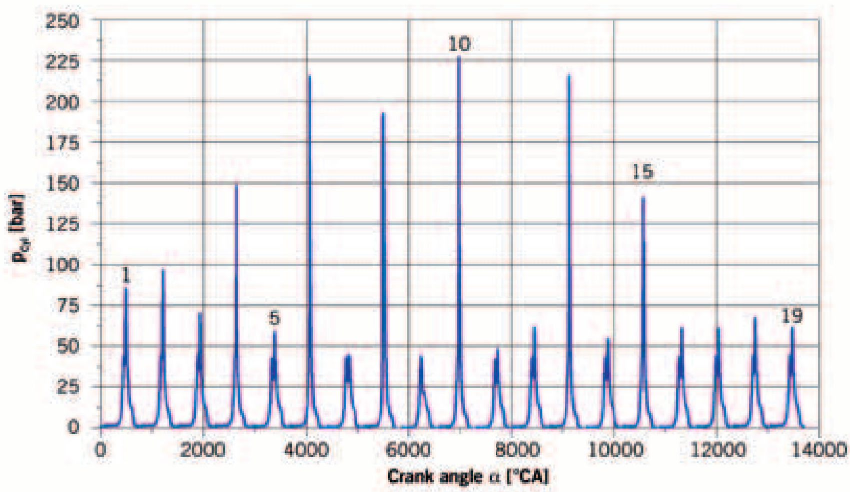

❶ Pre-ignition sequence

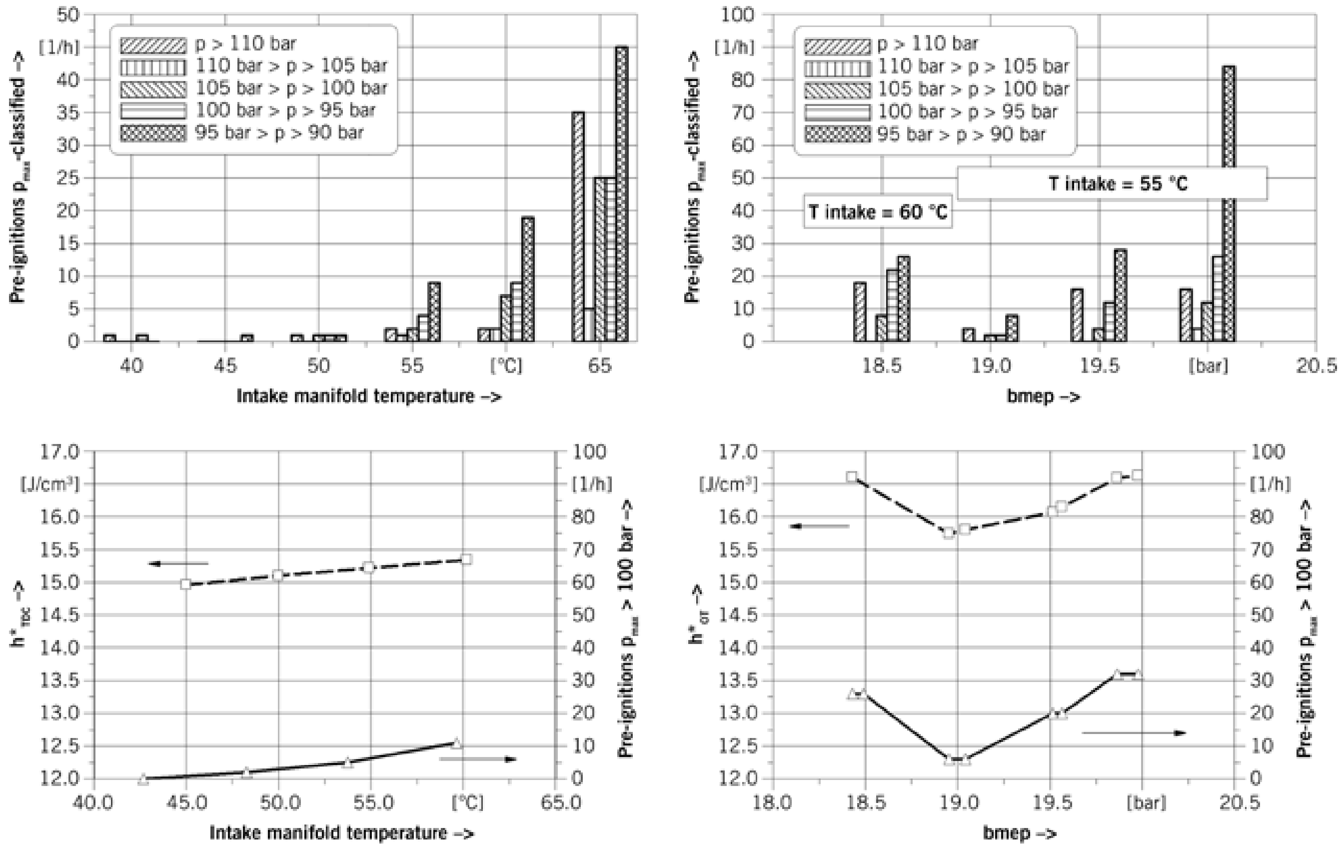

❷ Pre-ignition sensitivity in relation to inlet temperature and mean pressure

enthalpy level was kept constant in testing. Compensation for the higher level of fuel vaporization enthalpy at lambda = 0.95 was made by increasing cylinder charge, as can be seen by the different mean pressure. It becomes clear that in spite of enthalpy remaining virtually the same on varying lambda, pre-ignition tendency is significantly lower.

The piston-ring set was systematically modified for each individual cylinder to determine the influence of engine oil on pre-ignition tendency, ③. A mass spectrometer was used for measuring the concentration of unburned lubrication oil in the exhaust gas of the operating engine. Investigations revealed a pre-ignition frequency proportionate to oil emission.

SENSITIVITY OF INDIVIDUAL ENTHALPIES

❹ compares the effect of individual variables. Proceeding from a basic operating point, it separately varies several parameters. The effect of engine-based measures on specific enthalpy was shown to be predominantly linear.

In this example, lowering charge-air temperature by $\Delta T = 15$ K is capable of increasing mean pressure by $\Delta pme =$ 0.6 bar without affecting enthalpy. Varying injection timing reflects the correlation between charge temperature and the timing of vaporization in relation to BDC in the enthalpy characteristic [5].

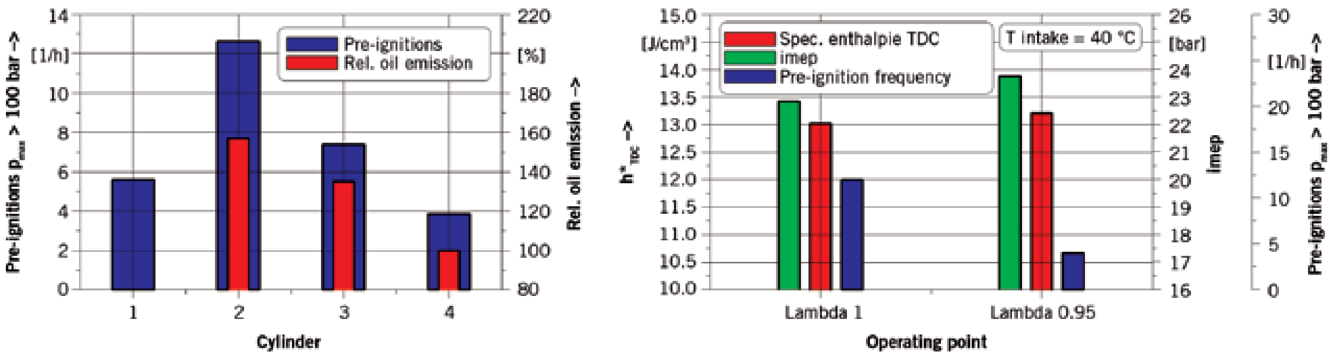

❸ Parameters influencing the limit enthalpy level

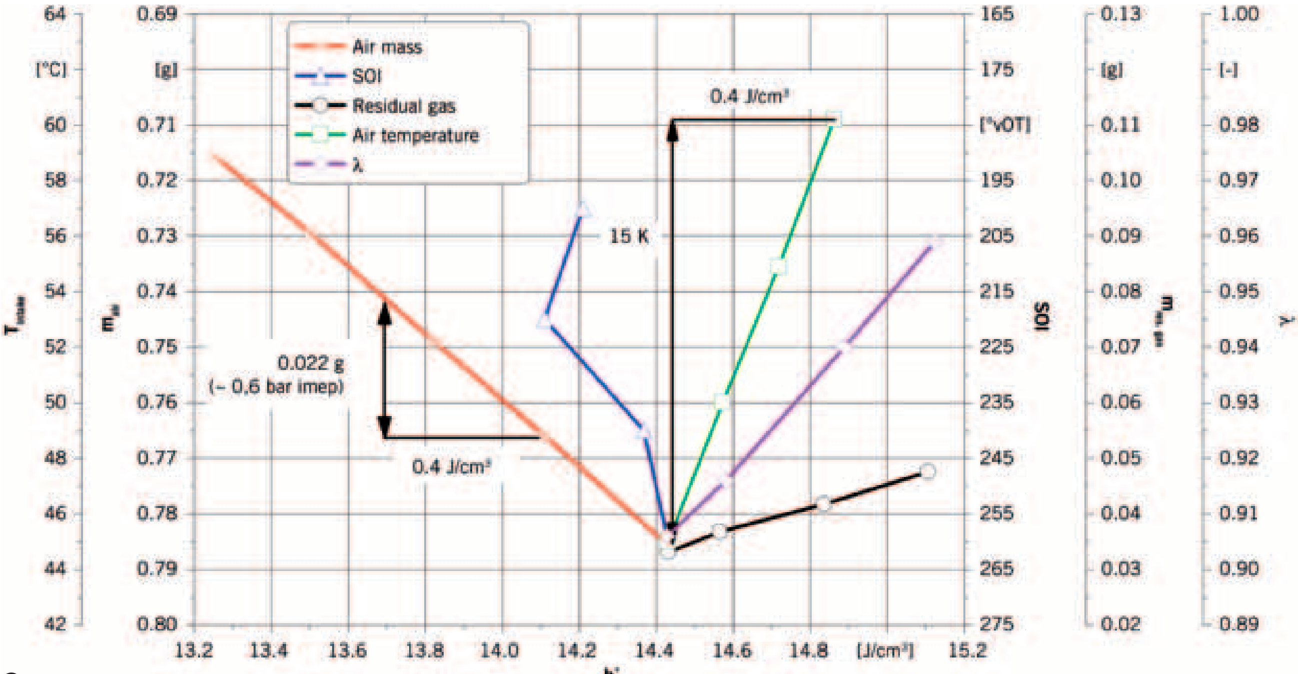

❹ Sensitivity of selected enthalpy components

TOTAL ENTHALPY BALANCE

❺ shows an enthalpy balance for a selected operating point. The largest effect is produced by the enthalpy components of compression work and fresh air. Keeping fresh-air mass constant, fresh-air temperature can provide an effective influencing lever. This, however, produces demands on charge-air cooling. The change in enthalpy produced by compression work is, by nature, extensively governed by the compression ratio, demanding an adjusted mass of fresh gas if mean pressure remains unchanged.

Influencing the effective compression ratio (IC to TDC), for example by retarding inlet closure (Atkinson process), produces effects that significantly reduce enthalpy. Enthalpy entrained is easy to influence with residual-gas mass and/or temperature. Scavenging concepts using positive purge pressure have already proven effective in mass-production concepts. Although the contribution residual gas makes to enthalpy is relatively small, a high share of free radicals – particularly in conjunction with retarded combustion – at the same time lowers the critical enthalpy level while boosting the effect the residual gas share has on pre-ignition tendency [4]. Reduced enthalpy from fuel is governed by the timing of vaporization timing in relation to BDC [5]. On the other hand, the rising proportion of fuel mass in the cylinder directly increases the negative enthalpy component. The contribution from wall heat

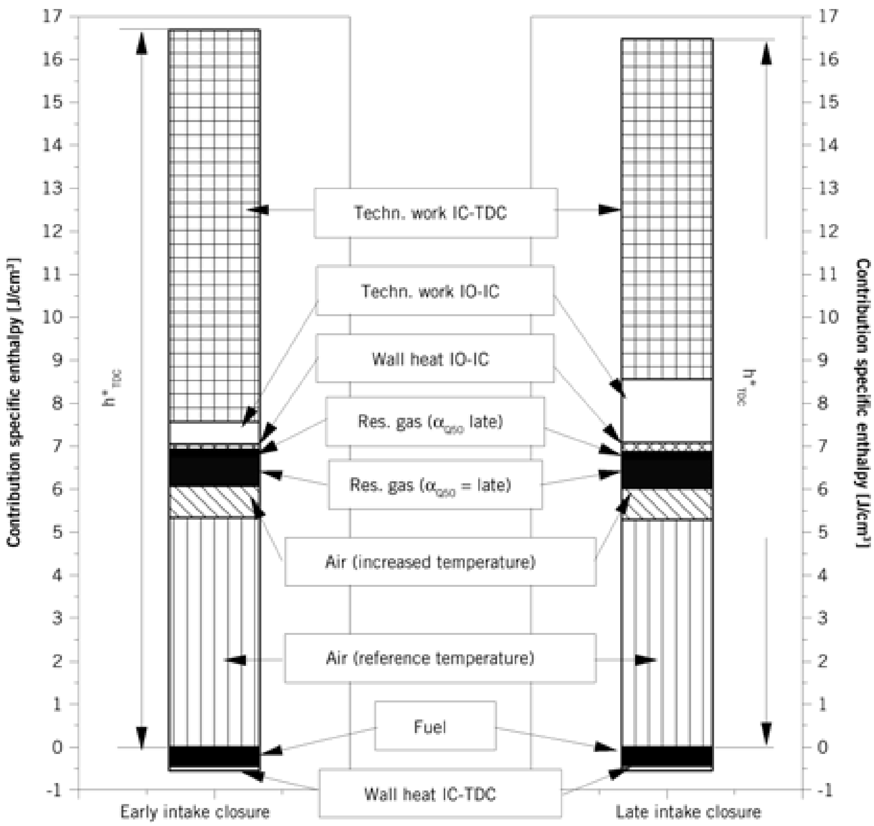

❺ Enthalpy balance at the pre-ignition limit

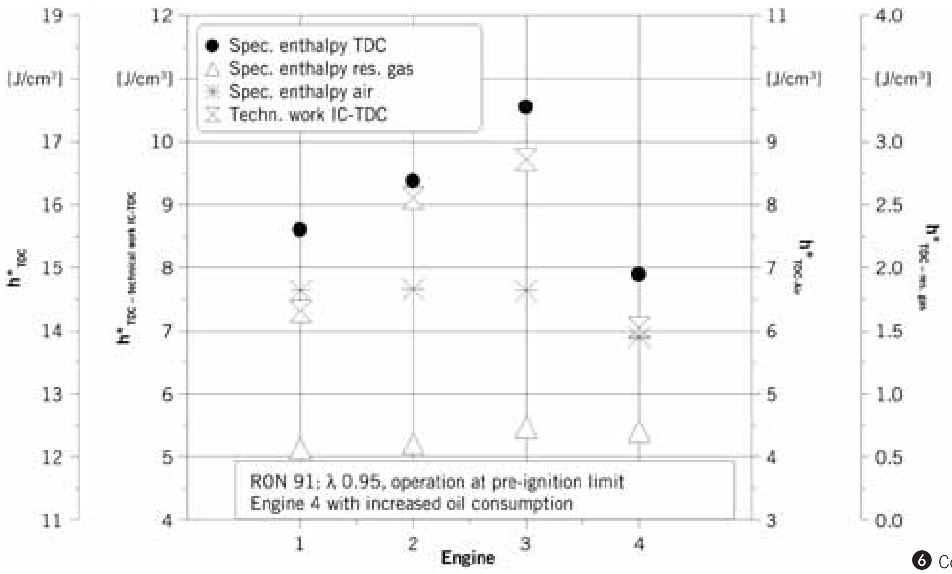

❻ Comparison of engine concepts

must be viewed in the light of controllable variables, such as wall temperature and heat transfer resulting from charge motion. Although the effect they have on total enthalpy appears slight, they can significantly contribute toward reducing the pre-ignition tendency under specific conditions.

ENTHALPY BALANCE FOR DIFFERENT ENGINE CONCEPTS

In addition to the effect produced by the concentration of lubrication oil in the fresh charge, circumstances, such as the shape of combustion chamber, charge motion or degree of homogenization, are also of significance. In the same way as the knock limit is established, systematic experimentation on the test bench can provide the basis for determining the limit for any specific engine. The enthalpy criterion developed in this study provides the basis for comparing and classifying engines in relation to critical enthalpy at the pre-ignition limit. ❻ shows the maximum levels of enthalpy at the pre-ignition limit for different engines. The fresh air enthalpy is seen to be comparable for engines 1 to 3 at similar charge air temperatures and mean pressures. Engine 1 differs from engines 2 and 3 to the extent that compression work is significantly reduced as a result of late inlet closure. Comparison also reveals the severe effect resulting from high quantities of lubrication oil entering combustion air (engine 4). Quantifying the sources of energy entrained permits classification of development stages in relation to the relevance of individual enthalpies.

SUMMARY

The above discourse describes a criterion that can be used as the basis for evaluating an engine's pre-ignition tendency. The specific enthalpy at TDC emerged as a parameter that is well-suited for evaluating the tendency to pre-ignition. Quantifying individual components within the overall enthalpy level delivers information about the specific influence they have on energy level. This provides the basis for comparing development stages or engine concepts on the basis of simple indication by determining global states in the cylinder. In particular, and depending on concept, it is possible to use the variables of combustion air temperature, mass and temperature of the residual gas remaining in the cylinder, timing of fuel vaporization in relation to BDC as parameters that can be influenced directly. When configuring turbocharged spark-ignition engines, the overall equation must include the variables of charge motion, effective compression ratio, cooling concept and effectiveness of the charge air system. If the engine concept's critical enthalpy level is known from measurements, it is only a short step to inferring the development stage reached.

REFERENCES

[1] Spicher, U.; Mass, U.; Dahnz, C.; Han, K.-M.; Magar M.: Vorentflammungen bei Ottomotoren (Pre-Ignition in SI Engines). Final Report FVV (ICE Research Association) Project No. 931, 2010
[2] Günther, M.; Zwahr, S.: Thermodynamische Analyse von Vorentflammungserscheinungen (Thermodynamic Analysis of Pre-Ignition Phenomena). Tagung Motorische Verbrennung (Engine Combustion Conference), Munich, 2009
[3] Zahdeh, A.; Rothenberger, P.; Schäfer, J.: Diagnosing Engine Combustion Using High Speed Photography in Conjunction with CFD. Symposium für Verbrennungsdiagnostik (Symposium on Combustion Diagnostics), Baden Baden, 2008
[4] Hoffmeyer, H.; Montefrancesco, E.; Beck, L.; Willand, J.; Ziebart, F.; Mauss, F.: Catalytic Reformated Exhaust Gases in Turbocharged DISI-Engines, SAE Paper 2009-01-0503
[5] Eichert, H.; Günther, M.; Zwahr, S.: Simulationsrechnungen zur Ermittlung optimaler Einspritzparameter an DI-Ottomotoren (Simulation for Determining Optimum Injection Parameters in DISI Engines). In: AEP No. 9-10, 2005
[6] Günther, M.; Tröger, R.; Zwahr, S.: Enthalpiebasierter Ansatz zur Quantifizierung und Vermeidung von Vorentflammungen (Enthalpy-Based Approach to Quantifying and Preventing Pre-Ignition events). 3rd Conference on Ottomotorisches Klopfen – Irreguläre Verbrennung (SI Engine Knock – Irregular Combustion), Berlin, 2010

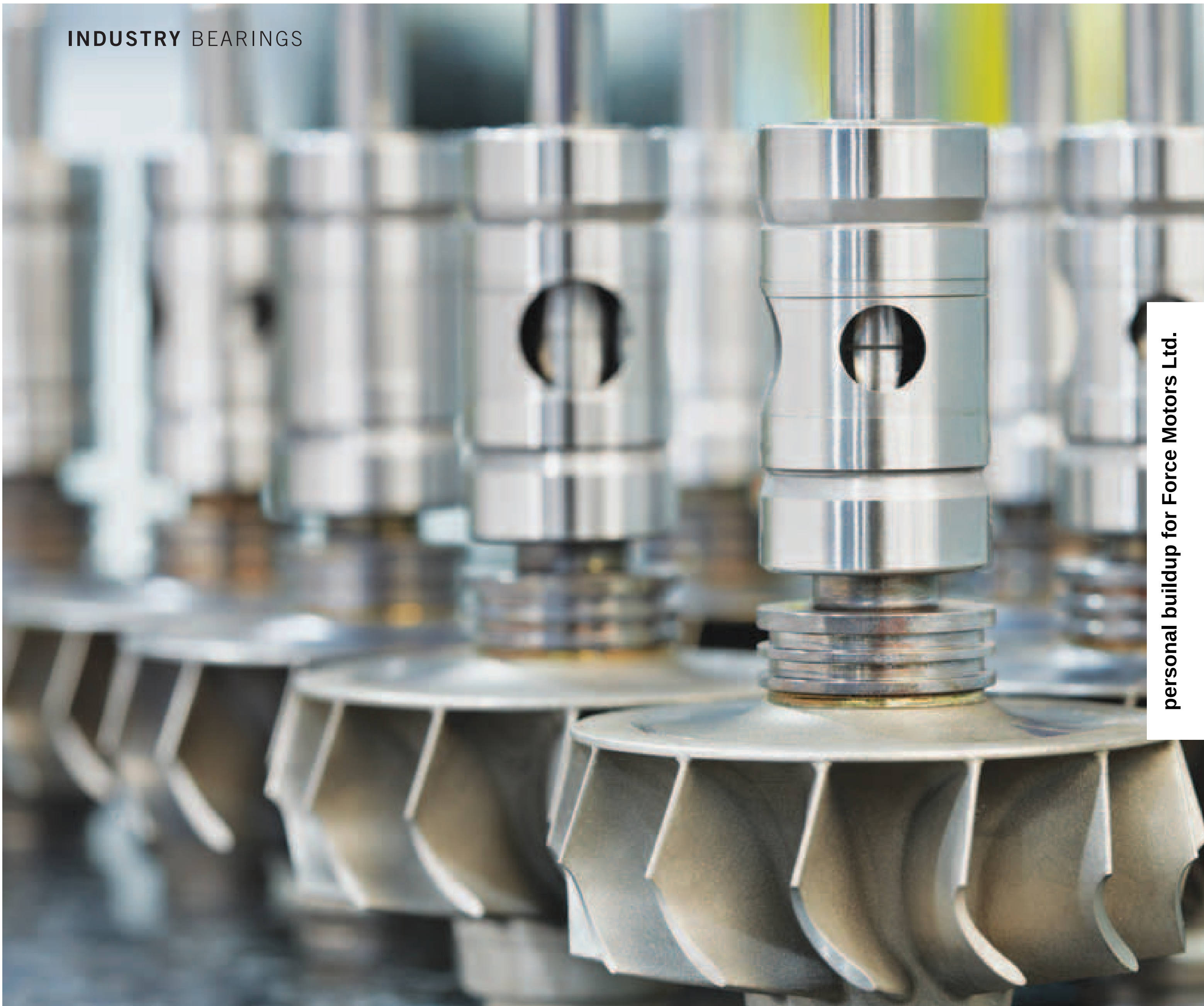

HIGH VOLUME SERIES PRODUCTION OF BALL BEARING TURBOCHARGERS

Ball bearing turbochargers have made their transition from motorsport to series production automotive engineering. The development of a modular system enables Honeywell to meet the different requirements of regional markets efficiently.

AUTHORS

KARL-HEINZ BAUER
is Vice President and Chief Technology Officer at Honeywell Transportation Systems in Rolle (Switzerland).

CRAIG BALIS
is Vice President Engineering at Honeywell Turbo Technologies in Rolle (Switzerland).

DAVID PAJA
is Vice President Marketing at Honeywell Turbo Technologies in Rolle (Switzerland).

PETER DAVIES
is Large Diesel Platform Director at Honeywell Turbo Technologies in Thaon-les-Vosges (France).

DAMIEN MARSAL
is Ball Bearing Component Manager at Honeywell Turbo Technologies in Thaon-les-Vosges (France).

TASK

Powertrain manufacturers throughout the world are faced with the simultaneous demands of improving performance and reducing emissions and CO_2. At the same time, they are uniformly calling for compact, high efficiency turbocharging systems that are both durable and affordable.

While there are many ways to achieve this – and many trade-offs from seemingly conflicting targets and competing technologies – perhaps the one common theme that all researchers and developers agree on is that improved efficiency is a good thing, since it advances all technical targets simultaneously.

From a turbocharger perspective, one area that has remained largely unchanged for decades is the bearing sub-system. However, recent developments in analytical techniques have opened up great potential here and rotor dynamics can be optimised analytically in a fraction of the time needed previously, leaving the developer new freedom to concentrate on the performance aspects of the design.

In 2010, Honeywell launched several new hydrodynamic bearing systems. These kinds of evolutionary development steps will continue in the future. However, the year also saw the bar raised to an entirely new level with the release of three all-new "low friction" ball bearing systems covering a wide range of Honeywell's extensive global portfolio. The systems set a new performance benchmark for the future in the high end passenger car, light duty and heavy duty truck segments, ❶.

MARKET REQUIREMENTS

Previously an end in themselves, high specific torque and power ratings have now reached a level that enable significant engine down-speeding and downsizing from eight to six cylinders, from six to four, from four to three, and so on. These two strategies are being implemented to achieve a reduction in CO_2 and to ensure compliance with present and future fuel efficiency and emissions standards. In turbocharger terms, this means higher and broader range efficiency from each of the three major sub-systems, the compressor, turbine stage and bearings.

Designing for steady-state operation is easy. Optimizing a package for vehicle applications which are highly transient and operate for significant periods at part load, on the other hand, requires a deep understanding both of varied operating conditions and of the many system interactions. It is at part load and low speed "off the map" where bearing performance becomes the key player in overall system efficiency.

The turbocharger must fulfil its function to deliver air and help to provide a predictable backpressure to drive EGR not only in a new state but equally when the turbocharger is operating across its full performance spectrum over its entire life. Successive emission standards have simultaneously reduced target levels and extended the period over which a vehicle must remain compliant.

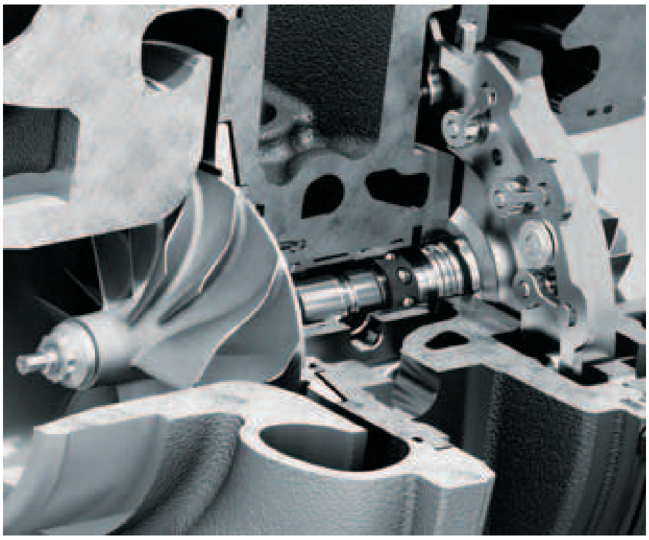

❶ Ball bearing turbocharger

In order to meet these constantly increasing requirements, Honeywell has continued its 2008 development of ball bearings and recently unveiled several production releases with three new sizes of bearing to meet these specific challenges.

ADVANTAGES OF BALL BEARINGS

The advantages of ball bearings stem from the fundamental change in the friction mechanism present in the system. Multiple rolling elements replace a thin oil film in high shear, significantly reducing the system friction, ❷. This results in

: a 50 % improvement in system friction at operating temperature and
: an 80 % improvement or more during cold start.

When applied to a turbocharger, this effect starts a virtuous upward spiral that flows all the way from turbo to engine and on to the vehicle performance. Independent testing commissioned at IAV GmbH in 2007 and published jointly in 2008 showed that tangible benefits could be demonstrated in engines > 2.2 l under EU5 diesel conditions [1].

A 2.5 % reduction in NEDC fuel consumption was achieved at ISO load, while other studies showed that this would increase to around a 4 % reduction in real world conditions. At the same time, a 10 % increase in low end steady-state torque and significant reductions in time-to-boost were demonstrated in warm conditions.

: a 41 % reduction in time-to-boost at 1500 rpm
: a 69 % reduction in time-to-boost at 1000 rpm
: a 3 % reduction in time-to-boost at 2000 rpm.

This shows that the ball bearing effect is most pronounced at low engine speeds – just where a down-speeding or downsizing concept needs the most help from the turbocharger system. The same study showed that a different approach to fuel economy could be taken and that an 8 % reduction in NO_x and a 9 % reduction in HC emission across the NEDC cycle could be demonstrated at ISO fuel consumption.

DESIGN

Since the debut in the motorsport arena in the 1990s, Honeywell's ball bearing systems have become part of the generic "double row angular contact ball bearings" family, but over time they have evolved into a single basic architecture, ❸.

Analytical techniques such as handbook calculations, industry standard codes and

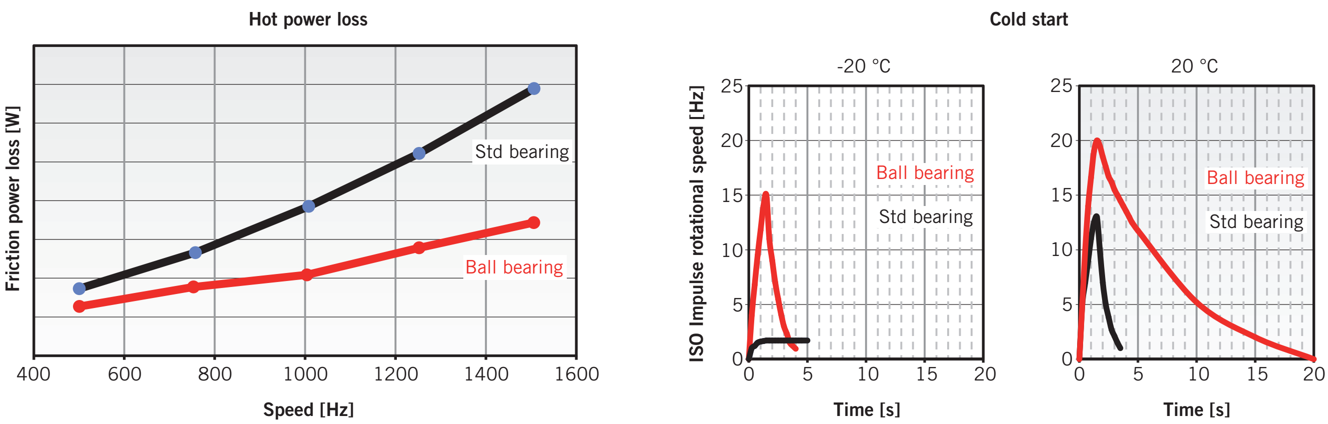

❷ Advantages of ball bearings

❸ Modular ball bearing family

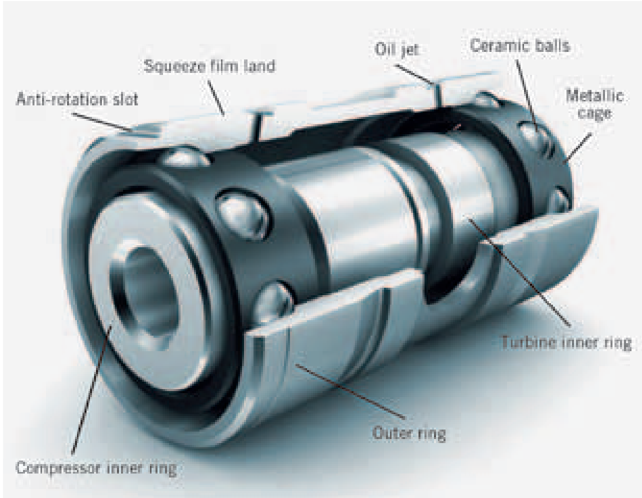

❹ Ball bearing cartridge

even bespoke supplier software have long existed to specify ball bearing size and durability appropriate for the multitude of duty cycles required for modern passenger car and commercial vehicle applications. Honeywell also benefits from an extensive field and test database developed by its Aerospace business and from its 1990s experience in motorsport and commercial vehicle applications, which allows it to calibrate classic bearing lifting theory in line with the real world.

The design consists of two inner rings made from heat-resistant bearing steel, press fitted onto a precision shaft. In this generation, the balls are now ceramic and are separated and guided by coated steel cages, while the outer ring is also made from a bearing steel, ❹.

Each system runs with a small but precise axial clearance in all operating conditions. This maximises performance and durability.

The oil supply system is the key to the system's functionality and longevity. The oil lubricates and cools multiple surfaces, damps vibration through the outer squeeze film and hence limits transmission to the surrounding structure and subsequent noise in the vehicle. The detailed design and balance of the oil network from a single inlet accommodates highly variable temperatures and pressures. It is a complex system that has been fully tested in all conditions.

The assembly process is critical and contributes strongly to the balanceability of the turbocharger.

CURRENT APPLICATIONS

The 2010 launches not only span three continents, three vehicle segments and cover three bearing and turbo frame sizes. They also meant that the technology had to be taken from niche to large volume production, ❺.

The 3.0 l V6 diesel application for a European car is an example of the true potential of ball bearing technology.

The engine is a V6 and is therefore most suited to a single turbocharger application, but it had to compete against two-stage boosted engines, which meant that the project team had very precise targets around maximising low end performance. The intrinsic low losses and good cold start of the ball bearing contributed to the vehicle's launch dynamics and agility, as well as to its improved fuel economy.

Launched in Dresden [2] and Aachen [3] and at the Paris Motor Show in October 2010, the application's performance statistics of 620 Nm of torque and 195 kW of power exceed those of the early two-stage boosted equivalents.

OUTLOOK

The breadth of the 2010 applications shows the performance, robustness and maturity of the technology. The production launches represent more than a tenfold increase in annual production volumes, turning the niche technology into a mainstream component of modern turbocharging systems. The next target is the systematic introduction of this technology for turbocharging four-cylinder engines. The dream of more than one million ball bearing turbochargers per year is now closer than ever before.

❺ Ball bearing turbine

REFERENCES

[1] Davies; Marsal; Jeckel; Tietze: A new Turbocharger Bearing System as a further step to improve overall turbocharger efficiency. 13. ATK Dresden, September 2008

[2] Davies; Marsal; Daguin; Genin; Jeckel: Downspeeding and Upgrading a Product Line for US'07 Tier 2 Bin 5, EU5 and EU6. 15. ATK Dresden, September 2010

[3] Werner; Schommers; Engel; Spengel; Reckzügel; Paule; Maderstein; Eibler; Hoppenstedt: The new V6 Diesel Engine from Mercedes-Benz. 19. Aachener Kolloquium Fahrzeug- und Motortechnik 2010

WASTE HEAT RECOVERY IN DRIVE SYSTEMS OF TODAY AND TOMORROW

Efforts to achieve a further reduction in CO_2 emissions require further reductions in fuel consumption. Closed steam cycles that make use of waste heat can contribute to this. On the basis of series-production stationary systems for waste heat recovery, Voith has developed the first mobile systems for rail vehicles, ships and commercial vehicles. They demonstrate the technical feasibility and the potentials.

AUTHORS

DIPL. PHYS. EBERHARD BREDEL
is Managing Director of Voith Turbo Verdichtersysteme GmbH & Co. KG in Zschopau (Germany).

DR.-ING. JÖRG NICKL
is Manager of Development at Voith Turbo Verdichtersysteme GmbH & Co. KG in Zschopau (Germany).

DIPL.-ING. STEPHAN BARTOSCH
is Vice President Product Lines Engine Technology and SteamDrive, Powertrain Technologies at Voith Turbo GmbH & Co. KG in Heidenheim (Germany).

INITIAL SITUATION

Internal combustion engines are the dominating power source in a wide variety of applications. This applies to on-road applications ranging from two-wheel vehicles to cars and commercial vehicles, or non-road applications from hand-operated devices to inland vessels and locomotives or major stationary applications. The application areas and fields are as diverse as the specific requirements and regulations.

Despite the high level of engine development, still only about 40 % of the energy in the fuel is converted into torque at the crankshaft. Most of the remaining energy is dissipated unused as heat via exhaust gases and through the cooling water.

An important approach towards further increasing the system efficiency of drive systems is to make technical use of this waste heat. For this purpose, Voith Turbo has developed waste heat recovery (WHR) systems based on the Clausius-Rankine cycle. By means of a closed steam cycle, some of this waste energy is reconverted into usable power and made available as additional tractive output or for driving auxiliary systems.

STEAMTRAC WHR SYSTEM

In order to be suitable for a broad application spectrum, the development and design of exhaust heat recovery systems must take different operating conditions and load profiles, as well as design and market specific requirements, into consideration. This applies not only to components such as the expander, the feed pump, the condenser and the steam generator. Depending on the heat sources that can be utilised, as well as the heat sinks available for dissipating the condensation heat, it is also necessary to select a suitable operating medium and a relevant process. This means that the selected design should result in the highest possible savings and/or benefits in the relevant operating cycles of the target application, ❶.

A heat recovery system in stationary biogas plants is, for example, very different from cyclical applications. There are also major differences between applications in diesel railcars or installations in inland vessels or commercial vehicles.

The design of the basic system is illustrated in ❷. The operating medium is directed into the operating cycle via a controlled feed pump rated at 10 to 60 bar. In a heat exchanger integrated into the exhaust line, the heat in the exhaust gas is used to warm up, evaporate and superheat the operating medium. The superheated steam is decompressed in an expander. This generates additional mechanical energy that can be redirected to the driveline or used as drive power, for example for auxiliary systems. The expanded operating medium is condensed in the condensing heat exchanger and then redirected to the operating medium tank in a closed cycle. The condensing heat exchanger is integrated into the cooling circuit of the drive system.

Via a specifically developed control unit, the heat recovery system is controlled and monitored in line with the available temperature and mass flows. Relevant links to the engine, vehicle and systems control enable an interchange of control systems and the integration into the overall system.

Apart from selecting and developing a suitable expander and appropriate operating media, other components such as the evaporator, the fuel pump and the control valves also had to be newly designed, produced and tested, as they are currently not available from other sources.

It was then a question of adapting these basic findings to the various fields of application and the broad utilisation spectrum.

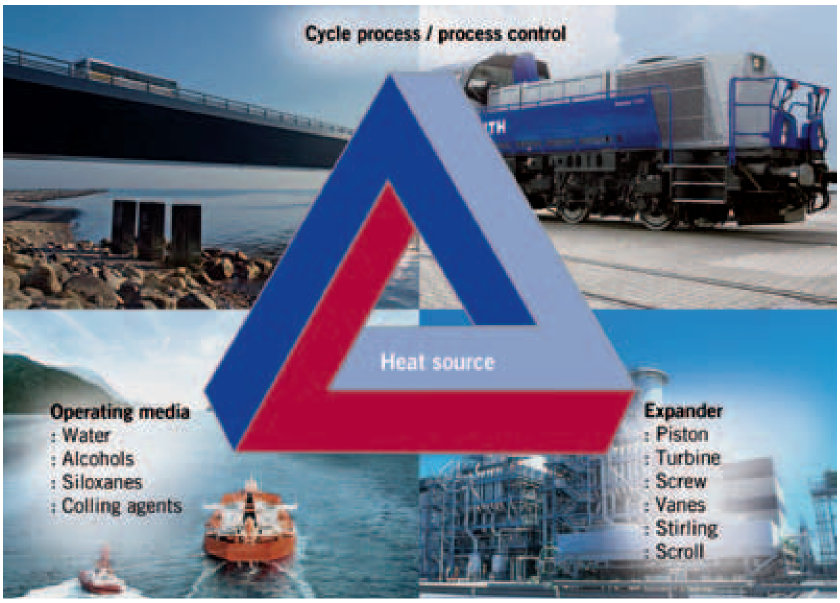

❶ Fields of application for a waste heat recovery system

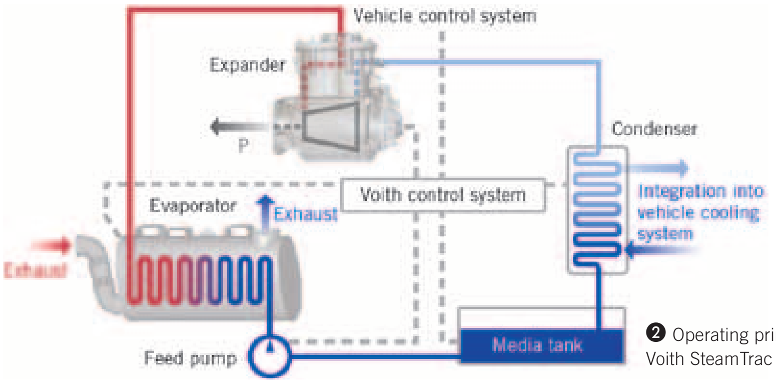

❷ Operating principle of the Voith SteamTrac system

Taking the wide variety of operating conditions, load profiles, constructive and market-specific requirements into consideration, the further design and series development of the respective heat recovery systems differentiates between on-road and non-road applications.

NON-ROAD DEVELOPMENT

The core component of the current SteamTrac system for non-road applications, ❸, is a two-stroke piston expander with an alternating flow principle, valve control and integrated lubrication system. The two-cylinder variation in serial design has an expansion volume of 800 cm^3 and is designed for a speed range of 600 to 3500 rpm. At 370 °C and an operating pressure of 60 bar it achieves a nominal output of 40 kW.

The first series applications of the waste heat recovery system can be found in combined heat and power stations.

In the UK, plants for generating energy from gas deposits have been in operation for about six months; in Germany, the first biogas applications entered service a few months ago.

Depending on the application and the existing engine technology, the feed-in power can be increased by 6 to 11 %, while the fuel consumption remains the same. Through cogeneration, the condensation heat can be utilised further. The operating medium is clean tap water.

In the marine industry, a first prototype application has already been projected, simulated and built. The integration and commissioning installation into the vessel was scheduled for March 2011. Calculations and simulations have shown that, depending on the operating loads, input power increases of up to 10 % can be expected, or, alternatively, a reduction in fuel consumption and CO_2 reductions of up to 6 %. Here, too, the first applications run with clean tap water.

Due to their differing transient load profiles, rail applications were used as a design and test basis right from the beginning of the development. The first integration trials in a diesel railcar drivetrain took place as early as May 2009. After several validation phases, two applications are currently integrated in railcars. A complete Powerpack with integrated SteamTrac system has been installed, following conclusive tests in the systems test field. A further system will be integrated into an existing vehicle during the course of a major overhaul. This project is being sponsored by the German State of Baden-Württemberg as part of a public transport innovation program.

Both systems are being thoroughly tested in trial runs, followed by applications in everyday public transport operation. According to the latest measurements of real-time transient operating profiles on the test stand, fuel savings and CO_2 reductions in the range of 5 to 8 % can be expected. In order to comply with downsizing efforts, future applications can run with a smaller diesel engine, as the SteamTrac improves the vehicle performance by up to 10 %. These applications use an eco-friendly, water-based medium.

Apart from the aforementioned add-on systems, future applications in rail systems will also use engine-integrated solutions.

The basis of these developments is the new Voith V8 diesel engine with a nominal output of 500 kW that has been designed specifically for rail applications.

Through the application of two-stage exhaust gas turbocharging with cooled exhaust gas recirculation, the Voith V8 complies with the exhaust norm Stage IIIB. The exhaust gas treatment is restricted to a maintenance-free particle catalyser.

❸ Expander R2/800 for NRMM applications – examples: train, biogas plant, tug boat, engine integration

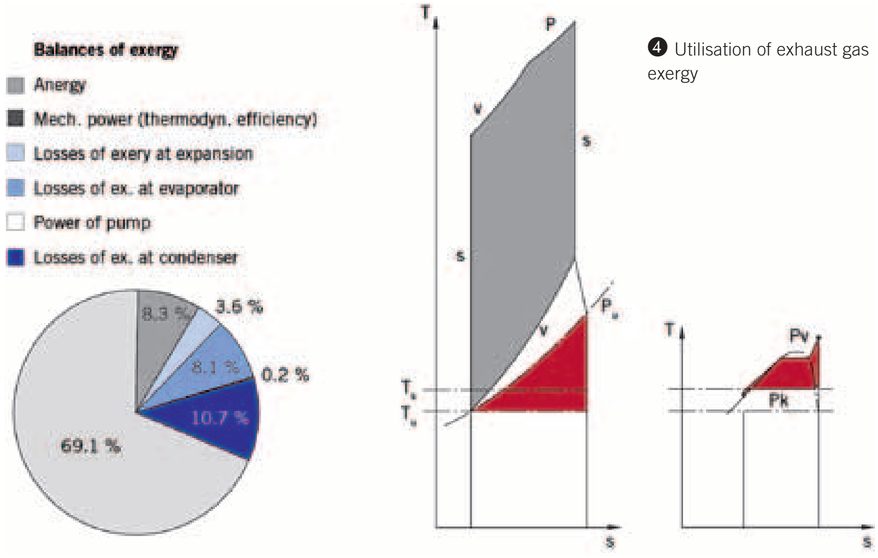

❹ Utilisation of exhaust gas exergy

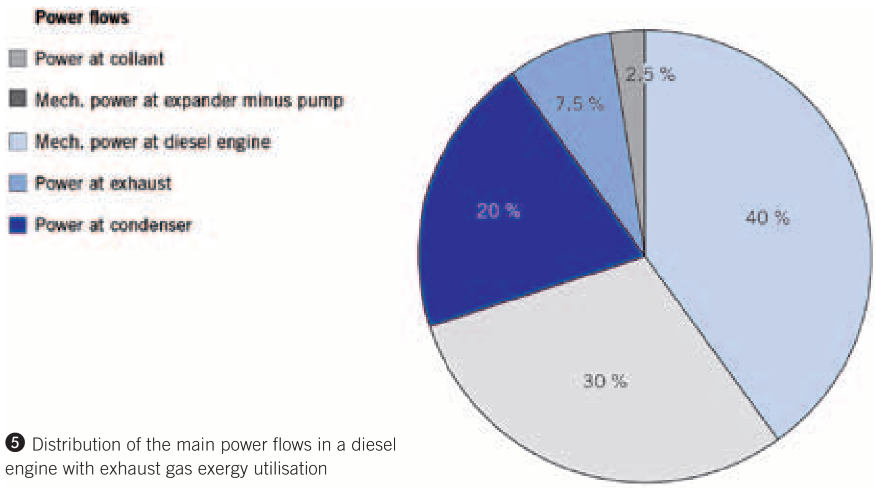

❺ Distribution of the main power flows in a diesel engine with exhaust gas exergy utilisation

By utilising waste heat via the SteamTrac system, which adds extra torque to the crankshaft, fuel savings of 5 to 7 % are currently achieved in the relevant C1-cycle-point for railcars. As approximately 25 % of the weighting takes place in the idling range, the total cyclical savings amount to nearly 5.4 %.

Due to the weighting (60 % idling speed), the overall cyclical advantage in the locomotive-relevant F-cycle amounts to about 2.8 %.

At present, the system is integrated into the engine periphery. The purpose of this exercise is to utilise waste heat and simultaneously reduce the output of the cooling system. Additionally, the complexity of downstream exhaust gas treatment systems in non-road applications is constantly rising. It is therefore increasingly important that any impact on these emission and approval-relevant units is excluded.

Apart from the development of waste heat recovery evaporators, the emphasis also lies on a single-cylinder expander that is adapted to the installation conditions and directly mounted on a PTO of the diesel engine. The fuel and lube pump, the control components and the condenser are also adapted to the engine periphery.

First measurements on the test stand with all relevant components showed an output increase from the expander of 16.5 kW. At the same time, the load on the low-temperature cycle is reduced by 48 %, i.e. the design of the LT cooling system can be adapted to the smaller dimensioned WHR aftercooler. The condensation of the waste heat recovery system moves into the high-temperature cycle, where the design is less critical in relation to the exterior temperature.

The values shown refer to the current application of the diesel engine. The engine-proof integration of the WHR system allows a further criterion for the emission and fuel behaviour. After the completion of the component tests, the overall applications for various rail installations are carried out.

ON-ROAD DEVELOPMENT

Voith Turbo Verdichtersysteme GmbH & Co. KG based in Zschopau is a company of the Voith Turbo Market Division Road and has been looking at on-road applications of the Voith Waste Heat Recovery (WHR) system since 2009. Here, too, the basic principle is the Clausius-Rankine steam process. The immediate goal and the first development stage is the development of a fully functioning system that takes the truck environment into account. Moreover, it is intended to prove that such a system is technically and economically viable.

Conditions for commercial vehicle applications such as:

: the lowest possible impact on payload, i.e. the system's mass should definitely be less than 150 kg
: cost amortisation for the truck users within one to two years
: integration into the existing vehicle installation space possible
: use of the front surface for heat removal, possible with modified cooling system of the vehicle.

The latter is less relevant if the focus is mainly on long-distance trucks. Unlike rail vehicles with their strong fluctuations (starting – coasting), long-distance trucks level out on a so-called 80 kW operating point with low fluctuations. The reason for this is the higher rolling and air resistance of commercial vehicles. Although there are manufacturer-related engine differences, one can still assume an exhaust mass flow of approximately 720 kg/h at about 600 K (327 °C), which results in a heat output into the environment of approximately 60 kW. To simplify matters, the values under review are the average values of the exhaust and the WHR mass flow. The temperature levels of other heat sources are too low.

If one directs this heat output to a heat process downstream from the combustion engine, the exergy of this heat out-

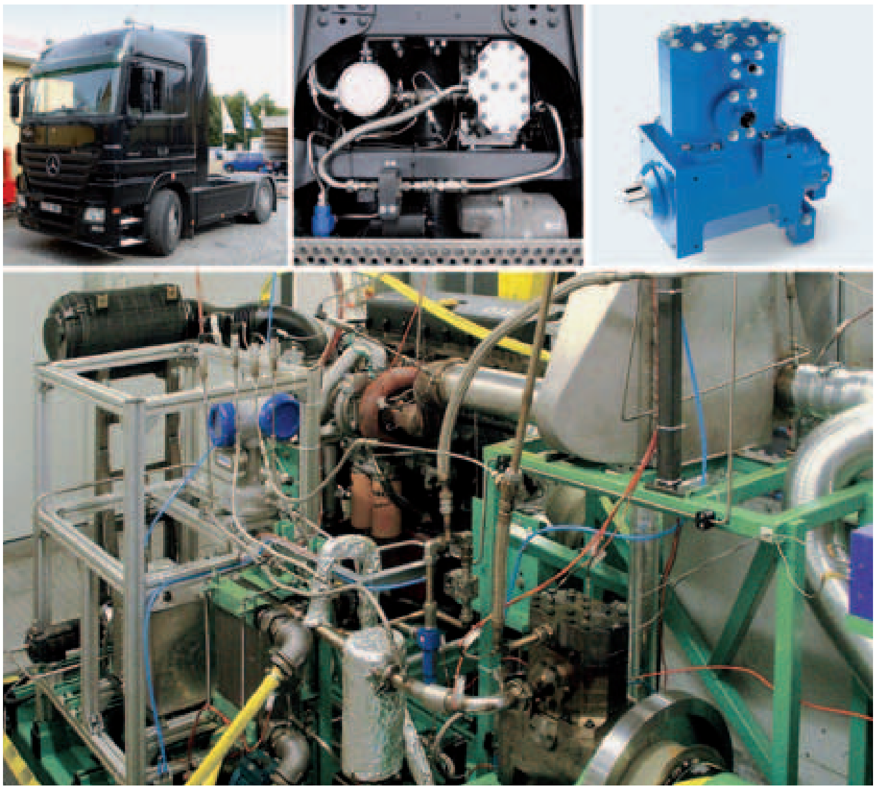

❻ Expander for on-road applications on a stationary test stand and integration into a rolling test stand

put can, to some degree, be converted into mechanical power. The exergy at an ambient temperature of approximately 300 K (27 °C) is still about 18.5 kW. This results in a maximum thermal efficiency of just under 31 % in terms of exhaust heat output. ❹ illustrates the situation. The example uses a simple Seiliger process (without a turbocharger), which should be sufficient with a view to the exhaust gas exergy balance.

On the left hand side, one can see the theoretically usable exergy as a triangular shape. These exergy characteristics with a continuously rising temperature when heat is added, but a constant temperature when heat is dissipated, are only offered by the classic steam power process, consisting of a feed pump, evaporator, expander and condenser with a fluid that provides trans-critical heat supply and sub-critical heat dissipation at proportionally low pump outputs. Such fluids have a critical temperature of approximately 200 °C and are comparably light molecules. ④ (centre) therefore shows an optimised steam power process using ethanol as fluid. Apart from its thermodynamic properties, ethanol is also preferred because of its anti-freeze qualities, as well as for ecological reasons and due to its wide availability. The illustration on the right also shows that the highest exergy losses occur because of the relatively high temperature difference during the heat dissipation in the condenser. Additional exergy losses take place mainly in the evaporator and during expansion, so that the utilisation of ethanol results in a performance increase and fuel savings of at least 6 %, ❺.

Apart from the problem of finding a suitable connection for feeding the mechanical power of the expander at the diesel engine (if possible before the coupling), it is necessary to dissipate an additional 60 % or so of the exhaust gas output to the environment via a heat exchanger. The temperature of the exhaust gas should be lower than that of the usual cooling water temperature of approximately 95 °C. If it is not possible for this to be done via the front surface, there is also the option of installing an additional air-cooled condenser with an exhaust steam-driven fan.

In this varying output and pressure range, the expander has been designed as a piston machine, which allows expansion efficiencies of more than 65 %.

This specific Voith WHR system for trucks is currently being tested on stationary and rolling test stands, ❻.

The core piece is an 800 cm^3 two-stroke expander with integrated pumps for lube oil and operating medium (including a thermostatic bypass valve).

SUMMARY

Compliance with future standards regarding CO_2 reduction is only possible with higher fuel efficiency. On the basis of a steam cycle process in which waste heat is utilised, fuel savings of at least 6 % can be achieved.

With the Voith WHR systems, the first waste heat recovery systems are already in series operation. Early applications in rail vehicles, vessels and trucks demonstrate the broad technical feasibility of waste heat recovery systems.

Relevant applications of the complete 'engine-waste heat recovery unit' system and the integration of a waste heat recovery system into the engine periphery offer the most viable potential in terms of fuel optimisation and reduction of emissions. It is therefore unlikely that future engine-driven systems can operate efficiently without a waste heat recovery system.

PEER REVIEW ATZ | MTZ

PEER REVIEW PROCESS FOR RESEARCH ARTICLES IN ATZ AND MTZ

STEERING COMMITTEE

Prof. Dr.-Ing. Lutz Eckstein	RWTH Aachen University	Institut für Kraftfahrzeuge Aachen
Prof. Dipl.-Des. Wolfgang Kraus	HAW Hamburg	Department Fahrzeugtechnik und Flugzeugbau
Prof. Dr.-Ing. Ferit Küçükay	Technische Universität Braunschweig	Institut für Fahrzeugtechnik
Prof. Dr.-Ing. Stefan Pischinger	RWTH Aachen University	Lehrstuhl für Verbrennungskraftmaschinen
Prof. Dr.-Ing. Hans-Christian Reuss	Universität Stuttgart	Institut für Verbrennungsmotoren und Kraftfahrwesen
Prof. Dr.-Ing. Ulrich Spicher	Universität Karlsruhe	Institut für Kolbenmaschinen
Prof. Dr.-Ing. Hans Zellbeck	Technische Universität Dresden	Lehrstuhl für Verbrennungsmotoren

ADVISORY BOARD

Prof. Dr.-Ing. Klaus Augsburg
Prof. Dr.-Ing. Bernard Bäker
Prof. Dr.-Ing. Michael Bargende
Prof. Dipl.-Ing. Dr. techn. Christian Beidl
Dr.-Ing. Christoph Bollig
Prof. Dr. sc. techn. Konstantinos Boulouchos
Prof. Dr.-Ing. Ralph Bruder
Dr. Gerhard Bruner
Prof. Dr. rer. nat. Heiner Bubb
Prof. Dr. rer. nat. habil. Olaf Deutschmann
Dr. techn. Arno Eichberger
Prof. Dr. techn. Helmut Eichlseder
Dr.-Ing. Gerald Eifler
Prof. Dr.-Ing. Wolfgang Eifler
Prof. Dr. rer. nat. Frank Gauterin
Prof. Dr. techn. Bernhard Geringer
Prof. Dr.-Ing. Uwe Grebe
Prof. Dr.-Ing. Horst Harndorf
Prof. Dr. techn. Wolfgang Hirschberg
Univ.-Doz. Dr. techn. Peter Hofmann
Prof. Dr.-Ing. Bernd-Robert Höhn
Prof. Dr. rer. nat. Peter Holstein
Dr. techn. Heidelinde Holzer
Prof. Dr.-Ing. habil. Werner Hufenbach
Prof. Dr.- Ing. Roland Kasper
Prof. Dr.-Ing. Tran Quoc Khanh
Dr. Philip Köhn
Prof. Dr.-Ing. Ulrich Konigorski
Dr. Oliver Kröcher
Dr. Christian Krüger
Univ.-Ass. Dr. techn. Thomas Lauer
Prof. Dr. rer. nat. Uli Lemmer
Dr. Malte Lewerenz
Prof. Dr.-Ing. Markus Lienkamp
Prof. Dr. rer. nat. habil. Ulrich Maas
Prof. Dr.-Ing. Martin Meywerk
Prof. Dr.-Ing. Klaus D. Müller-Glaser
Dr. techn. Reinhard Mundl
Prof. Dr. rer. nat. Cornelius Neumann
Dr.-Ing. Lothar Patberg
Prof. Dr.-Ing. Peter Pelz
Prof. Dr. techn. Ernst Pucher
Dr. Jochen Rauh
Prof. Dr.-Ing. Konrad Reif
Prof. Dr.-Ing. Stephan Rinderknecht
Dr.-Ing. Swen Schaub
Prof. Dr. sc. nat. Christoph Schierz
Prof. Dr. rer.-nat. Christof Schulz
Prof. Dr. rer. nat. Andy Schürr
Prof. Dr.-Ing. Ulrich Seiffert
Prof. Dr.-Ing. Hermann J. Stadtfeld
Prof. Dr. techn. Hermann Steffan
Prof. Dr.-Ing. Wolfgang Steiger
Prof. Dr.-Ing. Peter Steinberg
Prof. Dr.-Ing. Christoph Stiller
Dr.-Ing. Peter Stommel
Prof. Dr.-Ing. Wolfgang Thiemann
Prof. Dr.-Ing. Helmut Tschöke
Dr.-Ing. Pim van der Jagt
Prof. Dr.-Ing. Georg Wachtmeister
Prof. Dr.-Ing. Jochen Wiedemann
Prof. Dr. techn. Andreas Wimmer
Prof Dr. rer. nat. Hermann Winner
Prof. Dr. med. habil. Hartmut Witte

Scientific articles of universities in ATZ Automobiltechnische Zeitschrift and MTZ Motortechnische Zeitschrift are subject to a proofing method, the so-called peer review process. Articles accepted by the editors are reviewed by experts from research and industry before publication. For the reader, the peer review process further enhances the quality of the magazines‘ content on a national and international level. For authors in the institutes, it provides a scientifically recognised publication platform.

In the ATZ | MTZ Peer Review Process, once the editors has received an article, it is reviewed by two experts from the Advisory Board. If these experts do not reach a unanimous agreement, a member of the Steering Committee acts as an arbitrator. Following the experts' recommended corrections and subsequent editing by the author, the article is accepted.

In 2008, the peer review process utilized by ATZ and MTZ was presented by the WKM (Wissenschaftliche Gesellschaft für Kraftfahrzeug- und Motorentechnik e. V. / German Professional Association for Automotive and Motor Engineering) to the DFG (Deutsche Forschungsgemeinschaft / German Research Foundation) for official recognition.

LIFETIME PREDICTION OF COMPRESSOR WHEELS

AUTHORS

DIPL.-ING. PHILIPP VON HARTROTT is Scientist in the Group Lifetime-concepts, Thermomechanics at the Fraunhofer Institute for Mechanics of Materials IWM in Freiburg (Germany). He was responsible as Project Manager at Fraunhofer IWM.

DIPL.-PHYS. CHRISTOPH SCHWEIZER is Scientist in the Group Lifetime-concepts, Thermomechanics at the Fraunhofer Institute for Mechanics of Materials IWM in Freiburg (Germany).

DR.-ING. KARL-HEINZ LANG is Head of the Section Fatigue at the Institute of Materials Science and Engineering I of the Karlsruhe Institute of Technology (KIT) (Germany). He was responsible as Project Manager at the KIT.

DIPL.-ING. OSAMA KHALIL was Scientific Assistant of the Research Project at KIT. He is now working as a Material Engineer in the Plant Monitoring Section at the BP Gelsenkirchen GmbH (Germany).

Further engine optimisation will in the future result in even higher requirements being placed on the material of compressor wheels in exhaust gas turbochargers. To address this issue, a computer model has been developed within the framework of the FVV research project No. 897 “Enhanced methods for the lifetime calculation of exhaust gas turbocharger radial compressor wheels made of high temperature resistant aluminium alloys” at the Fraunhofer Institute for Mechanics of Materials (IWM) and the Karlsruhe Institute of Technology (KIT) that enables material fatigue in the compressor wheel material to be predicted.

THE SEAL OF APPROVAL FOR SCIENTIFIC ARTICLES IN MTZ.
MTZ PEER REVIEW
RECEIVED 2010-12-09
REVIEWED 2010-12-23
ACCEPTED 2011-01-17
REVIEWED BY EXPERTS FROM RESEARCH AND INDUSTRY.

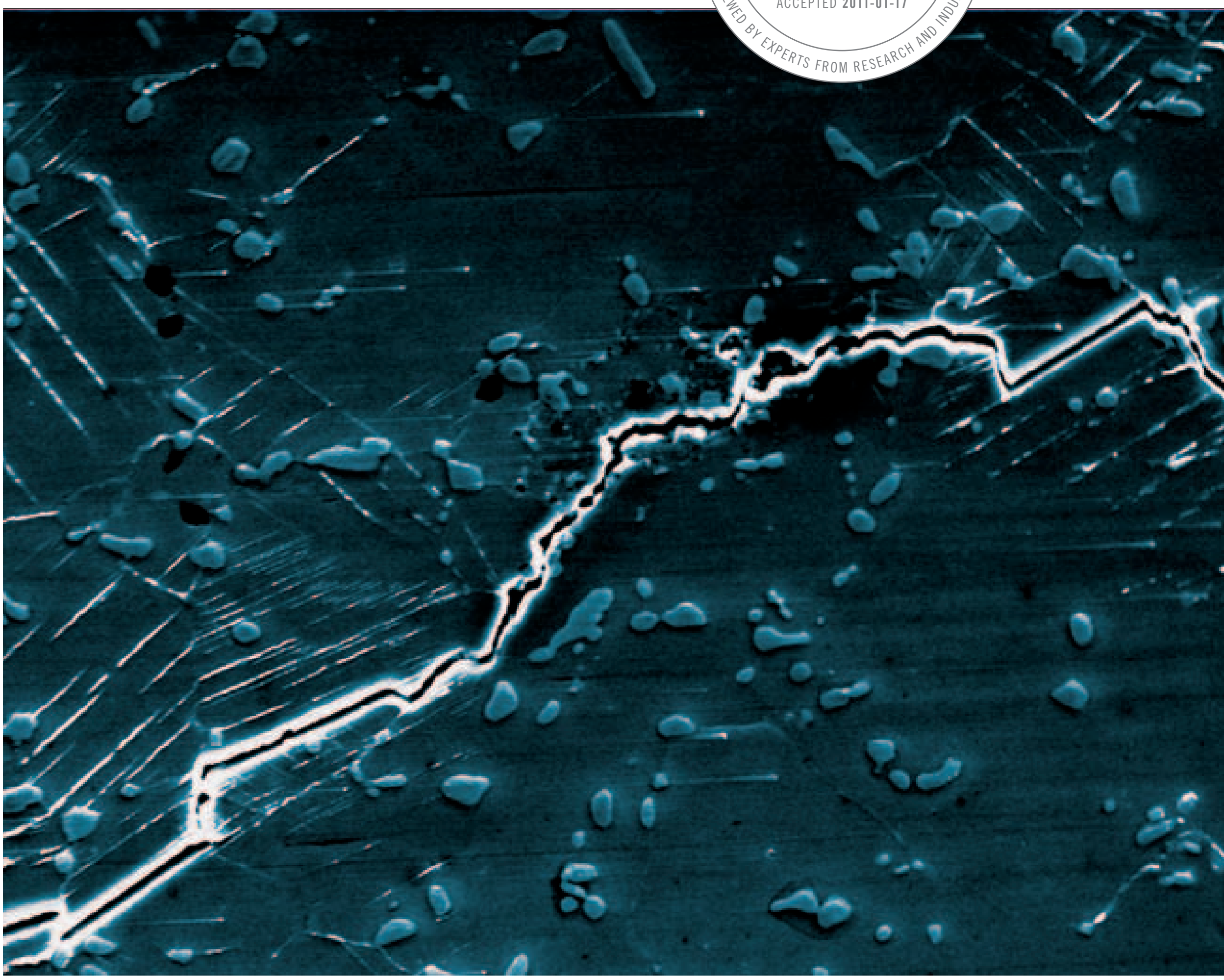

1 INCREASING MATERIAL REQUIREMENTS

The high temperature resistant aluminum alloy of the type 2618 is currently used as standard material for turbo-chargers in engines of passenger cars, trucks and large ships. Since future demands go along with higher circumferential velocities and compressor temperatures, the material will be exposed to higher loadings. Thus, simulation tools are needed, which help to optimize the component during the initial design stage with regard to lifetime and material usage. The development of such simulation tools was the objective of the FVV-research project "Improved methods for lifetime prediction of high temperature aluminum alloy compressor wheels for turbochargers" [1]. To this end the material properties were determined in an experimental part of the project. The theoretical part contained the development of suitable plasticity and lifetime models, which were fitted to the experimental data. All models were implemented in commercial finite element programs and applied to a component test.

2 EXPERIMENTAL PROGRAM FOR THE MATERIAL CHARACTERIZATION

As a basis for the numerical lifetime prediction under operation loading conditions a sound database of experimental data was generated. This data comprises deformation and damage related data. To this end hot tensile and compressive tests, short term relaxation tests, creep tests, isothermal and nonisothermal low cycle fatigue (LCF) tests as well as tests with changing maximum loads and deformation velocities were conducted at service-relevant temperatures. The isothermal LCF life was studied on smooth and notched specimens. An important contribution was the investigation of the damage evolution on polished specimens in interrupted LCF experiments. The data and material parameters were identified in the temperature range from 20 °C to 180 °C. For the observed features the interaction of cyclic loading and temperature dependent material behavior is of importance. The LCF life increases for a given strain amplitude with increasing temperature from room temperature to 150 °C. This can be ascribed to decreasing stresses, especially decreasing maximum stresses, which are primarily responsible for the fatigue damage. The effect is on one hand related to the decreasing Youngs modulus. On the other hand the decreasing strain hardening for bigger amplitudes leads to lower stresses. The maximum life is at about 150 °C. Further increase of the temperature leads to a small decrease in LCF life, although the cycling limit of 100,000 cycles was reached with a strain amplitude of 0.3 % at 180 °C. From 150 °C onward, especially at low and medium strain amplitudes, cyclic softening can be observed. Subsequently the damage evolution was studied in detail at two typical service temperatures (T = 80 °C and T = 180 °C) on polished specimens using scanning electron microscopy.

The study of the fatigue damage evolution confirms the different crack initiation behaviors for the investigated temperatures. At 80 °C crack initiation was exclusively observed on grain boundaries. The areas close to grain boundaries experienced heavy plastic deformations. The first micro cracks were observed there. This might be attributed to poor precipitation hardening in these areas [2]. These areas can be deformed plastically more easily but the cyclic durability is much weaker. This makes the grain boundaries the week links of the microstructure. During the crack growth phase the weak grain boundaries dominate, on the surface as well as inside the specimen. The final failure of the specimen at room temperature is a brittle fracture. The fracture surface shows a semi-circular crack (fatigue crack) with isolated grains lying open. At 180 °C the areas close to the grain boundaries are also heavily plasticized. Additionally pronounced slip bands can be observed inside the grains, which is attributed to the softening of the material with the higher temperature. The micro cracks appear on grain boundaries as well as on slip bands inside grains. The intergranular cracks grow faster than the transgranular cracks. Therefore mostly intergranular crack growth is observed at 180 °C. With an increasing number of cycles to failure the fraction of transgranular cracks increases but the intergranular cracks still dominate. ❶ shows the observed surface crack length over the cycles to failure for 80 °C and 180 °C. The crack initiation phase takes about one third of the total fatigue life at 180 °C. At 80 °C the initiation phase can take up to 80 %. The subsequent stable crack growth at 180 °C is significantly slower than at 80 °C. Apparently the bigger ductility of the material at 180 °C leads to earlier crack initiation but subsequently to slower crack growth because of the higher amount of plasticization at the crack tip.

3 MODEL FOR CYCLIC PLASTICITY

In order to describe the deformation phenomena in a compressor wheel, a time and temperature dependent plasticity model according to Chaboche [3] and Jiang [4] was implemented, which allows

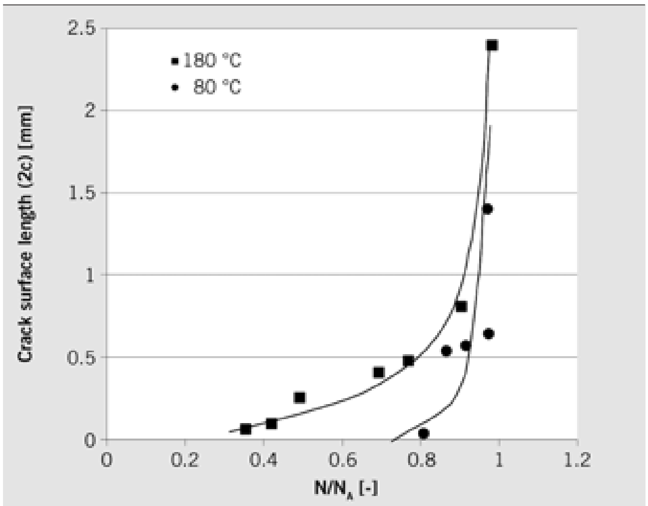

❶ Surface crack length over nomalized number of cycles to failure for $\varepsilon_{a,tot}$ = 0.4 % at T = 80 °C and 180 °C to account for strain rate, relaxation and ratchetting effects. In the following the model equations are presented. The stresses are computed from

EQ. 1

$$\dot{\sigma}_{ij} = C_{ijkl}(\dot{\varepsilon}_{kl} - \dot{\varepsilon}^{th}_{kl} - \dot{\varepsilon}^{vp}_{kl}) + \frac{\partial C_{ijkl}}{\partial T} C^{-1}_{klmn}\sigma_{mn}\dot{T}$$

where C_{ijkl} is the forth-order elasticity tensor and T is the temperature. The thermal strain rate is calculated with the differential expansion coefficient α^{th}:

EQ. 2

$$\dot{\varepsilon}^{th}_{ij} = \alpha^{th}\dot{T}\,\delta_{ij}$$

δ_{ij} is the second order unity tensor. For the viscoplastic strain rate a power-law relationship is used:

EQ. 3

$$\dot{\varepsilon}^{vp}_{ij} = \frac{3}{2}\,\dot{p}\,\frac{\beta_{ij}}{\beta_{eq}} \text{ with } \dot{p} = \left\langle\frac{\beta_{eq} - \sigma_Y}{K}\right\rangle^{n}$$

$\beta_{ij} = \sigma'_{ij} - \alpha_{ij}$ is the effective stress, where σ'_{ij} is the deviatoric part of the stress tensor and α_{ij} denotes the backstress tensor. β_{eq} is the von Mises equivalent stress. Two backstresses are used, whose evolution equations are given in the following:

EQ. 4

$$\dot{\alpha}^{(k)}_{ij} = C^{(k)}\,\dot{\varepsilon}^{vp}_{ij} - \gamma^{(k)}\,W^{(k)}\,\varphi^{(k)}\,\dot{p}\,\alpha^{(k)}_{ij} - R^{(k)}\alpha^{(k)}_{ij} + \frac{\partial C^{(k)}}{\partial T}\,\frac{1}{C^{(k)}}\,\dot{T}\alpha^{(k)}_{ij},\; k = 1,2$$

The function $W^{(k)}$ accounts for ratchetting effects:

EQ. 5

$$W^{(k)} = \left(\frac{\gamma^{(k)}}{C^{(k)}}\,\alpha^{(k)}_{eq}\right)^{\chi^{(k)}}$$

The function φ is introduced to model cyclic hardening and softening:

EQ. 6

$$\varphi^{(k)} = \varphi^{(k)}_{ss} + (1 - \varphi^{(k)}_{ss})e^{\omega^{(k)}p}$$

The model contains the following temperature dependent material parameters:

: E and α^{th} describing the thermoelastic properties of the material
: K and n describing the viscous properties of the material
: σ_Y, $C^{(k)}$, $\gamma^{(k)}$, $R^{(k)}$, $\varphi_{ss}^{(k)}$, $\omega^{(k)}$ and $\chi^{(k)}$, describing the plastic and hardening properties of the material.

In order to efficiently determine the model parameters, cyclic tests with a complex strain history were performed. They comprise two different strain amplitudes (0.5 and 0.7 %), different strain rates (10^{-5}–10^{-3}/s) as well as dwell times in tension and compression. ❷ shows the complex strain history. ❸ shows the stress response of the material (symbols) and the model adjustment (lines) as a function of time for 80 °C, 150 °C and 180 °C. The corresponding stress-strain hysteresis loops are shown in ❹.

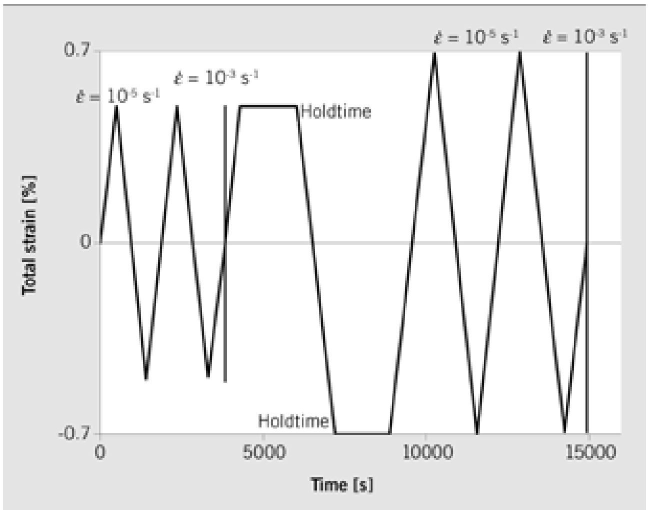

❷ Strain-time history of a complex cyclic test to efficiently determine the model parameters

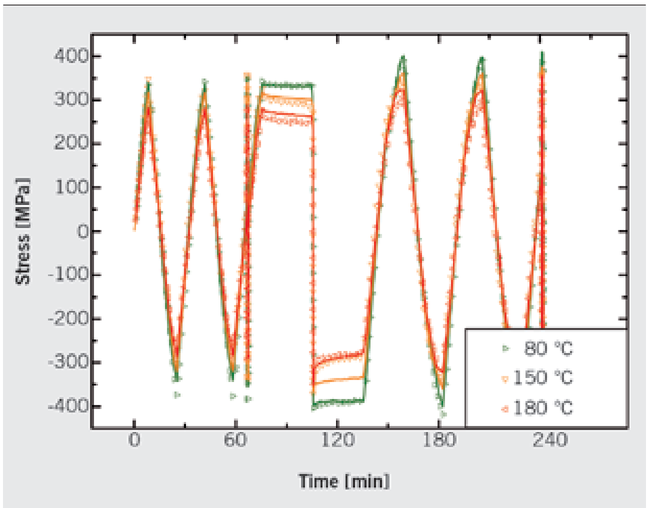

❸ Stress history for the complex cyclic test program (lines = model, symbols = tests)

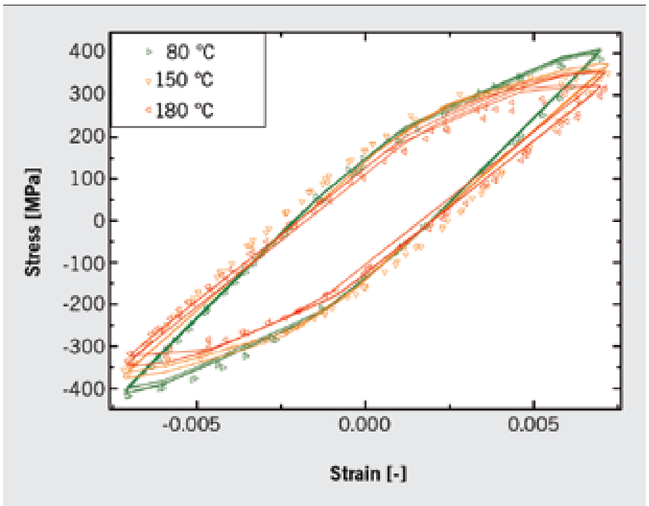

❹ Stress-strain hysteresis loops from minute 150 to minute 241 (lines = model, symbols = tests)

The plasticity model is capable of describing the time dependent and cyclic plasticity of the material over a wide loading range. In the course of the research project, single tests on aged specimens were performed. The mechanical properties strongly differ from the original heat treated T6 state. Thus, long term tests at high temperatures cannot be described by the model due to the change of microstructure, which is not accounted for in the model. To incorporate microstructural changes in a mechanical model will be the subject of future works.

4 MODELING OF LIFETIME

The lifetime model has its origin in a physical model, which is based on the growth of small fatigue cracks. It is assumed that the fatigue crack growth increment per cycle da/dN is proportional to the cyclic crack-tip opening displacement ΔCTOD:

EQ. 7

$$\frac{da}{dN} = \beta \Delta CTOD$$

Using elastic-plastic fracture mechanics ΔCTOD can be computed as follows:

EQ. 8

$$\Delta CTOD = d_N \frac{Z_D}{\sigma_{cy}} a$$

Here a denotes the crack length, σ_{cy} is the cyclic yield stress and d_N is a function of the macroscopic hardening behavior. For power-law hardening materials, which follow a Ramberg-Osgood type law, d_N is given by the singular crack-tip fields according to Hutchinson, Rice and Rosengren [5-7]. The damage parameter according to Heitmann Z_D [8] is valid for small semicircular surface cracks and a Poisson's ratio of 0.3 and proportional loadings:

EQ. 9

$$Z_D = 1{,}45 \frac{\Delta\sigma^2_{I,\,eff}}{E} + 2{,}4 \frac{\Delta\sigma_I^2 \Delta\varepsilon_{e,\,pl}}{\Delta\sigma_e \sqrt{1+3N}}$$

Δσ and $\Delta\varepsilon_{pl}$ are the stress and plastic strain range, respectively. The indices I and e refer to the maximal principal and equivalent stresses and strains, respectively. Young's modulus is denoted by E and N is the hardening exponent according to Ramberg-Osgood. Z_Da is an approximation for the effective cyclic J-integral ΔJ_{eff}. Crack closure, which is important for fatigue crack growth, is accounted for by the use of an effective stress range $\Delta\sigma_{eff}$. E. g. $\Delta\sigma_{eff}$ can be computed by the crack closure formula according to Newman [9], which has proved its validity for aluminium alloys. Beside the load ratio R the crack closure formula according to Newman also accounts for maximum stress effects. The model predicts an increasing amount of damage with higher load ratios and maximum stresses.

In order to receive an expression for the lifetime, it is assumed that the crack growth phase dominates the lifetime. Integration of Eq. 7 from an initial crack length to a technical crack length at failure leads to the following functional expression:

EQ. 10

$$N_A = A\left(d_N \frac{Z_D}{\sigma_{CY}}\right)^{-B}$$

Here A and B are adjustable parameters. For the computation of the part in brackets of Eq. 10, E, N and σ_{CY} are taken from a stabilized hysteresis loops at midlife.

The fracture mechanics parameter $d_N Z_D/\sigma_{cy}$ is correlated with the experimental lifetimes in ❺. The model parameters A and B were fitted by a least square fit. The model line corresponds to a medium probability of failure. The fracture mechanics parameter in combination with the crack closure formula according to Newman is able to describe the lifetimes very well. Altogether only eight out of 78 LCF-tests fall out of a scatterband of factor two (dashed lines).

5 APPLICATION TO A COMPONENT TEST

The plasticity and lifetime model were implemented into the commercial finite element programs Abaqus and Ansys using the function interface Umat and Usermat, respectively. The finite element

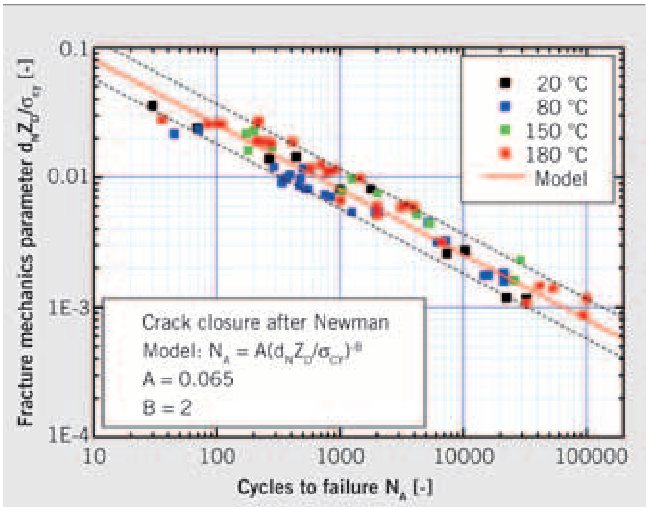

❺ Fracture mechanics parameter over the number of cycles to failure for the crack closure formula according to Newman (lines = model with scatter band of factor 2, symbols = tests)

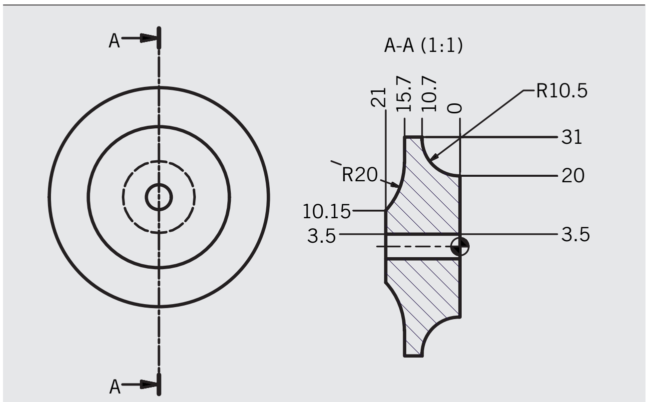

❻ Geometry of the component for the centrifuging test (all numbers in mm)

personal buildup for Force Motors Ltd.

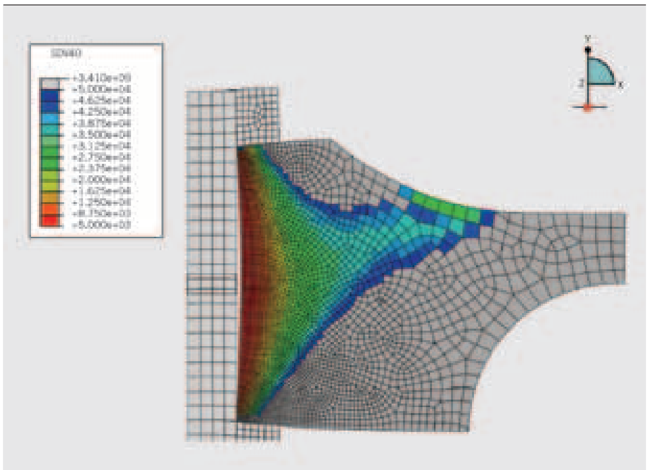

❼ Calculated lifetime distribution of the model (the colour code indicates shorter (red) and longer (blue) life of the component)

software was used to simulate a component like specimen. The geometry is shown in ❻. The specimen was tested by the working group member Voith Turbo Aufladungssysteme GmbH & Co. KG in a centrifuging test.

The lifetime was calculated by the Abaqus implementation. To this end, a pretension was applied to the component in a first step to fix it on the shaft. In a second step, three load cycles were calculated and the final cycle was used for the lifetime calculation. The cycle time was chosen to be 40 s according to the centrifuging test. The minimum and maximum rotational velocities were 10,000 and 200,000 rpm, respectively. The distribution of the calculated lifetime is shown ❼. Areas with a short lifetime are red. The element with the minimum lifetime (6250 cycles) determined the lifetime of the whole component. It is assumed that the 1 mm crack length criterion of the model predicts the life of the component, because of fast crack growth thereafter. The centrifuging test ended after 5550 cycles with fracture of the specimen. An overview picture of fractured specimen is illustrated in ❽.

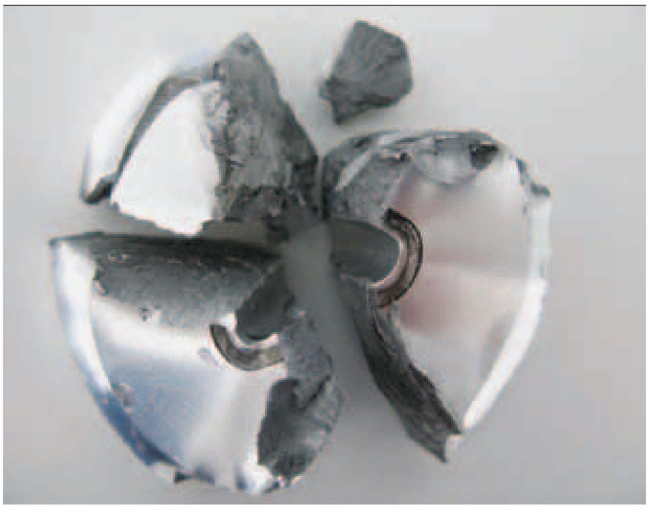

❽ Specimen tested at Voith Turbo (T = 50 °C, N_f = 5550 cycles)

6 CONCLUSIONS

The finite element implementations of the models are available to predict a component life with acceptable computational time. For the component like specimen the visco-plastic model took about six times the computation time of a purely elastic computation.

The models developed within this project predicted 6250 cycles to failure. This is in very good agreement with the experimental findings. The assessment of the specimen test was successful. It has to be noted that uniaxial tests with comparable conditions (temperature, R-ratio, cycles to failure) had an average scatter of factor 1.2 with single occurrences up to a factor of 1.65. The authors have no information about scatter of comparable component tests.

The very successful work of the FVV working group will be continued in a continuation-project focusing on over-ageing of material during service.

REFERENCES

[1] Verbesserte Methoden zur Lebensdauerberechnung von Abgasturbolader-Radialverdichterrädern aus hochwarmfesten Aluminiumlegierungen. Abschlussbericht des FVV-Vorhabens Nr. 897, Heft 911, 2010

[2] Vasudevan, A. K.; Doherty, R. D.: Grain boundary ductile fracture in precipitation hardened alloys. In: Acta Metall 35 (1987), No. 6, p. 1193-1219

[3] Lemaitre, J.; Chaboche, J.-L.: Mechanics of Solid Materials. Cambridge University Press, 1995

[4] Jiang, Y.; Sehitoglu, H.: Modelling of cyclic ratchetting plasticity, Part II: Comparison of model simulations with experiments. In: J. Appl. Mech. 63 (1996), p. 726-733

[5] Hutchinson, J. W.: Singular behaviour at the end of a tensile crack in a hardening material. In: J Mech Phys Solids 16 (1968), p. 13-31

[6] Rice, J. R.; Rosengren, G. F.: Plane strain deformation near a crack tip in a power-law hardening material. In: J Mech Phys Solids 16 (1968), p. 1-12

[7] Shih, C. F.: Relationships between the J-Integral and the crack opening displacement for stationary and extending cracks. In: J Mech Phys Solids 29 (1981), No. 4, p. 305-326

[8] Heitmann, H. H.; Vehoff, H.; Neumann, P.: Advances in Fracture Research 84 – Proc. of ICF6 vol 5 (eds. Valuri et al.). Oxford/New York: Pergamon Press Ltd., 1984, p. 599-606

[9] Newman, J. C.: A crack opening equation for fatigue crack growth. In: International Journal of Fracture 24 (1984), p. 131-135

THANKS

The authors thank the Bundesministerium für Wirtschaft und Technologie and the Arbeitsgemeinschaft industrieller Forschungsvereinigungen e. V. for the funding under grant no. 14651. The Forschungsvereinigung Verbrennungskraftmaschinen FVV e. V. is thanked for the coordination of the project under project no. 897. The FVV working group under the guidance of Dr. Böschen, MTU Friedrichshafen GmbH is thanked for the guidance of the project with inspiring discussions and valuable advice.

IMPRINT

MTZ WORLDWIDE

www.MTZonline.com

Founded 1939 by Prof. Dr.-Ing. E. h. Heinrich Buschmann and Dr.-Ing. E. h. Prosper L'Orange

Organ of the Fachverband Motoren und Systeme im VDMA, Verband Deutscher Maschinen- und Anlagenbau e.V., Frankfurt/Main, for the areas combustion engines and gas turbines
Organ of the Forschungsvereinigung Verbrennungskraftmaschinen e.V. (FVV)
Organ of the Wissenschaftliche Gesellschaft für Kraftfahrzeug- und Motorentechnik e.V. (WKM)
Organ of the Österreichischer Verein für Kraftfahrzeugtechnik (ÖVK)
Cooperation with the STG, Schiffbautechnische Gesellschaft e.V., Hamburg, in the area of ship drives by combustion engine

04 I 2011 _ April 2011 _ Volume 72
Springer Automotive Media I Springer Fachmedien Wiesbaden GmbH
P. O. Box 15 46 · 65173 Wiesbaden · Germany I Abraham-Lincoln-Straße 46 · 65189 Wiesbaden · Germany
Amtsgericht Wiesbaden, HRB 9754, USt-IdNr. DE811148419

Managing Directors Dr. Ralf Birkelbach (Chairman), Armin Gross, Albrecht Schirmacher I **Senior Advertising** Armin Gross I **Senior Marketing** Rolf-Günther Hobbeling
Senior Production Christian Staral I **Sales Director** Gabriel Göttlinger

EDITORS-IN-CHARGE
Dr. Johannes Liebl,
Wolfgang Siebenpfeiffer

EDITORIAL STAFF

EDITOR-IN-CHIEF
Johannes Winterhagen (win)
phone +49 611 7878-342 · fax +49 611 7878-462
johannes.winterhagen@springer.com

VICE-EDITOR-IN-CHIEF
Ruben Danisch (rd)
phone +49 611 7878-393 · fax +49 611 7878-462
ruben.danisch@springer.com

CHIEF-ON-DUTY
Kirsten Beckmann M. A. (kb)
phone +49 611 7878-343 · fax +49 611 7878-462
kirsten.beckmann@springer.com

SECTIONS
Electrics, Electronics
Markus Schöttle (scho)
phone +49 611 7878-257 · fax +49 611 7878-462
markus.schoettle@springer.com
Engine
Ruben Danisch (rd)
phone +49 611 7878-393 · fax +49 611 7878-462
ruben.danisch@springer.com
Online
Katrin Pudenz M. A. (pu)
phone +49 6172 301-288 · fax +49 6172 301-299
redaktion@kpz-publishing.com
Production, Materials
Stefan Schlott (hlo)
phone +49 8191 70845 · fax +49 8191 66002
Redaktion_Schlott@gmx.net
Research
Johannes Winterhagen (win)
phone +49 611 7878-342 · fax +49 611 7878-462
johannes.winterhagen@springer.com
Service, Event Calendar
Martina Schraad (mas)
phone +49 611 7878-276 · fax +49 611 7878-462
martina.schraad@springer.com
Transmission
Dipl.-Ing. Michael Reichenbach (rei)
phone +49 611 7878-341 · fax +49 611 7878-462
michael.reichenbach@springer.com

Dipl.-Ing. (FH) Moritz-York von Hohenthal (mvh)
phone +49 611 7878-278 · fax +49 611 7878-462
moritz.von.hohenthal@springer.com

PERMANENT CONTRIBUTORS
Richard Backhaus (rb), Dipl.-Reg.-Wiss. Caroline Behle (beh), Prof. Dr.-Ing. Stefan Breuer (sb), Jürgen Grandel (gl), Ulrich Knorra (kno), Prof. Dr.-Ing. Fred Schäfer (fs), Roland Schedel (rs)

ENGLISH LANGUAGE CONSULTANT
Paul Willin (pw)

ADDRESS
P. O. Box 15 46, 65173 Wiesbaden, Germany
redaktion@ATZonline.de

MARKETING I OFFPRINTS

PRODUCT MANAGEMENT AUTOMOTIVE MEDIA
Sabrina Brokopp
phone +49 611 7878-192 · fax +49 611 7878-407
sabrina.brokopp@springer.com

OFFPRINTS
Martin Leopold
phone +49 2642 9075-96 · fax +49 2642 9075-97
leopold@medien-kontor.de

ADVERTISING

HEAD OF SALES MANAGEMENT
Britta Dolch
phone +49 611 7878-323 · fax +49 611 7878-140
britta.dolch@best-ad-media.de

KEY ACCOUNT MANAGEMENT
Elisabeth Maßfeller
phone +49 611 7878-399 · fax +49 611 7878-140
elisabeth.massfeller@best-ad-media.de

SALES MANAGEMENT
Sabine Röck
phone +49 611 7878-269 · fax +49 611 7878-140
sabine.roeck@best-ad-media.de

MEDIA SALES
Frank Nagel
phone +49 611 7878-395 · fax +49 611 7878-140
frank.nagel@best-ad-media.de

DISPLAY AD MANAGER
Petra Steffen-Munsberg
tel +49 611 7878-164 · fax +49 611 7878-443
petra.steffen-munsberg@best-ad-media.de

AD PRICES
Price List No. 54 (10/2010)

PRODUCTION I LAYOUT
Heiko Köllner
phone +49 611 7878-177 · fax +49 611 7878-464
heiko.koellner@springer.com

SUBSCRIPTIONS
VVA-Zeitschriftenservice, Abt. D6 F6, MTZworldwide
P. O. Box 77 77, 33310 Gütersloh, Germany
Renate Vies
phone +49 5241 80-1692 · fax +49 5241 80-9620
SpringerAutomotive@abo-service.info

YOUR HOTLINE TO MTZ
Editorial Staff
☎ +49 611 7878-393
Reader's Service
☎ +49 611 7878-151
Advertising
☎ +49 611 7878-395

SUBSCRIPTION CONDITIONS
The eMagazine appears 11 times a year at an annual subscription rate 199 Euro for private persons and 299 Euro for companies. Special rate for students on proof of status in the form of current registration certificate 98 €. Special rate for VDI/ÖVK/VKS members on proof of status in the form of current member certificate 172 €. Special rate for studying VDI members on proof of status in the form of current registration and member certificate 71 €. Annual subscription rate for combination MTZworldwide (eMagazine) and MTZ (print) 398 €. The subscription can be cancelled in written form at any time with effect from the next available issue.

HINTS FOR AUTHORS
All manuscripts should be sent directly to the editors. By submitting photographs and drawings the sender releases the publishers from claims by third parties. Only works not yet published in Germany or abroad can generally be accepted for publication. The manuscripts must not be offered for publication to other journals simultaneously. In accepting the manuscript the publisher acquires the right to produce royalty-free offprints. The journal and all articles and figures are protected by copyright. Any utilisation beyond the strict limits of the copyright law without permission of the publisher is illegal. This applies particularly to duplications, translations, microfilming and storage and processing in electronic systems.

CALIBRATION OF SOLENOID INJECTORS FOR GASOLINE DIRECT INJECTION USING THE KNOCK SENSOR

Precise fuel metering is essential for lower exhaust emissions and increased fuel economy of modern combustion engines. This calls for compensating manufacturing dispersions of fuel injectors as well as maintaining a stable operating behavior during their entire lifetime. To meet this challenge, a method for calibrating solenoid injectors of gasoline direct injection engines has been developed at the Karlsruhe Institute of Technology (KIT).

AUTHORS

DIPL.-ING. KONRAD CHRIST is Research Associate at the Institute of Industrial Information Technology, Karlsruhe Institute of Technology (KIT) (Germany).

DIPL.-ING. KRISTINE BACK is Research Associate at the Institute of Industrial Information Technology, Karlsruhe Institute of Technology (KIT) (Germany).

DIPL.-ING. MEHDI JIQQIR wrote his Master Thesis at the Institute of Industrial Information Technology, Karlsruhe Institute of Technology (KIT) (Germany).

PROF. DR.-ING. UWE KIENCKE was Head of the Institute of Industrial Information Technology, University of Karlsruhe (TH) (Germany).

PROF. DR.-ING. FERNANDO PUENTE LEÓN is Head of the Institute of Industrial Information Technology, Karlsruhe Institute of Technology (KIT) (Germany).

THE SEAL OF APPROVAL FOR SCIENTIFIC ARTICLES IN MTZ.
MTZ PEER REVIEW
RECEIVED 2010-10-05
REVIEWED 2010-11-24
ACCEPTED 2011-01-18
REVIEWED BY EXPERTS FROM RESEARCH AND INDUSTRY.

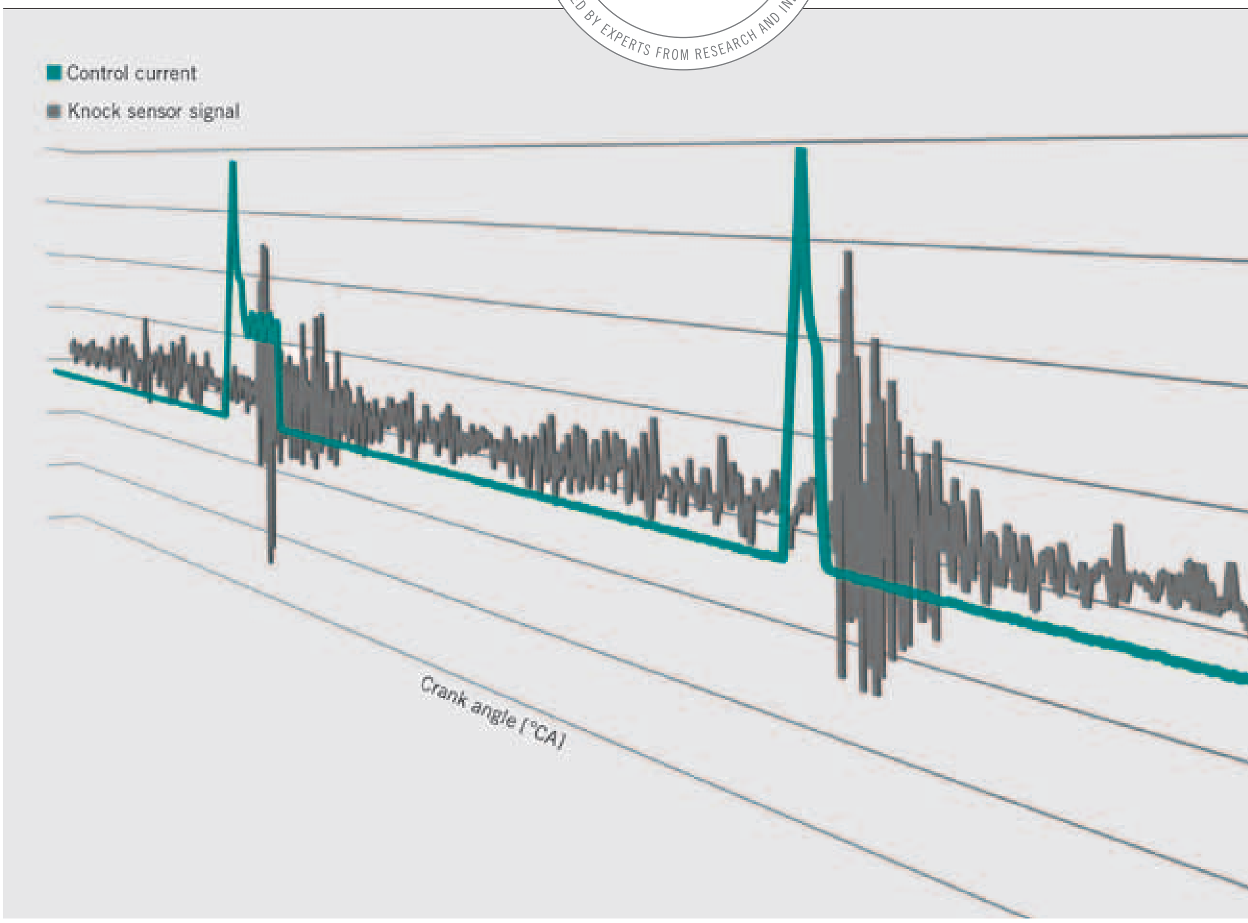

❶ Injector calibration with knock sensor

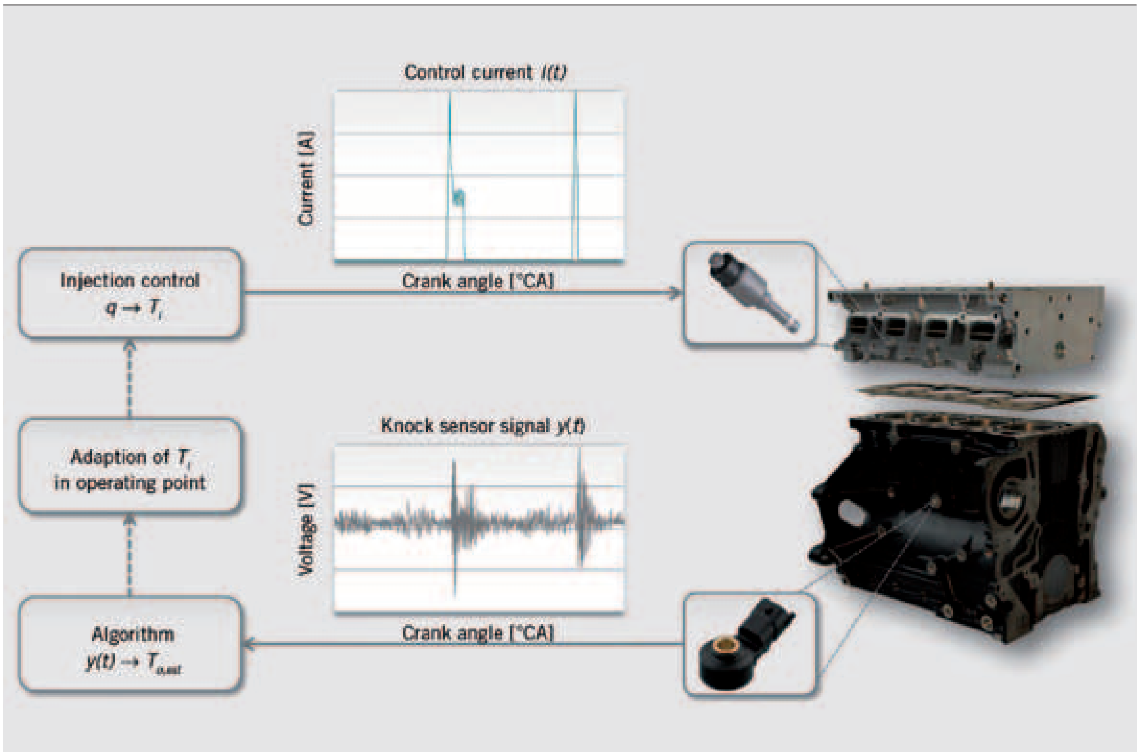

1 INTRODUCTION

Due to manufacturing and component tolerances, the performance of different solenoid injectors for gasoline direct injection (GDI) systems varies. Assembly and wear lead to further deviations from the desired injection duration, i. e. opening duration T_o of the fuel injector, and thus to imprecise fuel dosage. These discrepancies can be met by adapting the supply control duration T_i. At a constant fuel pressure p, the injection process can be characterized by the injector's opening duration T_o. Therefore, the method in [1] is based on retrieving the relation between the injection duration and the supply control duration. The ensemble of all pairs (T_i, T_o) yields a characteristic curve, describing the operating behavior of each individual injector. Correction values for the control duration in a specific operating point can be deduced from this characteristic. According to [1], the injection duration can be determined by specifically positioning an acceleration sensor at the injection valve. In order to avoid higher costs and modifications, neither of the injector nor the cylinder head, the method proposed in this article is aimed at utilizing the standard knock sensor. The strategy is outlined in ❶. The algorithm evaluates the structure borne sound emitted by the fuel injector onto the engine block for determining the begin and the end of injection.

2 THE SOLENOID INJECTOR

Gaining an insight into the injection process is a prerequisite for analyzing the knock sensor signal. ❷ shows a schematic cross-cut of a solenoid controlled injector [2]. The injector basically consists of a pintle and a solenoid, which is powered by the current $I(t)$. The current is activated at the start of injection (SOI). The pintle is lifted after a certain delay of magnetization and the injection

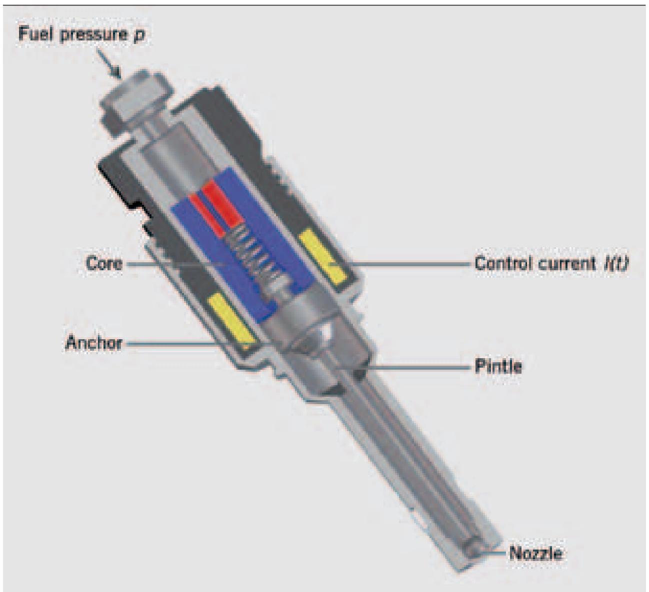

❷ Cross-cut of a solenoid controlled injector

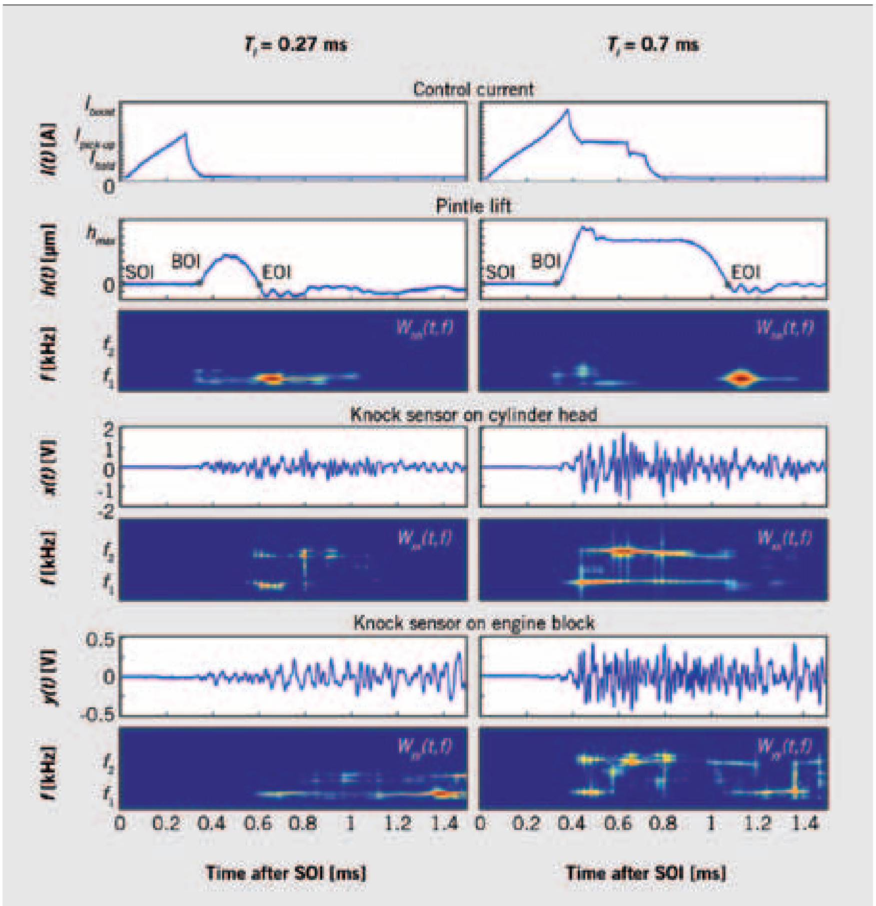

❸ Measured pintle lift as reference and corresponding knock sensor signals for $T_i = 0.27$ ms (left) and $T_i = 0.7$ ms (right) at $p = 10$ MPa

begins (BOI). If the energization is long enough, the anchor hits the solenoid's core (EPL). On deactivating the current, the magnetic field drops and the pintle shuts the nozzle, ending the injection (EOI). The injection process mainly depends on the supply control duration T_i, the fuel pressure and the ambient temperature.

As mentioned before, the production process entails dispersions in the accuracy of different fuel injectors. Due to wear, these dispersions are aggravated during the operation time. The resulting variations in the injected fuel mass can mainly be ascribed to deviations in certain components. Some of these directly influence the injection duration, such as specific values of the solenoid system, the length of the pintle lift, the spring constant and properties of the anchor. Variations in the nozzle's diameter [3] and fuel pressure pulsations [4] lead to further uncertainties in fuel metering.

3 ANALYSIS OF THE KNOCK SENSOR SIGNAL

During the injection process the cylinder head is excited, which leads to structure borne sound emissions on the cylinder head and the engine block. An analysis of the knock sensor signal is performed to find out if the BOI and the EOI can be determined. For this purpose, an adaptive quadratic time-frequency representation is employed, because linear methods, such as the short-time Fourier transform (STFT) and the wavelet transform [5], are unsuitable due to the uncertainty principle. A representation based on the Wigner-Ville distribution is applied according to Eq. 1 [6], whereas the tuning parameter σ is optimized w. r. t. the signal under consideration. This allows assigning the observed frequencies to different events of the injection process.

In the following, measurements of the structure borne sound on the cylinder head are examined and compared to simultaneously recorded laser vibrometer measurements of the pintle lift [7] in order to get an accurate reference for the BOI and the EOI. The resulting findings are the basis for the investigation of the knock sensor signal on the engine block. Subsequently, the knock sensor signals are evaluated with the engine running in combustion.

EQ. 1

$$W_{xx}(t,f) = \int_{-\infty}^{\infty} \int_{-\infty}^{\infty} \frac{\sqrt{\pi\sigma}}{|\tau|} e^{-\frac{\pi^2\sigma(t-u)^2}{\tau^2}} x\left(u+\frac{\tau}{2}\right) x^*\left(u-\frac{\tau}{2}\right) e^{-j2\pi f\tau} \mathrm{d}u\,\mathrm{d}\tau$$

3.1 KNOCK SENSOR ON CYLINDER HEAD

First, the knock sensor is mounted on the cylinder head in the vicinity of the injector. The reference measurements $h(t)$ and the knock sensor signal $x(t)$ are each shown in ❸ for two different T_i. In case of $T_i = 0.27$ ms, the anchor does not hit the solenoid's core. The begin of injection can be determined directly out of the signal amplitude $x(t)$. The end of injection, however, is superimposed by structure borne sound waves of preceding events. Hence, its detection is not trivial in the time domain signal. For this reason, the presented time-frequency method is applied. The respective time-frequency representations $W_{hh}(t,f)$ and $W_{xx}(t,f)$ are depicted in ③ as well, whereas high signal energies are encoded in red color and low energies in blue color. By means of these representations, the excited frequencies can be related to the occurring events. It stands out that the pintle oscillates at the end of injection with frequencies around $f = f_1$.These frequencies are also present when the anchor hits the core, which can be seen between 0.4 ms and 0.6 ms after the SOI for $T_i = 0.7$ ms. The oscillations are transmitted via the injector body to the cylinder head where they are captured by the knock sensor. Furthermore, the knock sensor signal contains a second dominant frequency $f = f_2$, a sensor resonance, which is excited at the end of injection as well as the anchor impact. The end of injection can be determined exactly, as can be seen in the figure. If the time span between the anchor impact and the end of injection is very short, superimposed structure borne sound waves hamper the detection. At a system pressure of $p = 10$ MPa, this occurs for $T_i = 0.3...0.5$ ms.

3.2 KNOCK SENSOR ON ENGINE BLOCK

According to the above considerations, the injection duration can be determined using a knock sensor on the cylinder head. In the next experiment, the knock sensor is mounted on the specified position on the engine block (type Volkswagen EA111). The same injector as in Section 3.1 is used. The knock sensor signals recorded in this setup are displayed in ③ as well. The propagation delay of the structure borne sound is estimated and compensated accordingly. Compared to $x(t)$, the signal amplitude $y(t)$ is damped. Nevertheless, the begin of injection is clearly visible. The time-frequency analysis of the measurements on the engine block yields similar results to the previous examinations. The dominating frequencies f_1 and f_2 can be observed at the corresponding time instants. Thus, detecting the end of injection can be achieved.

3.3 KNOCK SENSOR SIGNALS DURING ENGINE RUN

When the engine is running in combustion, besides the fuel injection, events such as the clicking of the intake and exhaust valves take place. Those cause structure borne sound emissions, which are also contained in the knock sensor signal. ❹ shows the signals of the two standard knock sensors of a four cylinder GDI engine of type GM L850 running in combustion. Laser vibrometer reference measurements are not available in this case. Knock sensor A, located between cylinders 1 and 2, mainly records the injections of injector 1 and 2. Respectively, knock sensor B, which is mounted between cylinders 3 and 4, captures the corresponding fuel injections. These two signals are measured for 50 engine cycles depending on the crank angle. In each cycle, one main (MI) and one post injection (PI) per cylinder is carried out. The control duration of the post injection is chosen according to the operating point of the injector calibration.

In spite of background noise, a detailed consideration of the post injection (SOI at -235° CA) reveals a highly systematic behavior. The disturbances can be modeled as additive white Gaussian noise and attenuated by calculating the mean of all measurements. As previously, the characteristic frequency f_1, which is excited by the bouncing of the pintle, can be observed in the time-frequency domain. Besides the fuel injection, the clicking of the inlet and exhaust valves causes transients in the sensor signals. Their analysis shows, however, that these events do not exhibit a systematic behavior.

4 ALGORITHM FOR INJECTOR CALIBRATION

The injection duration can be estimated by evaluating the measured knock sensor signals in the time-frequency plane. However,

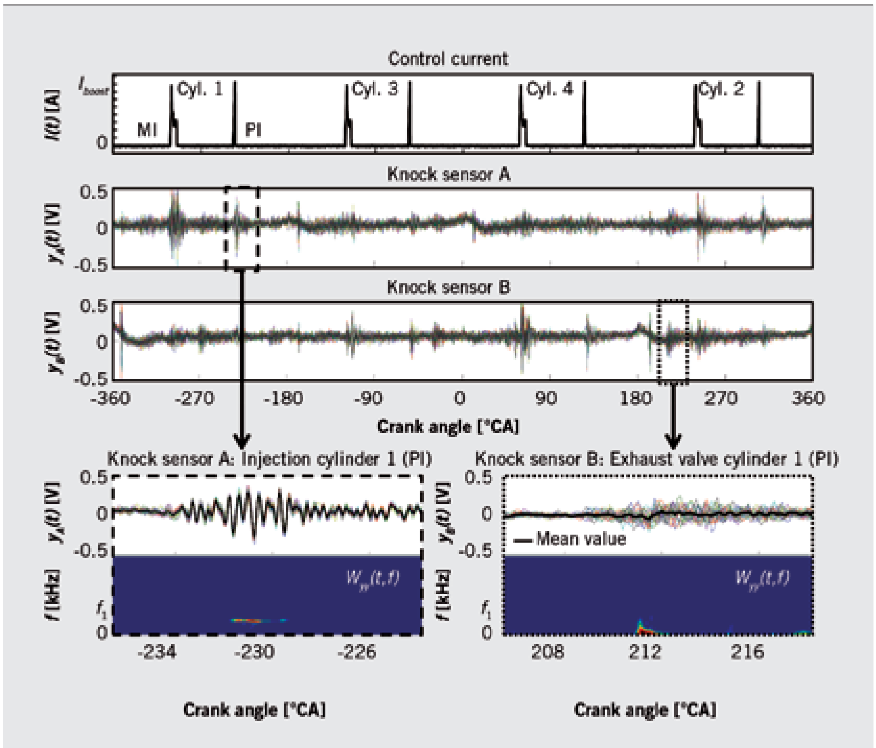

❹ Knock sensor signals during engine run (GM L850) for n_{mot} = 1000 rpm, p = 10 MPa, MI: T_i = 1.1 ms, PI: T_i = 0.29 ms, ignition in cylinder 1 at -28,5° CA

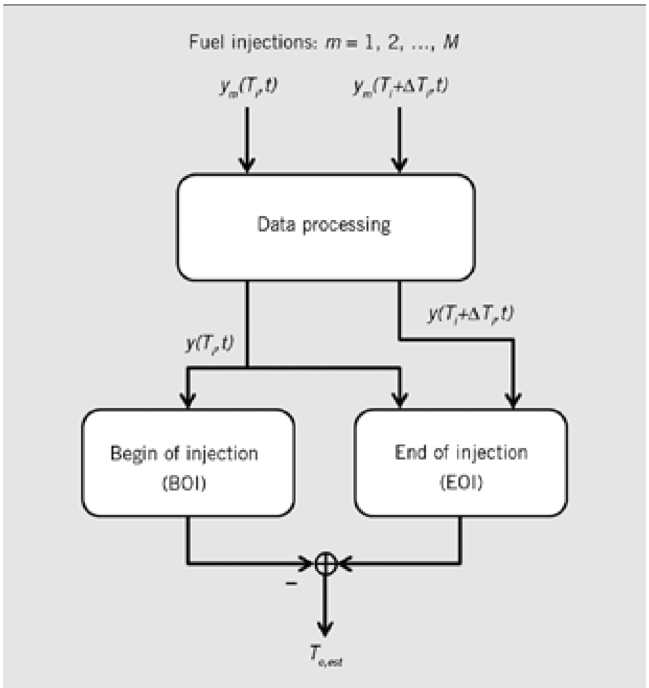

❺ Algorithm for estimating the actual duration of injection

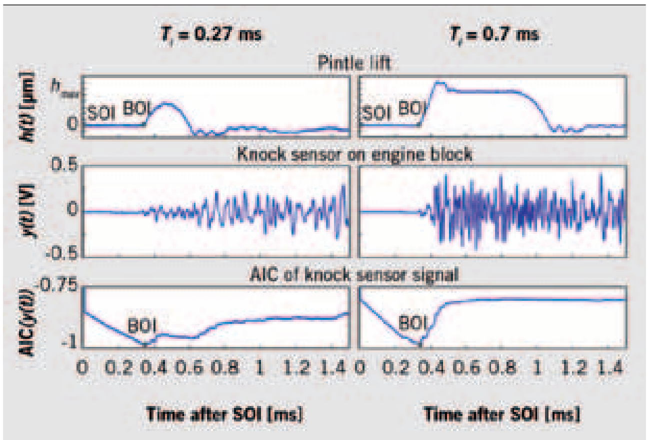

❻ Determination of the begin of injection (BOI) for $T_i = 0.27$ ms (left) and $T_i = 0.7$ ms (right) at $p = 10$ MPa

the computational cost of this approach is very high, limiting its practical use for implementation on an ECU. Hence, the proposed method is based on simple signal processing in time domain. ❺ outlines the developed algorithm. To obtain the injection duration, knock sensor signals are recorded for several injections at a constant fuel pressure. The SOI is chosen in a way that no other noise sources, such as the intake valves, are active during the injection. For noise reduction, the mean values $y(T_i, t)$ and $y(T_i + \Delta T_i, t)$ of the measured signals are calculated after dealing with outliers. Subsequently, based on this data, the estimation of the actual injection duration is performed.

4.1 BEGIN OF INJECTION

The BOI can be detected by thresholding the knock sensor signal $y(T_i, t)$ since it causes a sudden rise in energy. A simple and robust method for acoustic emissions analysis [8] is adapted to the task at hand. The signal $y(T_i, t)$ is split into two segments by means of the Akaike Information Criterion (AIC) [9]. The time instant of optimal segmentation corresponds to the BOI and is calculated by minimizing Eq. 2 [10], in which $w(t)$ is a windowing function and τ a time index in the interval $[t_{soi}, t_e]$, ❻.

EQ. 2

$$AIC(y(t)) = t \cdot \log[\mathrm{var}(y(t) \cdot w(\tau))] + (t_e - t) \cdot \log[\mathrm{var}(y(t) \cdot (1 - w(\tau)))],\ w(\tau) = \begin{cases} 1 \text{ für } t_{SOI} < \tau \le t \\ 0 \text{ für } t < \tau \le t_e \end{cases}$$

4.2 END OF INJECTION

Section 3 revealed that decaying structure borne sound waves of earlier events interfere with the end of injection, impeding its detection in the signal $y(T_i, t)$. To tackle this problem, it is compared to a second measurement $y(T_i + \Delta T_i, t)$ corresponding to a longer control duration $T_i + \Delta T_i$. The strategy is explained pictorially in ❼: The currents $I(T_i, t)$ and $I(T_i + \Delta T_i, t)$ are uniform in the time interval $[t_{SOI}, t_{SOI} + T_i]$, leading to identical pintle lifts and thus similar structure borne sound emissions. The curves of the two knock sensor signals are equal until a certain point in time, as the lower part of ⑦ shows. Only the pintle's impact onto the nozzle, which occurs at different time instants, causes the curves to diverge. This event constitutes the EOI. The practical realization of this approach

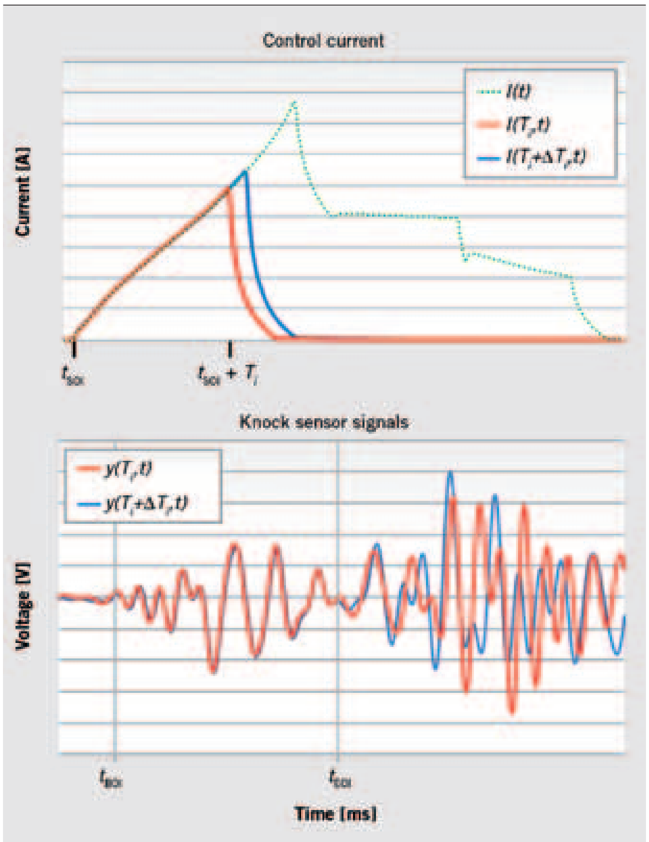

❼ Approach for estimating the end of injection (EOI)

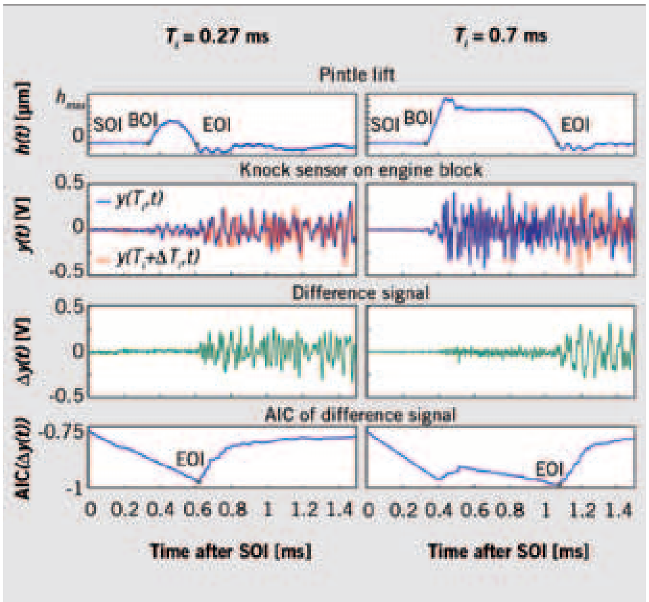

❽ Determination of the end of injection (EOI) for T_i = 0.27 ms (left) and T_i = 0.7 ms (right) at p = 10 MPa

uses the difference between $y(T_i, t)$ and $y(T_i + \Delta T_i, t)$. The choice of ΔT_i mainly depends on the slope of the injector's characteristic curve at the considered operating point. With the help of the difference signal $\Delta y(T_i, t)$, the end of injection can finally be detected by means of the AIC analogously to the begin of injection, ❽.

4.3 RESULTS

An assessment of the algorithm is performed by comparing the estimated injection duration $T_{o,est}$ to the laser vibrometer reference $T_{o,ref}$. At a fuel pressure of $p = 10$ MPa, the control duration is increased in steps of 5 µs from $T_i = 0.25$ ms up to $T_i = 1$ ms. In each operating point, $T_{o,est}$ is estimated out of five measurements. The resulting characteristic curve is depicted in ❾ along with the reference. In the ballistic mode, the algorithm determines the injection durations with a maximum relative error of 5 %. As laid out in Section 3.1., the detection of the EOI is strongly impaired for $T_i = 0.3\ldots0.5$ ms due to superpositions. Hence, some outliers can be found in this interval. Their number can be reduced by further processing. Since the respective injection durations can partly be realized by choosing different control durations, the operating points in this interval are of lower relevance.

During the engine run, the phenomena shown in the previous sections also occur, ❿. The proposed algorithm for detecting the BOI and the EOI yields a clear and plausible result.

5 SYNOPSIS

Solenoid injectors can be calibrated by estimating the actual duration of fuel injection using the knock sensor situated on the engine block. In this article, an easy to implement algorithm has been presented, which can be integrated in an engine control unit for in-situ injector calibration. Thereby, the mentioned systematic variations can be reduced during the injector's entire life-span. For a complete optimization of the fuel metering according to Eq. 3, the effects of fuel pressure pulsations and variances in the nozzle's diameter need to be taken into account.

The procedure detects the begin of injection by processing the time domain sensor signal. The end of injection is determined by comparing two signals of different control durations T_i. The proposed method for acoustic emissions analysis has proved to be suitable. Even for very short control durations the estimation yields reliable results. The evaluation based on the reference measurements shows that each injector's distinct characteristic, i. e. the relation between the control duration T_i and the injection duration T_o, can be determined precisely by applying the presented algorithm. The integration and testing on an ECU is yet to be performed.

EQ. 3	$\lvert q_{ist} - q_{soll} \rvert \rightarrow \min$

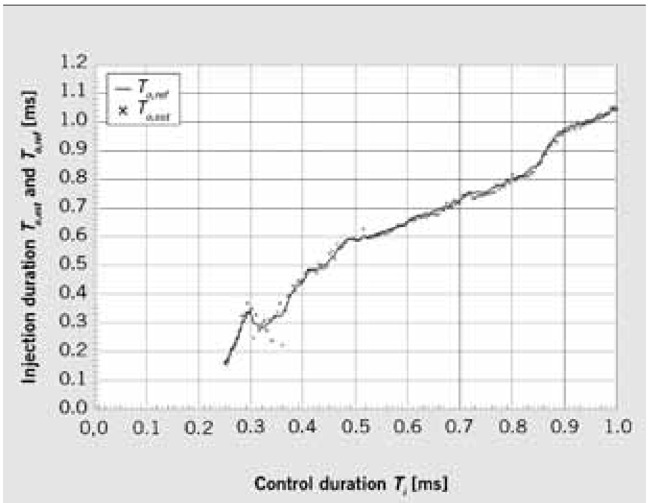

❾ Comparsion of the estimated injection duration $T_{o,est}$ to the reference $T_{o,ref}$ at p = 10 MPa

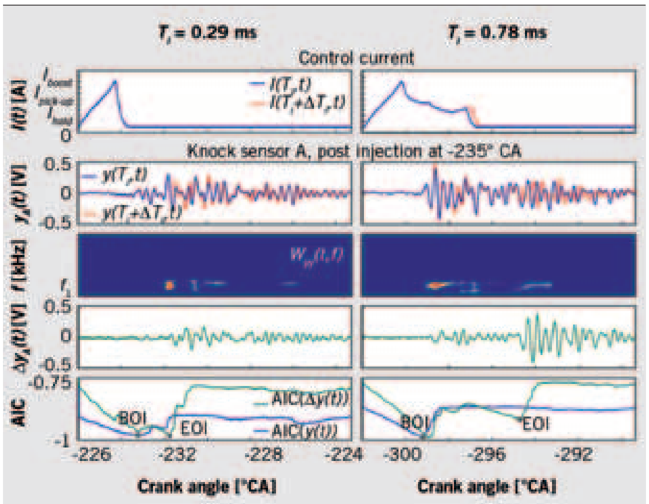

❿ Estimation of the actual injection duration during engine run (GM L850) for T_i = 0.29 ms (left) and T_i = 0.78 ms (right) at p = 10 MPa

VARIABLE	DESCRIPTION	UNIT
AIC*(y(t))*	Akaike-function of signal *y(t)* at time *t*	
BOI	Begin of injection	
EOI	End of injection	
EPL	End of pintle lift	
$h(t)$	Pintle lift	[µm]
h_{max}	Max. pintle lift	[µm]
$I(t)$	Control current	[A]
I_{boost}	Boost current	[A]
I_{hold}	Hold current	[A]
$I_{pick\text{-}up}$	Pick-up current	[A]
p	Fuel pressure at injector	[MPa]
q	Fuel mass	[mg/stroke]
SOI	Start of injection	
T_i	Supply control duration	[ms]
T_o	Injection duration	[ms]
$T_{o,est}$	Estimated injection duration	[ms]
$T_{o,ref}$	Injection duration according to reference signal	[ms]
u	Time index	[s]
$W_{hh}(t,f)$	Time-frequency representation of h(t)	
$W_{xx}(t,f)$	Time-frequency representation of *x(t)*	
$W_{yy}(t,f)$	Time-frequency representation of *y(t)*	
$w(t)$	Time window for AIC	
$x(t)$	Knock sensor signal on cylinder head	[V]
$y(t)$	Knock sensor signal on engine block	[V]
$\Delta y(t)$	Difference signal	[V]
ΔT_i	Difference of supply control durations	[µs]
τ	Time index	[s]
σ	Tuning parameter for time-frequency representations	

REFERENCES

[1] Hehle, M.; Willmann, M.; Remele, J.; Ziegler, T.; Schmidt,G.: In-Situ-Kalibration – Hochpräzise Kraftstoffeinspritzung für Off-Highway-Motoren. In: ATZoffhighway 2008, No. 4, p. 36-48
[2] Achleitner, E.; Koch, A.; Maier, J.; Marinai, A.: Magnetspulen-Injektoren für Benzin-Direkteinspritzung. In: MTZ 2006, No. 5, p. 332-339
[3] Tang, J.; Pischinger, S.; Grütering, U.; Keck, J.: Einflüsse auf die Belagsbildung bei Einspritzdüsen von Dieselmotoren mit Direkteinspritzung. In: MTZ 2008, No. 9, p. 754-761
[4] Baranowski, D.; Brunelli, M.; Taudt, C., Zander, E.: Theoretische und experimentelle Methoden der hydraulischen Auslegung von Common-Rail-Systemen. In: Tschöke, H. und Leyh, B. (Hrsg.): Diesel- und Benzin-Direkteinspritzung, Vol. 2, p. 36-57. Expert-Verlag, 2003
[5] Kiencke, U.; Schwarz, M.; Weickert, T.: Signalverarbeitung: Zeit-Frequenz-Analyse und Schätzverfahren. München: Oldenbourg, 2008
[6] Boashash, B.: Time-Frequency Signal Analysis and Processing: A Comprehensive Reference. New York: Elsevier, 2003
[7] Waibler, E.; Schumann, G.: Schnelle, berührungslose Nadelhubmessungen an innen öffnenden Einspritzventilen unter hydraulisch realistischen Bedingungen. In: Tschöke, H. und Leyh, B. (Hrsg.): Diesel- und Benzin-Direkteinspritzung, Vol. 2, p. 148-159. Expert-Verlag, 2003.
[8] Kurz, J. H.; Grosse, C. U.; Reinhardt, H.-W.: Strategies for Reliable Automatic Onset Time Picking of Acoustic Emissions and of Ultrasound Signals in Concrete. In: Ultrasonics (2005), No. 7, Vol. 43, p. 538-546
[9] Akaike, H.: Markovian Representation of Stochastic Processes and its Application to the Analysis of Autoregressive Moving Average Processes. In: Annals of the Institute of Statistical Mathematics (1974), No. 1, Vol. 26, p. 363-387
[10] Maeda, N.: A Method for Reading and Checking Phase Times in Auto-Processing System of Seismic Wave Data. In: Jishin (1985), No. 3, Vol. 38, p. 365-379